

# UNCLASSIFIED

AD NUMBER
AD839673
NEW LIMITATION CHANGE
TO Approved for public release, distribution unlimited
FROM Distribution authorized to U.S. Gov't. agencies and their contractors; Administrative/Operational Use; JUL 1968. Other requests shall be referred to Air Force Flight Dynamics Lab., Wright-Patterson AFB, OH 45433.
AUTHORITY
AFFDL ltr, 31 May 1973

THIS PAGE IS UNCLASSIFIED

AFFDL-TR-68-79

AD 339673

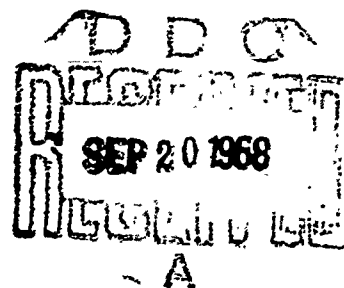
## HIGH ALTITUDE CLEAR AIR TURBULENCE MODELS FOR AIRCRAFT DESIGN AND OPERATION

EDWARD V. ASHBURN, DAVID T. PROPHET and DAVID E. WACO

*Lockheed-California Company*

TECHNICAL REPORT AFFDL-TR-68-79

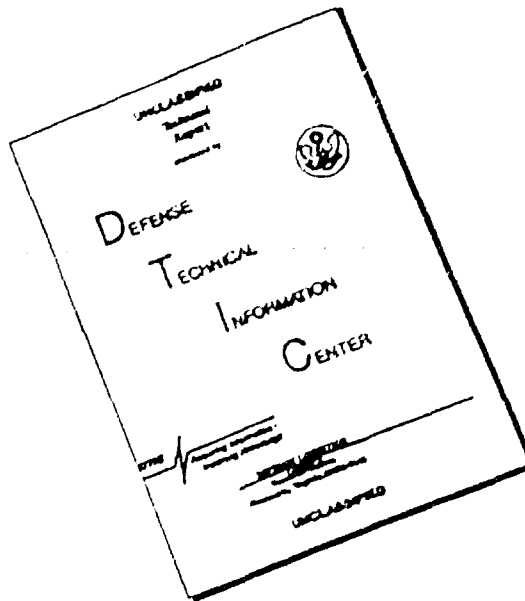
JULY 1968



This document is subject to special export controls and each transmittal to foreign governments or foreign nationals may be made only with prior approval of the Air Force Flight Dynamics Laboratory (FDTR), Wright-Patterson AFB, Ohio 45433.

AIR FORCE FLIGHT DYNAMICS LABORATORY  
AIR FORCE SYSTEMS COMMAND  
WRIGHT-PATTERSON AIR FORCE BASE, OHIO

# DISCLAIMER NOTICE



THIS DOCUMENT IS BEST  
QUALITY AVAILABLE. THE COPY  
FURNISHED TO DTIC CONTAINED  
A SIGNIFICANT NUMBER OF  
PAGES WHICH DO NOT  
REPRODUCE LEGIBLY.

# NOTICE

When Government drawings, specifications, or other data are used for any purpose other than in connection with a definitely related Government procurement operation, the United States Government thereby incurs no responsibility nor any obligation whatsoever; and the fact that the Government may have formulated, furnished, or in any way supplied the said drawings, specifications, or other data, is not to be regarded by implication or otherwise as in any manner licensing the holder or any other person or corporation, or conveying any rights or permission to manufacture, use, or sell any patented invention that may in any way be related thereto.

SECTION 12	
DATE	WHITE SECTION <input type="checkbox"/>
NO.	DIFF. SECTION <input checked="" type="checkbox"/>
DISTRIBUTION/AVAILABILITY CODES	
DIST.	AVAIL. and/or SERIAL
2	

Copies of this report should not be returned unless return is required by security considerations, contractual obligations, or notice on a specific document.

**AFFDL-TR-68-79**

## **HIGH ALTITUDE CLEAR AIR TURBULENCE MODELS FOR AIRCRAFT DESIGN AND OPERATION**

**EDWARD V. ASHBURN, DAVID T. PROPHET and DAVID E. WACO**

*Lockheed-California Company*

This document is subject to special export controls and each transmittal to foreign governments or foreign nationals may be made only with prior approval of the Air Force Flight Dynamics Laboratory (FDTR), Wright-Patterson AFB, Ohio 45433.

## FOREWORD

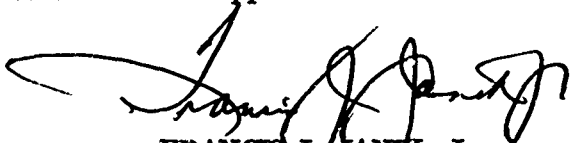
This report was prepared by the Lockheed-California Company, Burbank, California for the Air Force Flight Dynamics Laboratory, Wright-Patterson Air Force Base, Ohio under Contract AF 33(615)-3639. The contract title is "Research Investigation of High Altitude Clear Air Turbulence in the Altitude Layer of 50,000 to 80,000 Feet." The contract was initiated under Project No. 1367, "Structural Design Criteria," Task No. 136702, "Aerospace Vehicle Structural Loads Criteria." The Lockheed-California Company report number is LR 21501. The report covers work conducted from 1 March 1966 through May 1968.

The contract was administered by the Air Force Flight Dynamics Laboratory, Wright-Patterson Air Force Base, Ohio, with Mr. Paul L. Hasty (FDTR) as Project Engineer. The Lockheed-California Company Principal Investigators were Dr. W. W. Hildreth, Mr. G. E. Abrahms, and Mr. E. V. Ashburn.

Special acknowledgments are due to Dr. Arnold Court and Mr. U. Oscar Lappe, consultants for the program and to the following Lockheed-California Company personnel: Dr. D. T. Perkins, Division Scientist of the Physical and Life Sciences Laboratory; Mr. M. G. Childers, Department Scientist of the Physical Sciences Laboratory; Mr. S. I. Adelfang and Mr. F. A. Mitchell, staff members of the Atmospheric Physics Laboratory; and Mr. W. M. Crooks of the Flight Test Organization.

This report was submitted by the authors in June 1968.

This technical report has been reviewed and is approved.



FRANCIS J. JANIK, Jr.  
Chief, Theoretical Mechanics Branch  
Structures Division

ABSTRACT

This report presents the results of an analysis of the turbulence data derived from the high altitude clear air turbulence (HICAT) flight investigation and from the pertinent meteorological and geophysical data. The curves representing the power spectra have various slopes and shape. These curves are grouped into categories. One group of categories are predominantly cases of flights over mountains. A second group of categories are mostly from flights over flatland. Theoretical, statistical, and practical forecasting analyses in addition to flight records all indicate that large horizontal temperature gradients and large changes in vertical temperature gradients are closely associated with HICAT and conversely small horizontal temperature gradients and nearly constant vertical temperature gradients are closely associated with smooth air.

Evidence is presented that the relative frequency of occurrence of high altitude clear air turbulence by geographic area may be deduced from an analysis of the standard deviations of the 24 hour temperature changes at the HICAT flight altitude.

Turbulence was observed during 6.9% of the flight miles over mountains and 5.5% of the flight miles over water. The RMS of the vertical gust velocity during HICAT was 0.86 over water, 1.02 over flatland and 1.89 over mountains.

(This document is subject to special export controls and each transmittal to foreign governments or foreign nationals may be made only with prior approval of the Air Force Flight Dynamics Laboratory (FDTR), Wright-Patterson AFB, Ohio 45433.)

## TABLE OF CONTENTS

SECTION		PAGE
I	INTRODUCTION	1
II	OTHER STUDIES	3
III	TURBULENCE MEASUREMENTS	7
	Graphs and Maps	8
	Revised Turbulence Model	11
	Classification of Spectra of Gust Velocities	19
IV	UPPER AIR DATA	30
V	DISCUSSION	39
	An Interpretation of the Radiosonde Temperature Profiles in Terms of Vertical Wave Motion in the Atmosphere	39
	Calculation of Mean Square Vertical Acceleration from Radiosonde Data	41
	A Model for Clear Air Turbulence Based on Sloping Isen- tropic Surfaces	51
	Example of World Wide Application of Both Models	63
	Statistical Studies	68
	The Development of a Practical Procedure for Forecasting High Altitude Clear Air Turbulence	73
	Horizontal Temperature Gradients in Regions of Clear Air Turbulence	85
	Geographic Distribution of Turbulence	93
VI	CLASSIFICATION OF HICAT BY CHARACTERISTICS OF THE EARTH'S SURFACE	102
VII	CONCLUSIONS	105
VIII	REFERENCES	106
IX	BIBLIOGRAPHY	109

## LIST OF FIGURES

Figure		Page
1a	Time Histories. Gust Velocities, Altitude, and Air Temperature	9
1b	Time Histories. Air Speed, Roll Angle, Elevator Position, Longitudinal Acceleration, Lateral Acceleration, Normal Acceleration	10
2	Power Spectrum of Vertical Gusts. Flight 102, Run 15	11
3a	Flight Track Map Over Hawaii, Flight 76	13
3b	Flight Track Map Over Australia, Flight 102	14
4	Relative Spectral Density as Function of Longitudinal Scale of Turbulence ( $L$ )	17
5	$U_V$ Normalized Power Spectral Classes A Through D	21
6	$U_V$ Normalized Power Spectral Classes E Through F*	22
7	A Composite of $U_V$ Normalized Power Spectral Classes A Through F*	23
8	Unclassified $U_V$ Normalized Power Spectra	24
9	Normalized Power Spectra for Flight 107, Runs 9 and 10, ( $U_F, U_L$ ) and Flight 102 ( $U_V$ )	26
10	$U_F, U_L$ , and $U_V$ , Normalized Power Spectra for Flight 76, Runs 4, 5, and 6, and Flight 114, Runs 3, 13, and 14	28
11	Meteorological Station Locations. Hawaii	31
12	Meteorological Station Locations. New Zealand	32
13	Meteorological Station Locations. Australia	33
14	Meteorological Station Locations. Central America	34
15	Meteorological Station Locations. Great Britain	35
16a	Meteorological Station Locations. United States	36
16b	Meteorological Station Locations. Northeastern United States	37
17	Meteorological Station Locations. Alaska	38
18	Hypothetical Case of Balloon Ascent	40
19	Temperature Sounding, Las Vegas, Nevada, 30 Aug 1966, 0000Z (Flight 114)	44
20	Temperature Sounding, Ely, Nevada, 31 Aug 1966, 0000Z (Flight 115)	46
21	Temperature Sounding, Winnemucca, Nevada, 31 Aug 1966, 0000Z (Flight 115)	47

# LIST OF FIGURES (Continued)

Figure		Page
22	Temperature Sounding, Hilo, Hawaii, 17 May 1966, 0000Z (Flight 76)	48
23	Temperature Sounding, Hilo, Hawaii, 16 Apr 1966, 0000Z (Flight 58)	49
24	Temperature Sounding, Lihue, Hawaii, 16 Apr 1966, 0000Z (Flight 58)	50
25	Temperature Sounding, Eagle Farm, Australia, 27 Jul 1966, 2300Z (Flight 102)	52
26	Temperature Sounding, Williamstown, Australia, 27 Jul 1966, 2300Z (Flight 102)	53
27	Temperature Sounding, Cobar, Australia, 27 Jul 1966, 2300Z (Flight 102)	54
28	Temperature Sounding, Wagga, Australia, 27 Jul 1966, 2300Z (Flight 102)	55
29	Isentropic Height Analysis for $\theta = 450^{\circ}\text{A}$ , Southeastern Australia, 27 Jul 1966, 2300Z (Flight 102)	65
30	Isentropic Height Analysis for $\theta = 490^{\circ}\text{A}$ , Southeastern Australia, 27 Jul 1966, 2300Z (Flight 102)	66
31	Frequency Distribution of Meteorological Variables for Turbulent and Nonturbulent Cases	71
32	Frequency Distribution of Meteorological Variables for Turbulent and Nonturbulent Cases	72
33	Flight Track, Flight 266, 1 Dec 1967	75
34	70 mb Analysis, 2 Dec 1967, 0000Z	76
35	Temperature Soundings, 2 Dec 1967, 0000Z	78
36	Isentropic Analysis, 2 Dec 1967, 0000Z	79
37	Flight Track, Flight 218, 30 Jun 1967	81
38	700 mb Analysis, 30 Jun 1967, 1200Z	82
39	Temperature Soundings, 30 Jun 1967, 1200Z	83
40	Isentropic Analysis, 30 Jun 1967, 1200Z	84
41	Correlation Between Temperature Changes and RMS 2000 Values	86
42	Time Histories of Gust Velocity and Temperature Variations for Flight 100, Runs 6 and 9	87
43	Time Histories of Gust Velocity and Temperature Variations for Flight 107, Run 8 and Flight 265, Run 37	88

# LIST OF FIGURES (Concluded)

Figure		Page
44	Time Histories of Gust Velocity and Temperature Variations for Flight 202, Run 7 and Flight 102, Run 9	89
45	Time Histories of Gust Velocity and Temperature Variations for Flight 114, Runs 13 and 14	90
46	Time Histories of Gust Velocity and Temperature Variations for Flight 280, Run 10	91
47	Correlation Between Temperature and Gust Velocity Changes	94
48	Standard Deviation of 24 Hour Temperature Change at 100 mb (Jan - Mar 1964)	95
49	Standard Deviation of 24 Hour Temperature Change at 100 mb (Apr - Jun 1964-65)	96
50	Standard Deviation of 24 Hour Temperature Change at 100 mb (Jul - Sep 1964-65)	97
51	Standard Deviation of 24 Hour Temperature Change at 100 mb (Oct - Dec 1964-65)	98
52	Standard Deviation of 24 Hour Temperature Change at 100 mb (Southeastern Australia 17 Jul - 12 Aug 1966)	100

## SYMBOLS

$a$	Universal constant of turbulence
$a_N$	Normal acceleration in aircraft axes; positive upward
$B$	Stability and shear term
$E$	Energy
$f$	Coriolis parameter
$g$	Gravitational acceleration
$h$	Wave amplitude
$I^2$	Scorer's parameter
$L$	Longitudinal scale of turbulence
$i_u$	Scale parameter
$n$	Normal vector
$N$	Sample number
$p$	Slope of power spectral density curve
$P$	Pressure
$Ri$	Richardson number
$RMS$	Root Mean Square
$s$	Slope of isentropic surface
$t$	Time
$T$	Temperature
$u$	Component of $V$ in $x$ direction
$u_r$	Component of $V$ perpendicular to wind shear vector
$U_{de}$	Derived equivalent gust velocity
$U_F$	Longitudinal gust component
$U_L$	Lateral gust component
$U_V$	Vertical gust component
$v$	Component of $V$ in $y$ direction
$v_s$	Indicated airspeed
$V$	Horizontal component of wind speed
$w$	Component of wind in $z$ direction
$w_o$	Rate of rise of balloon with respect to air
$z$	Height

## SYMBOLS

$\alpha$	Wind direction
$\gamma$	Lapse rate
$\gamma_d$	Dry adiabatic lapse rate
$\Gamma$	Gamma function
$\varepsilon$	Dissipation rate of energy
$\theta$	Potential temperature
$\lambda$	Wavelength
$\nu$	Frequency
$\rho$	Density
$\sigma$	Standard deviation
$\sigma^2$	Variance
$\tau$	Wave period
$\omega$	Degrees latitude
$\bar{\varepsilon}$	Power spectral function
$\chi^2$	Chi-square
$\Omega$	Reduced frequency
$\Omega_e$	Angular speed of earth's rotation
$\nabla$	Del operator
$\nabla_H$	Horizontal component of Del operator

## SECTION I

### INTRODUCTION

This report consists of an extensive analysis of the meteorological and geophysical conditions associated with high altitude clear air turbulence. The basic turbulence data were obtained from Project HICAT (Investigation of High Altitude Critical Atmospheric Turbulence) of the Flight Dynamics Laboratory, Air Force Systems Command, Wright-Patterson Air Force Base, Ohio.

The discussion begins with a description of the basic turbulence data and of the method of selecting samples for analysis. Then the meteorological and geophysical data that were used in the study are described. Sections on case history studies, statistical studies, theoretical analysis and climatological studies follow.

The purpose of this report has been to present data, models, and summaries relating to high altitude clear air turbulence in a form that will provide a foundation for the development of improved methods for forecasting turbulence, calculating gust loads and vehicle responses, designing aerospace vehicles to withstand gusts, and analyzing fatigue.

#### CHRONOLOGY

The HICAT program, initiated in 1962, was divided into two distinct but complementary phases. One phase consisted of the design, installation, and flight of instruments that would yield data relating to the motions of the atmosphere. The first flight of the WU-2 aircraft under this program was made on 20 February 1964, and by 15 July 1964, 18 HICAT search flights were completed. Complete documentation of this portion of the HICAT program was presented by Crooks (1).

New and more sophisticated instruments were then installed in the WU-2 and HICAT search flights were resumed on 8 October 1965. By 1 March 1967, a total of 114 more flights were made. The details of the instrument development, data reduction, and flight program for the period ending in February 1967 were presented by Crooks, Hoblit, and Prophet (2). A report covering the flights made from March 1967 through February 1968 is in preparation.

The second phase of the HICAT program was initiated in July 1962. Work accomplished up to April 1965 was presented by Hildreth, et al. (3) and Hildreth, Court, and Abrahms (4). The present report covers the work accomplished up to May 1968.

The HICAT program is now part of a larger ALLCAT program on "Critical Atmospheric Turbulence" which was initiated by the Air Force Flight Dynamics Laboratory in June 1966. See Anonymous (5). The objective of the ALLCAT Program is to provide fine-scale true gust velocity measurements of continuous wavelength turbulence for all altitudes, seasons, and typical geographic areas. These turbulence data, correlated with meteorological conditions and synthesized with other

data, will be used to establish valid turbulence criteria for the design of advanced vehicle structures and flight control systems, and for human factors investigations. The turbulence data can be utilized in evaluating structural modifications and life determinations of existing flight vehicles. These data will assist meteorological agencies in verifying, changing, and establishing techniques for forecasting critical atmospheric turbulence. The turbulence data will also be useful to other technical disciplines, such as physiological and psychological investigations of crew members, crew accommodations, guidance, flight instrumentation, jet engine design, and mission planning in operational organizations.

## SECTION II

### OTHER STUDIES

Many reports and articles have appeared in the last few years on clear air turbulence and its effects upon aircraft. Of more than 300 entries in the Bibliography (Section V), many are efforts to define the meteorological and geophysical conditions associated with clear air turbulence at altitudes of 20,000 to 40,000 ft. Observations of clear air turbulence upon which these studies are based vary from subjective reports of airline and military pilots to specific and detailed measurements of the characteristics of the turbulence. Likewise, the discussions vary from purely theoretical treatments, to case histories and to extensive statistical studies.

With few exceptions, the meteorological data are the temperatures, pressures, wind velocities, and wind directions obtained routinely by national weather services. Horizontal and vertical temperature gradients and wind shears may be derived from these basic measurements by an analysis system that is nearly always partially subjective. Other functions of the temperature and wind fields such as Richardson number, deformation, divergence, etc. have also been used in statistical analyses and case history studies of relationships between meteorological conditions and the reports of turbulence. In general, derivation of such quantities from the basic temperature and wind data requires a significant amount of subjective judgment which, along with the errors in the original data, introduces an unknown uncertainty in the final results.

The basic meteorological data and the quantities derived from these data that have been used in statistical studies of clear air turbulence are summarized in Table 1. These studies have served as an important guide to the work described in this report.

TABLE I  
LITERATURE SURVEY OF RELATIONSHIP BETWEEN CLEAR AIR TURBULENCE  
AND METEOROLOGICAL & GEOPHYSICAL PHENOMENA

Author	Year	Place	Plane	Weight	Turb. Cases	Relationship with CAT	Peer Correlation
Port, W. G. A. (1949)	1948	England	Spitfire	20-40, 000'		$\Delta T/\Delta z < -2^\circ/1000'$ (In-flight temperatures)	Lapse rate; vert. wind shear; RI
Bannon, J. K. (1951)	1949	England	Comet Meteor F-86, etc.	28-40, 000'	7	Low pressure side of jet; horis. vert. wind shear; RI < 1; Add. Notes: wind Max 130-160 KT	Above or below jet
Lake, H. (1956)	1953	U.S.	Commercial Military	30-39, 000'	598 Pilot rpts	Negative vert. wind shear; lapse rate < dry adiab. > isothermal	Positive vert. wind shear; RI; adiab. inversion
Clam, L. H. (1957)	1954-55	N.E., N.W. & S.W. U.S.	USAF Fighters	25-45, 000'		Strong jet overhead or to south; below & on cyclonic side of jet; some corral; Upper level trough or low	
Estoque, M. A. (1958)	1957-58	U.S., Japan Europe	B-47 & U-2	23-40, 000'		2% of flight turbulent above 150 mb; 15% turbulent at 300 mb	
Balser, M. E. & Harrison, H. T. (1959)	1957-58	U.S.	Mostly Military	20-45, 000'	927 Pilot rpts	Pressure trough; at and below both jet stream and tropopause; Note: Results affected by flight frequencies	Cold or warm side of jet; warm air advection; horis. temp. gradient
Harrison, H. T. (1959)	1957-58	U.S.	Mostly Military	20-45, 000'	927 Pilot rpts	Horis. wind shear; near or to left of jet core; pressure trough; meandering polar jet	800 mb chart for indicating turbulence higher up
George, J. J. (1961)	1959	East U.S.		7-19, 000'	15 severe	Horis. wind shear > 80 KT/180 mi. plus max. of vert. shear combined; above base of vert. shear layer; Note: Max. vert. shear = 18 KT/1000'	Vert. shear < 8 KT/1000'
Harrison, H. T. (1961)	1960	U.S.	Commercial Military	25-44, 000'	Pilot rpts	Left of jet core (looking downwind) near level max. wind of polar jet; below level max. wind between jets; horis. & vert. wind shears; superadiabatic lapse rate	
Ball, J. T. (1962)	1961	U.S.	Commercial Military	18-38, 000'	Pilot rpts	Height of max. wind layer; horis. temp. gradient	Lapse rate; wind shear; RI
Briggs, J. & Roach, W. T. (1963)	1960	England	Canberra	28-38, 000'	22 flights	RI < 1; vert. wind shear; upper frontal zone; some corral; $V(3V/8d)/\text{vertical grad. of kinetic energy}$	Horis. shear, lapse rate, sign of vert. wind shear
Colson, D. (1963a)	1962	U.S.	Commercial Military	18-40, 000'	Pilot rpts	Vert. wind shear (exception in mountain waves); some corral; jet; RI < 1; pressure trough	Horis. shear
Colson, D. (1963b)	1960-62	U.S.	Commercial Military	18-70, 000'	12, 126 Pilot rpts	Jet stream; slight corral; cold side of jet; Note: % of flights with turb: 40-50, 000' = 60%; 50-60, 000' = 51%; 60-70, 000' = 34%	Pressure trough or ridge
Kadlec, P. W. (1963)	1960-63	East U.S.	Commercial	20-40, 000'	414 flights	4 cirrus pattern models; polar & subtropical jets; converging jets; upwind of trough	

TABLE 1  
LITERATURE SURVEY OF RELATIONSHIP BETWEEN CLEAR AIR TURBULENCE  
AND METEOROLOGICAL & GEOPHYSICAL PHENOMENA (Continued)

<u>Author</u>	<u>Year</u>	<u>Place</u>	<u>Plane</u>	<u>Height</u>	<u>Turb. Cases</u>	<u>Relationship w/ CAT</u>	<u>Poor Correlation</u>
Rai Sivar, N. C. & Varghese, K. P. (1963)	1961-63	India	Boeing 707	30-42, 000'	88 Pilot rpts	Near press. trough lines where large E-W wind gradient	Jet stream; horis. temp. gradient
Richardson, N.N. (1963)	1963	U.S.	Commercial Military	20-40, 000'		Laplace operator ( $\nabla^2$ ) applied to horis. shear field minus thermal wind shear	
Rustanbeck, J.D. (1963)	1960-61	U.S.	Commercial Military	18-40, 000'	163 Pilot rpts	$Ri \leq 5$ ; below both level max. wind & tropopause	Lapse rate
Endlich, R.M. (1964) Endlich, R.M. & McLean, G.S. (1965) Endlich, R.M., Mancuso, R. L. & Davies, J.W. (1966)	1957	U.S.	B-47	34-42, 000'	23 In-flight	Best: $V(\Delta\sigma/\Delta h) \approx$ normal to flow; also jet stream; trough & ridge; upper front; horis. & vert. shears (speed & direction); vert. velocity; $V(\partial\sigma/\partial h)$ ; Note: (in-flight measurements of wind, temp., turb.) flow perpendicular to jet axis	$Ri$
Kao, S. K. & Woods, H.D. (1964)	1957	U.S.	B-47	25-40, 000'		$Ri < 1$ ; energy spectra similar for perpendicular and parallel to jet	
Kadlec, P.W. (1964)	1963-64	U.S.	Commercial Military	20-40, 000'	179 flights	3 cirrus models; anticyclonic curvature of subtrop. jet; above straight jet in tropopause; downwind of developing surface low	
Kronebach, G.W. (1964)	1962	U.S.	Commercial Military	17-55, 000'	1063 Pilot rpts	Within 240 n. mi. of jet (71%); cyclonic jet or straight; $Ri < 1$ ; $V(\partial\sigma/\partial h)_{90}$ better than shear	Horis. shear; anticyclonic jet; cold or warm side of jet
Reiter, E.R. & Nemia, A. (1964)	1962	U.S.	Commercial Military	34, 000'	Pilot rpts	Merging jets; stable lapse rate; vert. & horis. direction shear; Scorer's $f^2$	Wind speed; scalar shear
Sorenson, J.E. (1964)	1963	U.S.	Commercial Military	25-41, 000'	264 $\geq M$ Pilot rpts	Horis. temp. gradient plus jet, trough or mountain; horis. direction shear; $\partial\sigma/\partial h$ or $\partial\sigma/\partial t$	
Burns, A. & Rider, C.K. (1965) (1966) - Reiter, E.R. & Burns, A. (1966)	1963	Australia	Camberra	26-33, 000'		Subtropical jet; stable lapse rate; $\partial\sigma/\partial h$ ; Spectra fit $\sim t^{-2/3}$ law at short wavelengths	
Endlich, R.M. & R. L. Mancuso (1965)	1962	U.S.	Commercial Military	18-40, 000'	337 Pilot rpts	$Ri$ ; $(V\partial\sigma/\partial h)$ ( $\partial^2\sigma/\partial h^2$ ); $\partial^2\sigma/\partial h^2$ ; horis. direction shear	
Kadlec, P.W. (1965) (1966)	1965-66	East U.S.	DC-8	20-41, 000'	963 flights	$\partial T/\partial h \geq 1^\circ\text{C}/\text{min}$ ; Total $\Delta T = 1^\circ\text{C}$ ; jet stream; dir-ns; anticyclonic jet	
Spillane, K.T. (1965) (1967)	1964 ?	Australia	Target Acft	20-65, 000'	54 Pilot-less flights	$Ri < 1$ ; static stability; sharp change in $\partial T/\partial h$ with ht; $\partial\sigma/\partial h$ only fair; secondary turb. max. 88, 000	
Wiegman, E.J. (1965)	1963	U.S.	Commercial Military	7-43, 000'	1043 Pilot rpts	Satellite cloud patterns; jet stream & troughs; frontal wave systems	

TABLE I LITERATURE SURVEY OF RELATIONSHIP BETWEEN CLEAR AIR TURBULENCE AND METEOROLOGICAL & GEOPHYSICAL PHENOMENA (Concluded)

Author	Year	Place	Plane	Height	Turb. Cases	Relationship with CAT	Poor Correlations
Brochet, G. (1966)	1964	Europe	Civil & Military	20-40,000'	Pilot rpts	Jet stream at 300 mb plus relief $\geq 6000'$ ; vert. wind shear for $z < 30,000'$	Vert. wind shear for $z > 30,000'$
Burns, A., Harrold, T.W., Burham, J. & Spavins, C.S. (1966)	1965	Oklahoma	Canberra	40-45,000'	5 flights	Near thunderstorms; vert. motion; $\Delta T/\Delta z$ ; (Note: oscillograph used)	Height above clouds
Clarke, R.H. (1966)	1963	Australia	Canberra	27-29,000'	2 flights	$\zeta^2 = \eta/u^2 - 1/u \partial^2 u/\partial z^2 + \eta/gu \partial u/\partial z$ ( $\eta = g \partial \ln \rho/\partial z$ ) max. upstream; $Ri < 1$ ; mountain lee	
Endlich, R.M., Mancuso, A.L. & Davies, J.W. (1966), Endlich, R.M. & Mancuso, R.L. (1967)	1962-65	U.S.	Commercial Military	20-40,000'	Several thousand Pilot rpts	Best: deformation; $\Delta \bar{V}/\Delta z$ ; def. times $\Delta \bar{V}/\Delta z$ ; $\Delta T = d(\partial T/\partial n)/dt$ ; Fair: $ \nabla \cdot \bar{V} $ , $\nabla \text{Rel. humid.}$ ; divergence; vorticity; $V (\partial \alpha/\partial z)$	$V: \Delta \bar{V}/\Delta z$
George, J.J. (1966)	1961-63	U.S.	Commercial	20-40,000'	Pilot rpts	Axis of temperature trough	
Harrison, H.T. (1966)	1963-65	U.S.	Commercial	20-40,000'	4000 $\geq$ M Pilot rpts.	Mountain lee plus jet stream shear; wind speed plus $\Delta P$ across mountain; horiz. temp. gradient upwind	
Kao, S.K. (1966)	1956-57	U.S.	B-47	25-40,000'	2752 Turb Cases	Divergence; curved jets; below & north of jet core	
McLean, J.C. (1966)	1962	East U.S.	Commercial Military	18-37,000'	Pilot rpts	Upper fronts; adiabatic layers	
Moore, R.L. & Krishnamurti, T.N. (1966)	1962	U.S.	Commercial	20-40,000'	Pilot rpts	$\nabla_H T \times \nabla (\nabla \cdot \bar{V})$	
Nanevitz, J.E., Vance, E.F. & Sorebreny, S.M. (1966)	1963	U.S.	DC-8	20-40,000'	Pilot rpts	Electrical activity	
Steiner, R. (1966)		U.S., Japan Europe	U-2	20-75,000'	11,500 ml	Extensive turb. & strong jet; max. turb. 30-40,000' elev. near jet & large shears	
Vinnichenko, N.K. (1966); Foltz, H.P. (1967) Reiter, E.R. & Foltz, H.P. (1967)	1964-65 1962-66	Russia West U.S.	TU-104, IL-18 Commercial Military	18-40,000'	9000 Pilot rpts	Spectral slopes $< -5/3$ Mountain lee; farther downstream of ridge for lighter intensities; stable layers; $-5/3$ law applied to long wavelengths	
Halvey, R.A. (1967)	1964	Sierra Nev. Mnts (Calif)	U-2	53-60,000'	2 flights	Static stability min.; downstream side of trough; wave amplitude local max.	
Pinus, N.Z., Reiter, E.R. Shur, G.N. & Vinnichenko, N.K. (1967)	1963-65	Russia Australia	TU-104 Canberra	25-35,000'		Unstable gravity waves & Archimedian forces act as sources & sinks of turbulent energy	

### SECTION III

#### TURBULENCE MEASUREMENTS AND THEORIES

The case histories and the statistical studies presented in this report are based directly upon the WU-2 HICAT flight program. From February 1965 to March 1968, a total of 47 hours of clear air turbulence were recorded in flights from bases in California, Massachusetts, Alaska, Hawaii, Puerto Rico, New Zealand, Australia, England, Florida, Panama, Maine, and Louisiana. The flights and measurements derived from the flights from February 1965 to March 1967 are discussed in detail by Crooks, Hoblit and Prophet (2) and this material was available for use in the present study. Portions of the turbulence data from the flights made after March 1967 were also available for use in the present report.

The identification of turbulent cases and the derivation of the relevant in-flight data was directed by Crooks and Hoblit. Because the selection of turbulence samples is of fundamental importance for the present study, the description of the method of selecting a turbulence sample will be summarized here.

The primary airborne data acquisition system is a digital pulse code modulation system. The system accepts both analog and digital data signals from various remote sources in the WU-2 aircraft and processes them into a digital format at the rate of 25 samples per second. The analog data signals are also recorded concurrently in analog form on an oscillogram. Analog signals are received from a gust probe, an inertial navigation system, accelerometers, thermometers, altimeter, and other sensors. The gust probe provides an indication of airspeed and gust forces. The inertial navigation system provides information on aircraft altitude, acceleration, velocity, and horizontal displacement.

The selection of clear air turbulence samples for data processing starts with an edit of the measurements recorded on the oscillogram. Turbulence samples were selected primarily through evaluation of the records of acceleration normal to the fuselage axis. This acceleration could be determined to within 0.01 g. Rapid variations in this acceleration for ten seconds or more, with amplitudes exceeding  $\pm 0.05$  g with occasional excursions of  $\pm 0.10$  g, indicated that the data were worth processing, unless records indicated that the aircraft was in a turn. Small, high-frequency oscillations in the gust probe records normally provided further evidence of the presence of turbulence. Usually, the pilot would have confirmed the presence of turbulence by activating the oscillograph event marker.

Each edited sample was characterized by a subjective description in words in addition to the estimated cg acceleration peak level. In general, the following classification, derived originally from HICAT pilot comments, was observed:

#### Frequency Occurring Peak Acceleration

#### CAT Description

$\pm 0.05$  to  $\pm 0.10$  g

Very Light (VL)

$\pm 0.10$  to  $\pm 0.25$  g

Light (L)

$\pm 0.25$  to  $\pm 0.50$  g

Moderate (M)

$\pm 0.50$  to  $\pm 0.75$  g

Severe (S)

$\pm 0.75$  or greater

Extreme (X)

These objective criteria were not complete enough to eliminate entirely some subjective judgments. However, the limits of the objective criteria were sufficiently broad that the role of subjective judgment in the selection of turbulence cases was relatively minor. For the purposes of this report the turbulence cases presented by Crooks, Hoblit, and Prophet (2) were accepted without modification.

#### GRAPHS AND MAPS

Once the specific times of turbulence were selected, records from all the various special instruments were processed by techniques given by Crooks et al. (2). The approximately 29 hours of turbulence found from February 1965 to March 1967 required processing 100 million data points. The end products of this data processing were time histories and power spectral densities. In addition, flight track maps were prepared.

The time histories were presented in a graphical form with 12 1/2 points per second along the time axis. Vertical, lateral, and longitudinal gust velocities, derived gust velocity, corrected altitude, ambient air temperature, true airspeed, roll angle, cg longitudinal, lateral and normal acceleration were all plotted as a function of time. Including selected time histories from the newer series of WU-2 flights a total of 322 time histories covering approximately 1500 minutes of turbulence were available at the time this report was written. A sample of the time histories is given in Figure 1a and b. Not all the time histories are complete because, at times, one or more of the instruments or signal recording devices did not operate satisfactorily. Thus, the number of hours of prepared time histories is less than the number of hours of turbulence.

Graphs and a detailed discussion of the power spectra of the vertical, lateral, and longitudinal gust velocity components were also presented by Crooks, Hoblit, and Prophet (2). Some of the graphs of the power spectra for the latest series of WU-2 flights were also available for use in the present study. Figure 2 is a sample of the power spectra used in this study. The problems associated with classifying the spectra and determining relationships between spectral types and meteorological and terrain conditions are discussed later in this section.

Flight track maps for the present study were prepared by two methods. In some cases they were prepared directly through interpretation of the records obtained from the LN-3 navigational system. A description of the instruments and the method of interpreting the records of the instrument signals is given by Crooks, Hoblit,

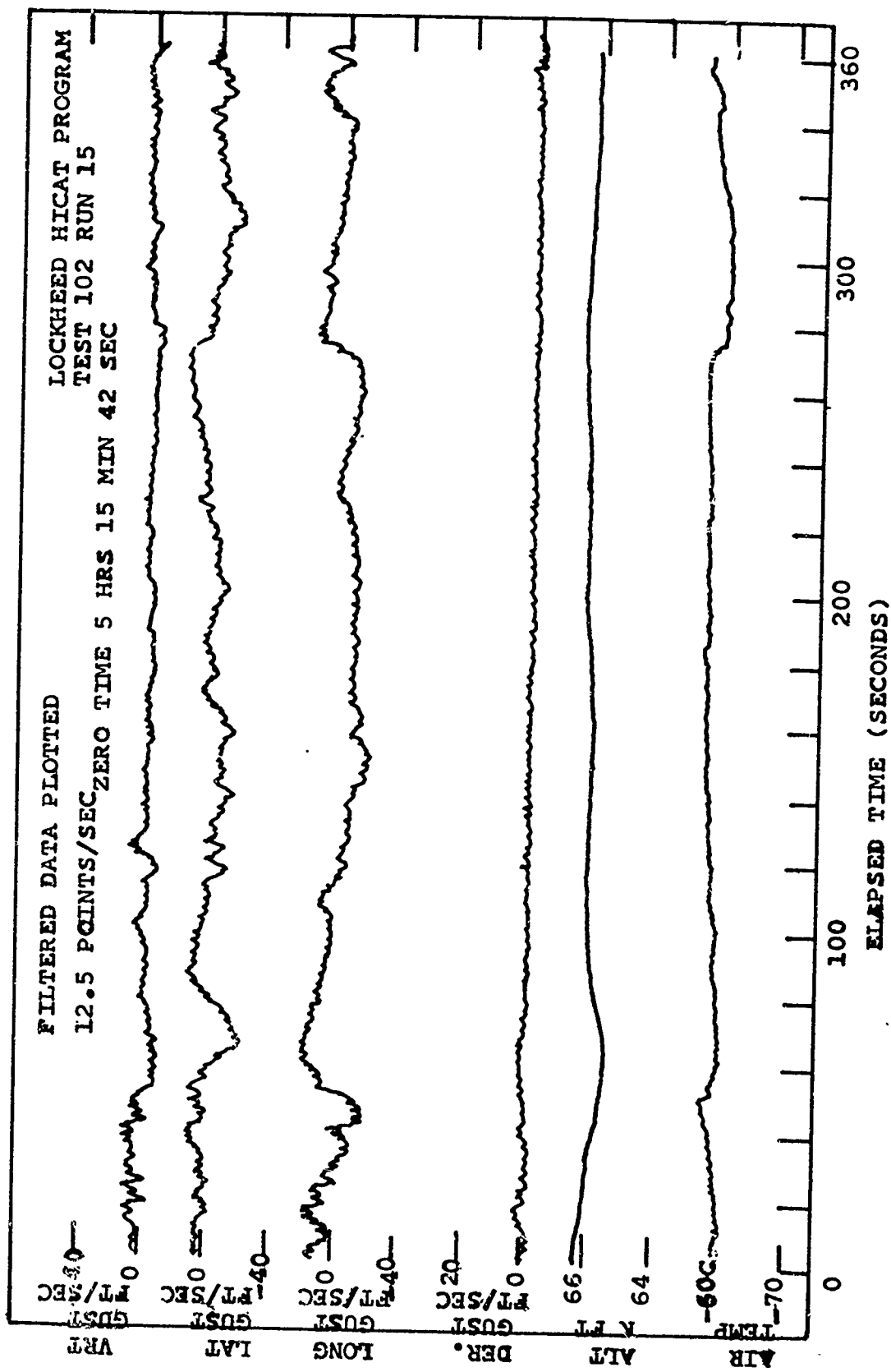


Figure 1a. Time Histories. Gust Velocities, Altitude, and Air Temperature

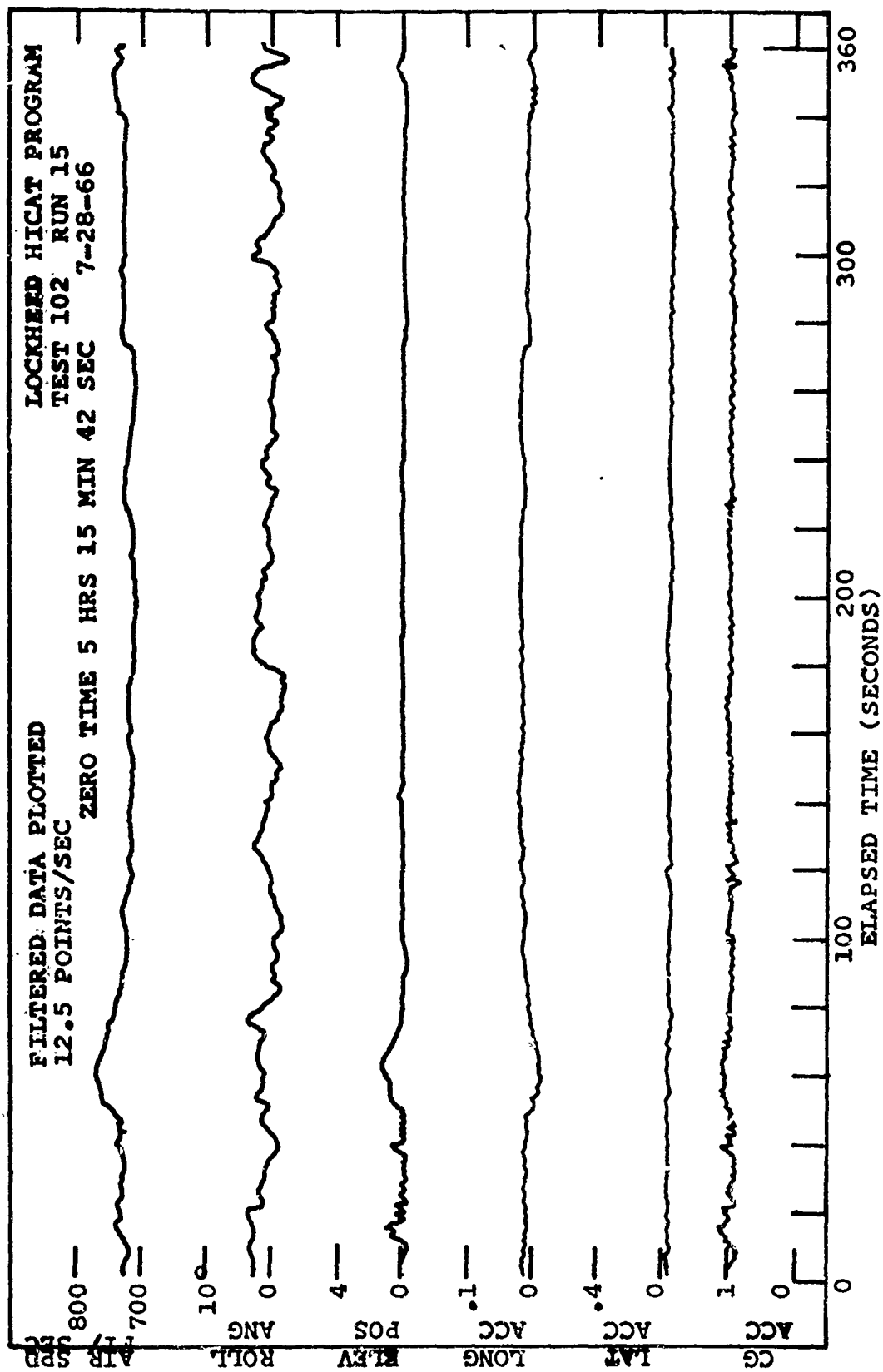


Figure 1b. Time Histories. Air Speed, Roll Angle, Elevator Position, Longitudinal Acceleration, Lateral Acceleration, Normal Acceleration

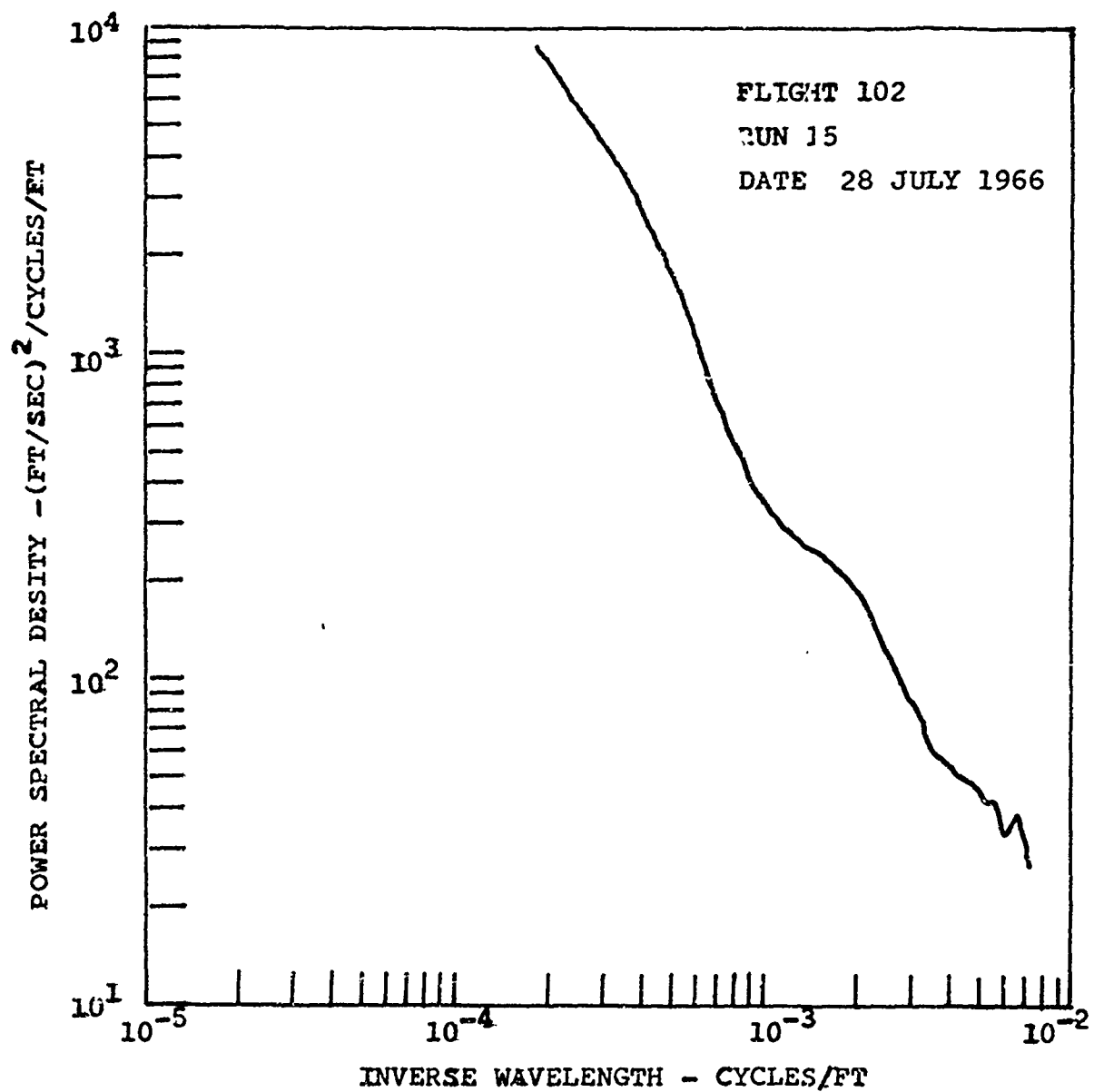


Figure 2. Power Spectrum of Vertical Gusts. Flight 102 Run 15

and Prophet (2). Flight track maps were based upon pilot reports when the LN-3 equipment did not operate as planned, or its data seemed unreliable. Samples of flight track maps are presented in Figure 3a and b.

#### REVISED TURBULENCE MODEL

Analysis of turbulence measurements requires a realistic mathematical model for the turbulence. For the present work, the model used for the previous study, Hildreth, Court, and Abrahms, (4) was revised after analysis of many such models.

Several decades of work on theoretical interpretation of experimental wind tunnel data led, by the late 1950's, to the general adoption in aeronautical engineering of an expression for the spectrum of vertical gusts:

$$\bar{\phi}_V(\Omega) = (\sigma_V^2 L/\pi) \left[ 1 + 3 (\Omega L)^2 \right] \left[ 1 + (\Omega L)^2 \right]^{-2} \quad (1)$$

Here  $\bar{\phi}_V(\Omega)$  is the power spectral density at frequency  $\Omega$  (radians per foot),  $\sigma_V^2$  is the variance of the vertical motion, or mean square gust velocity, and  $L$  is the longitudinal scale of turbulence, variously interpreted as the horizontal distance at which the correlation between horizontal speeds vanishes, or the "effective gust size".

This turbulence model assumed the turbulence to be isotropic and the correlation between the longitudinal wind components (in the direction of flow) to decrease exponentially with separation. It was used in many studies of aircraft response to atmospheric turbulence, and was adopted by Hildreth, Court, and Abrahms (4) for the analysis of high-altitude turbulence spectra obtained by Lockheed in 1963-64, in the immediate precursor of the studies reported here.

However, this isotropic-exponential model has certain theoretical drawbacks. Most important for its application to aircraft design, it provides that the spectral power at high frequencies varies inversely according to the square of the frequency. But at these frequencies the well-established similarity theory requires that the variation be according to the  $-5/3$ , not  $-2$  power. Hence von Karman (6) abandoned the exponential decrease of correlation with separation. "For the time being" he proposed "an interpolation formula" for isotropic turbulence which would satisfy the similarity hypothesis.

As developed in detail by Houbolt, Steiner, and Pratt (7) in Appendix B of their significant report, von Karman's "Interpolation formula" leads to

$$\bar{\phi}_V(\Omega) = (\sigma_V^2 L/\pi) \left[ 1 + 8/3 (1.339 \Omega L)^2 \right] \left[ 1 + (1.339 \Omega L)^2 \right]^{-11/6} \quad (2)$$

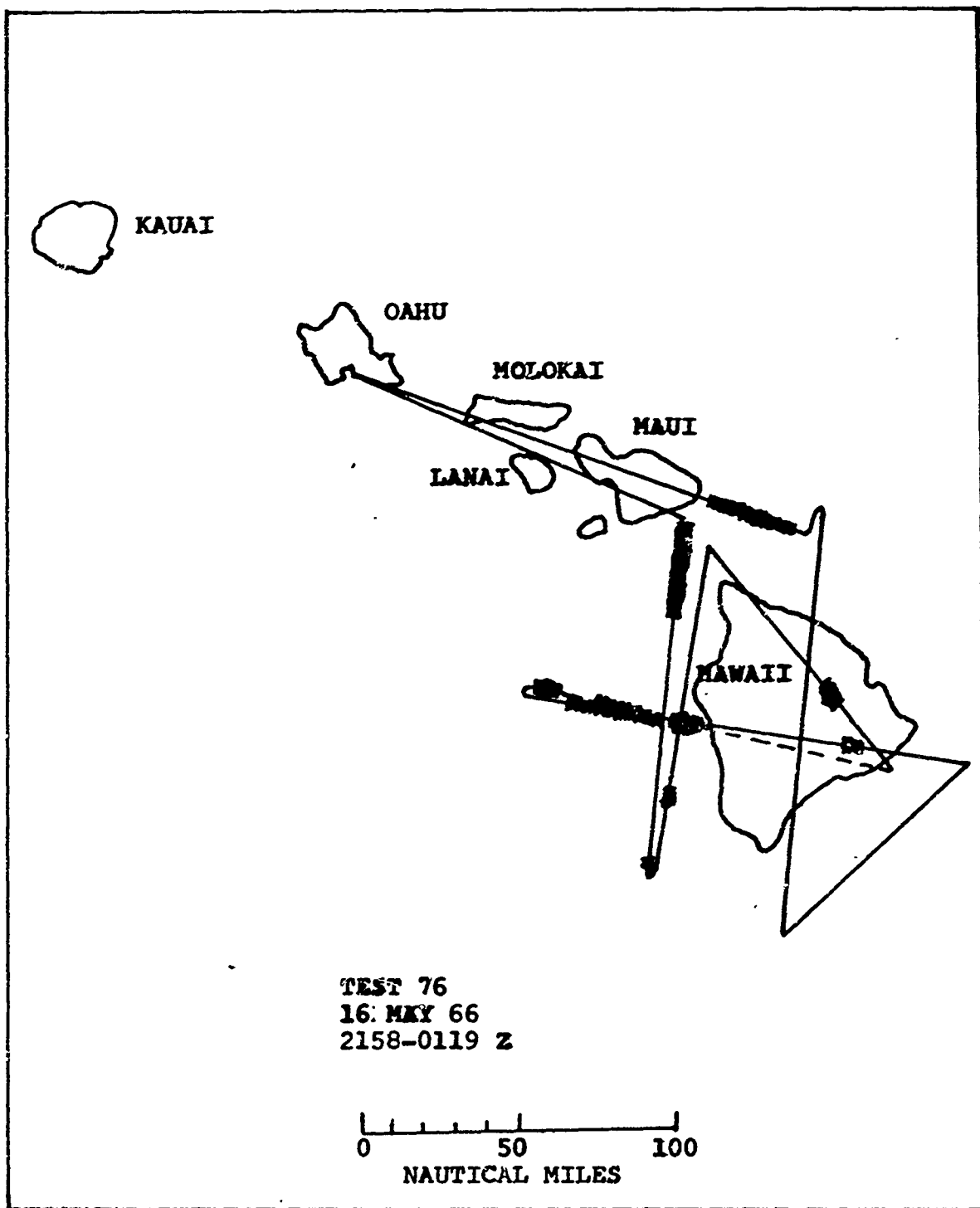


Figure 3a. Flight Track Map Over Hawaii, Flight 76.

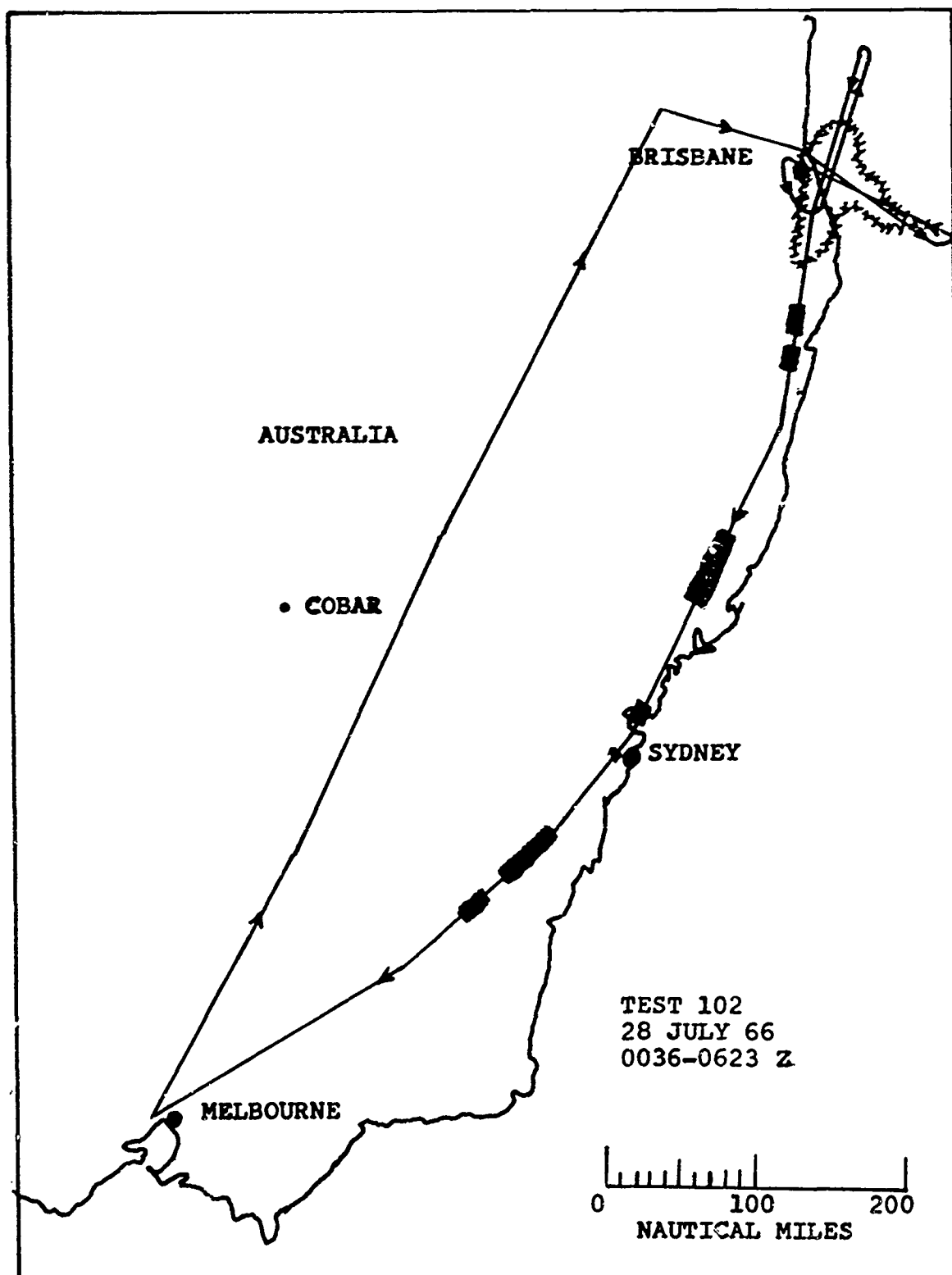


Figure 3b. Flight Track Map Over Australia. Flight 102

Thus the final term has an exponent of  $-11/6$  instead of  $-2$ , the coefficient in the second term is  $8/3$  instead of  $3$ , and a numerical constant, involving gamma functions, is introduced:

$$\Gamma(\frac{1}{3}) \Gamma(\frac{5}{6}) / \Gamma(\frac{1}{2}) = 0.339...$$

Extensive comparisons of these two formulas for the power spectra density of vertical gusts, by Rhyne and Steiner (8), and by others, led Houbolt, Steiner, and Pratt to conclude that the von Karman representation "best fits these data".

Consequently, this revised model has also been adopted for the analysis of atmospheric turbulence between 50,000 and 80,000 feet, and for the data obtained in the experimental flight program. However, the proper value of the scale length,  $L$ , in Eq. (2) requires investigation.

### Scale Length

Of greater interest, both theoretically and practically, than the absolute power density spectrum of Eq. (1) and (2) is the relative density,  $\hat{\epsilon}_w(\Omega) \sigma_w^{-2}$ , obtained by dividing both sides by the total variance of vertical gusts. This relative spectral density depends only on the longitudinal scale length,  $L$ , defined as

$$L = L_u = \int_0^{\infty} \left[ \overline{(u_x u_{x+k})} / \overline{(u_x^2)} \right] dk \quad (3)$$

the integral over horizontal distance ( $x$ ) of the correlation between simultaneous horizontal velocities at points separated horizontally by a distance  $k$ . This correlation decreases, more or less exponentially, with the separation  $k$ , and becomes essentially zero at separations greater than some value  $k_0$ . Hence the integral in Eq. (3) need be only from  $0$  to  $k_0$ , rather than to  $\infty$ .

However, the correlation can be computed only up to a maximum separation  $k^*$ , which must be much less than the total distance over which measurements are available, and usually  $k^* \ll k_0$ . Hence the integral cannot be computed from  $0$  to  $k_0$ , but instead must be truncated at  $k^*$ , for which the corresponding lowest observable frequency is  $\Omega^*$ .

In practice,  $L$  is evaluated not from the correlation, but by solving the spectral density function, Eq. (2), to yield, Rhyne and Steiner, (8)

$$L = 0.692 (\sigma_v / \sigma_v^*)^3 (\Omega_1^{-2/3} - \Omega_2^{-2/3})^{3/2} \quad (4)$$

where  $\sigma_v^2$  is the variance of vertical motions at all frequencies and  $\sigma_v^2 *$  the variance over the observable region, assuming that almost all the gust energy is in the observed region, and  $\Omega_1$  and  $\Omega_2$  are, respectively, the low and high frequency ends of the truncated spectrum.

In addition to the interpretations as maximum distance over which correlation is appreciable, and as maximum effective gust size, the scale length  $L$  has another application in practice. Logarithmic differentiation of the expression for the relative spectral density (details are given in Appendix I) shows that the spectral density becomes constant with respect to  $\Omega$  at

$$L_0 = (1/2.187)\Omega = 0.0728\lambda \quad (5)$$

where  $\lambda = 2\pi/\Omega$  is the wavelength, in feet. Thus, the scale length  $L$  should be about 7.3 percent of the wavelength at which the spectrum "levels off". (In contrast, the isotropic-exponential model used previously, Eq. (1), yields a criterion of  $L_0 = 1/1.752\Omega = 0.0919\lambda$ .) Hence, on plots of relative spectral density against frequency (or wavelength), values of  $L$  may be estimated, although some extrapolation may be required. Such plots, for various values of  $L$ , are shown in Figure 4.

Rhine and Steiner (8) found values of  $L$  from 2,000 to "as large as 5,000 feet for severe-storm turbulence above 25,000 feet in altitude". Reexamination of some clear-air turbulence data by Houbolt et al. (9) "yielded values of  $L$  of approximately 3,000 to 6,000 feet for the different runs and methods of evaluation". Hence they concluded "that  $L$  is fairly large, apparently of the order of 5,000 feet".

However, Hoblit et al. (9), from study of responses of various subsonic aircraft, accepted 2,500 feet as the best estimate of scale length for stratospheric turbulence. Summarizing this work, Stauffer, Hildreth, and Crooks (10) pointed out that, with realistic values for root-mean-square gusts and for aircraft operation, the maximum RMS accelerations for supersonic flight increased markedly between assumed scale lengths of 1,000 and 2,500 feet, but only negligibly when the length was further increased to 5,000 feet. "SST design, based on a turbulence scale of 2,500 feet," they concluded, "will not be significantly affected if additional research indicates a higher scale to be in order."

Reanalysis of data from the first HICAT study, Hildreth and Crooks (11), yielded spectral curves within the envelope of 384 turbulence spectra from B-66 flights at low levels, and overlapping the envelope of 67 spectra from 67 B-66 storm penetrations, as well as the envelope of 10 TOPCAT spectra, Reiter and Burns (12). In all the reanalyzed HICAT spectra, the scale of turbulence apparently was slightly more than 2,500 feet.

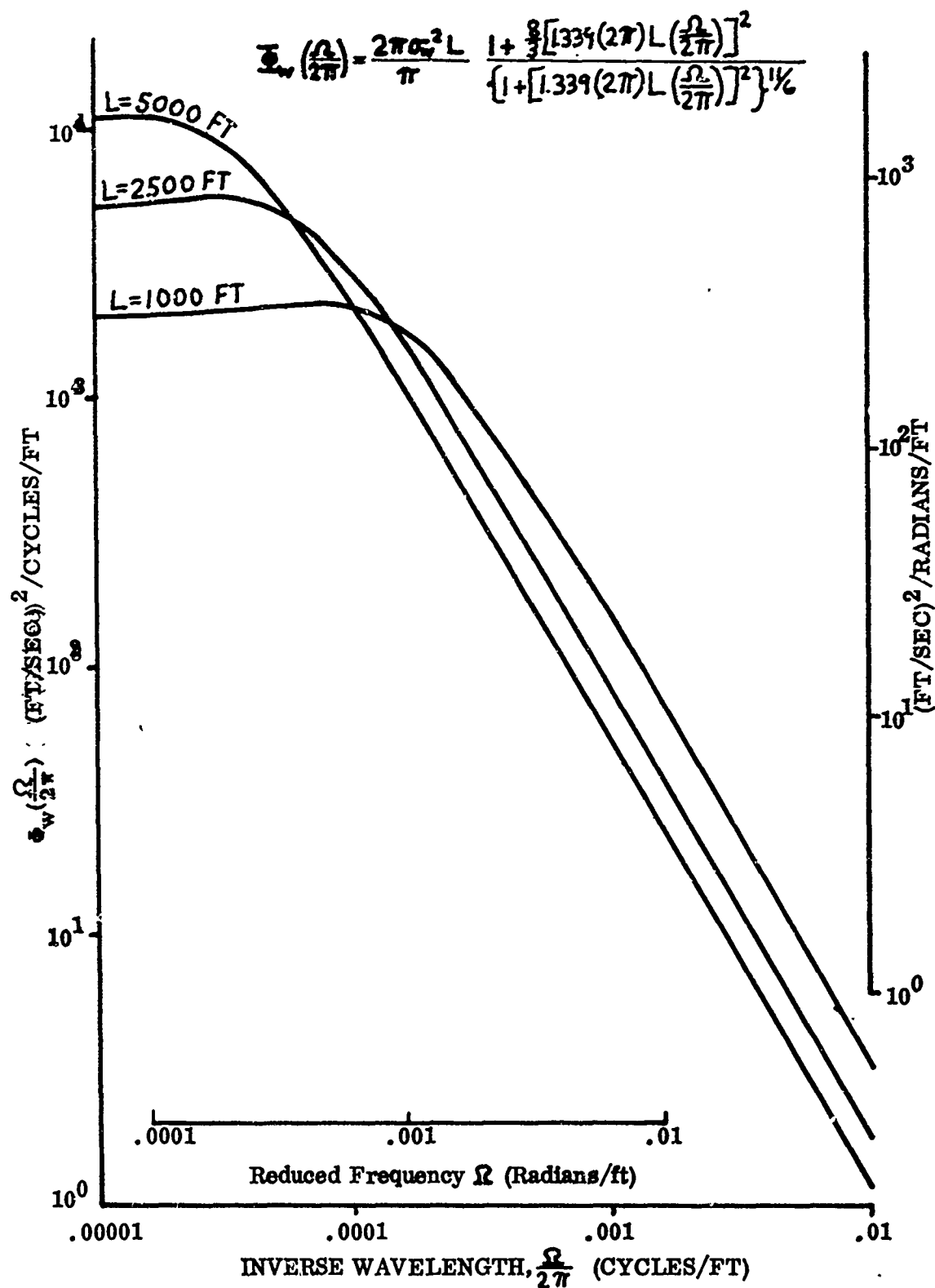


Figure 4. Relative Spectral Density as Function of Longitudinal Scale of Turbulence (L)

### Dynamic Considerations

The scale length,  $L$ , also is related to other atmospheric properties. Perturbation theory indicates that the large scale static stability, wind shear, and the mean wind speed of an atmospheric layer are the important parameters that determine the character of wave perturbations (undulance) in that layer when it is disturbed at its boundaries. These disturbances may result from low level air flow over the terrain, irregular distribution of heat sources, (convection in particular), as well as disturbances arising from dynamic instability. In general, the short waves are external waves which damp out quickly with height, have predominant vertical motion, and may be unstable if the wind profile is right. Long waves are internal waves which are generally stable, have predominantly horizontal motion, and propagate energy in the vertical.

The critical wavelength region separating the short external waves from the longer, internal waves appears to be determined principally by the wind speed near the boundary and the static stability of the layer. For a given wind speed, the greater the static stability the shorter is the critical wavelength. For a given static stability the greater the wind speed the longer the critical wavelength. Disturbances with frequencies or wavelengths near critical values may cause development of one or more resonant waves, with large vertical amplitudes, extending through deep layers.

Generally the static stability and the wind combine to make the critical wavelength in the stratosphere on the order of 1 km. However, near the cold side of a jet stream, where the static stability is generally less but the wind speed still high, the critical wavelength may be as great as a 100 km. To state the case differently, the greater the critical wavelength the greater the probability of a deep layer of rough air with a long scale length and greater rms gust intensity.

On the other hand, in the troposphere the critical wavelength generally is larger (10 - 50 km) than in the stratosphere. Hence any resonant mountain waves affecting the stratosphere would most likely be confined to thin layers, and cause horizontal internal waves to develop, except possibly over and on the cold side of jet streams, as indicated above. The longer external waves would also be confined to thin stratospheric layers but could cause internal waves to develop. The shorter external waves in the troposphere could excite external waves in the stratosphere, but both data and theory indicate that the energy in these tropospheric external waves would probably be negligible at the tropopause except when the mountains are high, the tropopause low and the wind speed large.

Disturbances with wavelengths longer than those critical in the troposphere should propagate energy upward. Theoretical estimates, Eliassen and Palm (13), indicate that waves shorter than about 20 km (usually external waves) are effectively reflected by the upper troposphere. Short internal waves (< 50 km) have approximately up to three fourths of the energy reflected while longer waves have progressively less energy reflected in the upper troposphere.

Disturbances from low level heat sources would have similar scale effects on the stratosphere. The importance of convection in perturbing stable layers has been investigated by Townsend (14). As the scale of thermals affecting the stratosphere

is on the order of 1 to 10 km, external waves and resonant waves could be excited as well as internal waves.

These considerations show that the important meteorological parameters are:

- (a) The critical wavelength in the stratosphere
- (b) The tropospheric critical wavelength for terrain effects, and
- (c) A measure of convective instability (such as the Showalter Index).

The geophysical parameters include a measure of the terrain roughness, as well as a height-to-width ratio for determining resonant waves. For heating effects, a measure of the irregularity of the surface vegetation character should be important. All of these eventually may provide a direct means for estimating the scale length,  $L$ , and other characteristics of a high altitude turbulence model. But until they have been investigated in detail, the most useful approach to analysis of high altitude spectra appears to be the application of the von Karman model, Eq. (2), assuming  $L = 2,500$  feet.

#### CLASSIFICATION OF SPECTRA OF GUST VELOCITIES

In the inertial subrange the power spectral density should depend on the frequency  $\Omega$  and the energy dissipation rate  $\epsilon$  according to

$$\Phi(\Omega) = a \epsilon^{2/3} \Omega^{-p} \quad (6)$$

where  $a$  is a universal constant and  $p$  is the slope of the power spectral density curve. Several authors, e.g., Reiter and Burns (15); Pinus, Reiter, Shur, and Vinnichenko (16), have obtained an experimental value of  $p = -5/3$  in the inertial subrange in agreement with that derived theoretically by Komogorov (17). Other values for  $p$  are of course possible, such as  $-2$ , Eq. (1), depending on the assumptions made in deriving an expression for  $\Phi(\Omega)$ . The HICAT spectra show significant deviations from both the  $-5/3$  and  $-2$  laws.

#### Spectral Slopes

Energy spectra derived from time histories of gust velocities are commonly presented by plotting the power spectral density divided by the inverse wavelength in units of  $(\text{ft/sec})^2/\text{cycles/ft}$  as a function of the inverse wavelength in cycles/ft (Figure 2). However, the spectra available from HICAT flights 54 through 265 have been normalized with respect to the energy by dividing the ordinate by the variance of the vertical gust velocity for wavelengths less than 2000 ft. The ordinate is hence no longer the same measure of turbulent energy as before and is in units of  $(\text{cycles/ft})^{-1}$ . The normalization process has effectively reduced to a minimum the differences in energy for  $\lambda < 2000$  ft and facilitated the comparison of spectral shapes, especially for  $\lambda > 2000$  ft. The 2000 ft cutoff was selected in order that all available spectra could be included.

Following normalization, spectra for the vertical component of the gust velocity ( $U_V$ ) were classified into several groupings according to shape. Only those cases were considered where  $RMS > 0.63$  because pilot-induced control movements or instrument malfunctions affect the spectra shapes appreciably at lower variances.

Figures 5 through 7 present the  $U_V$  spectra for various categories number A through F\*. The  $p = -5/3$  and  $p = -2$  lines have been entered for comparison purposes. The solid curved lines are composites of the several cases.

The distribution of spectra by classes is:

CLASS	A	B	C	D	E	E*	F	F*	Unclassified
NUMBER	21	8	13	15	30	10	17	3	9

In general, the average slope of the spectra increases with class from A to F\*. There are, however, singularities in the spectral shapes which will be described in more detail.

The spectrum curve for classes A and D has a value for  $p$  much less than  $-5/3$  for  $\lambda < 1000$  and  $2000$  ft, respectively. Class C spectra, in addition, has  $p < -5/3$  in the approximate range  $1000 \text{ ft} > \lambda > 150 \text{ ft}$ ; E and F spectral slopes are less than  $-5/3$  for  $\lambda < 2000$  ft. Approximately 80% of the classified spectra deviate towards shallowed slopes than  $-5/3$  for  $\lambda < 1000$  ft, contrary to the results of others (Pinus, Reiter, Shur, and Vinnichenko, (16); Reiter and Burns, (13), for flights at commercial jet altitudes (i.e., below 40,000 ft).

Approximately 70% of the spectra, including all the classes with the exception of D, F, and F\*, show a tendency towards constant or decreasing  $p$  with increasing  $\lambda$ . B spectra especially show a flattening out at longer wavelengths. Some portions of the E\*, F, and F\* curves, 43% of the total classified spectra, possess  $p \geq 2$  for  $\lambda > 900$  ft. The long wave portions of the spectra for runs 102 (16), 114 (14), and 219 (3) in the F\* category have  $-3$  slopes which agrees with the findings of Shur (1962).

A total of 9 individual cases vary substantially from the categories A through F\* and are grouped separately (Figure 8). Spectra from flight 100, run 16 and flight 257, run 13 (Figure 8a) fall within the C class for  $\lambda > 800$  ft but deviate from this at small  $\lambda$ . Flight 258, run 8, 10 and flight 264, run 14 (Figure 8b) are characteristic of the B class at shorter  $\lambda$  and E or E\* at  $\lambda > 900$  ft. The remaining four cases (Figure 8c) do not appear to fall into any basic category or combination of categories.

The spectra illustrated in Figure 9a provide an example that indicates that flight orientation with respect to the wind has no significant effect upon the shape of spectral curve. The runs were only 6 minutes apart and over the same course except run 107 (9) was into the wind and 107 (10) with the wind. The wind speed was around 65 KTS at the time.

Figure 9b shows how there can be but small variations in the spectral shapes for several cases over a wide range of distance. Eleven samples were taken in a 600 mile path along the lee side of the Great Dividing Range in Southeastern Australia.

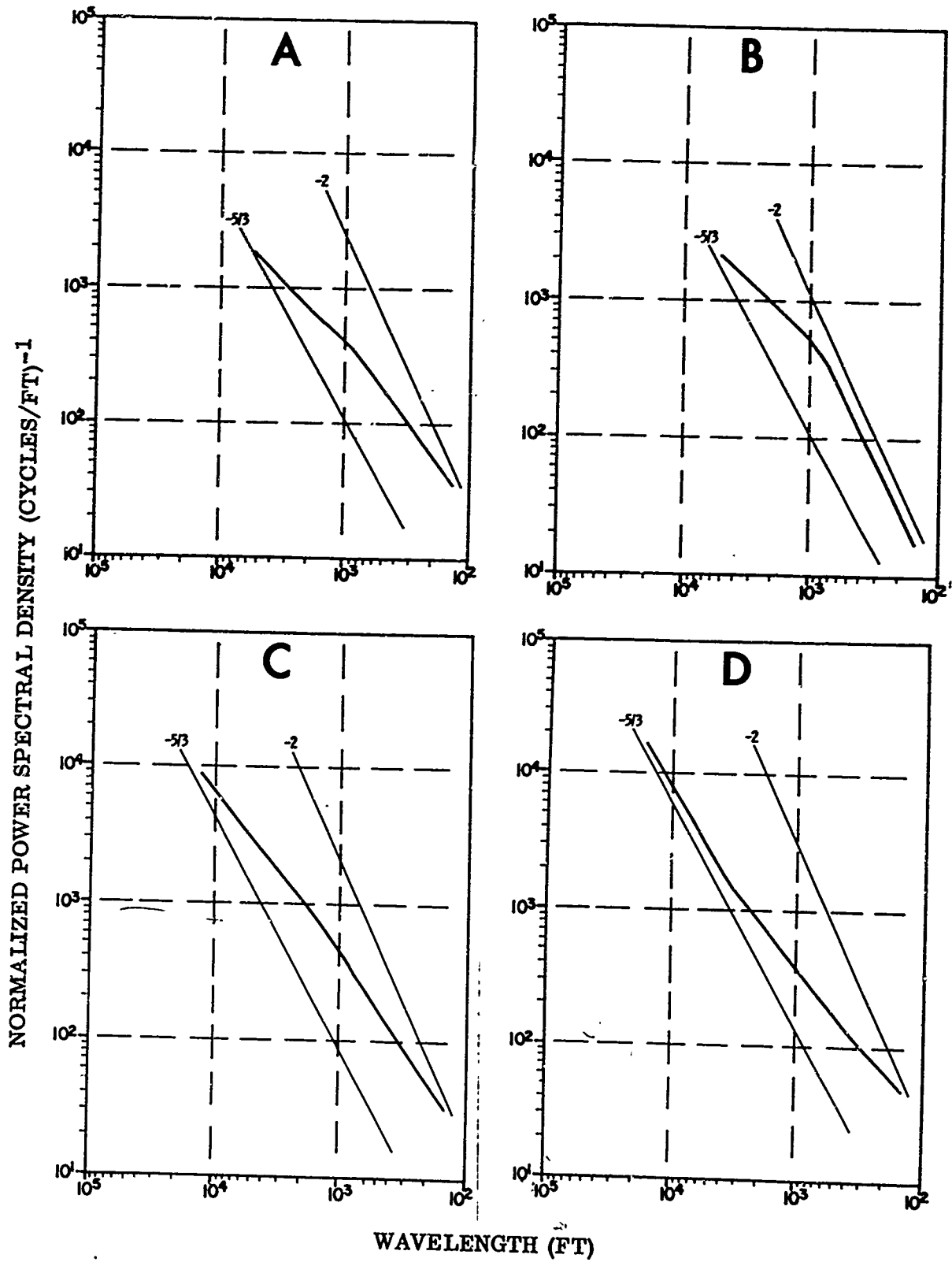


Figure 5.  $U_V$  Normalized Power Spectral Classes A Through D

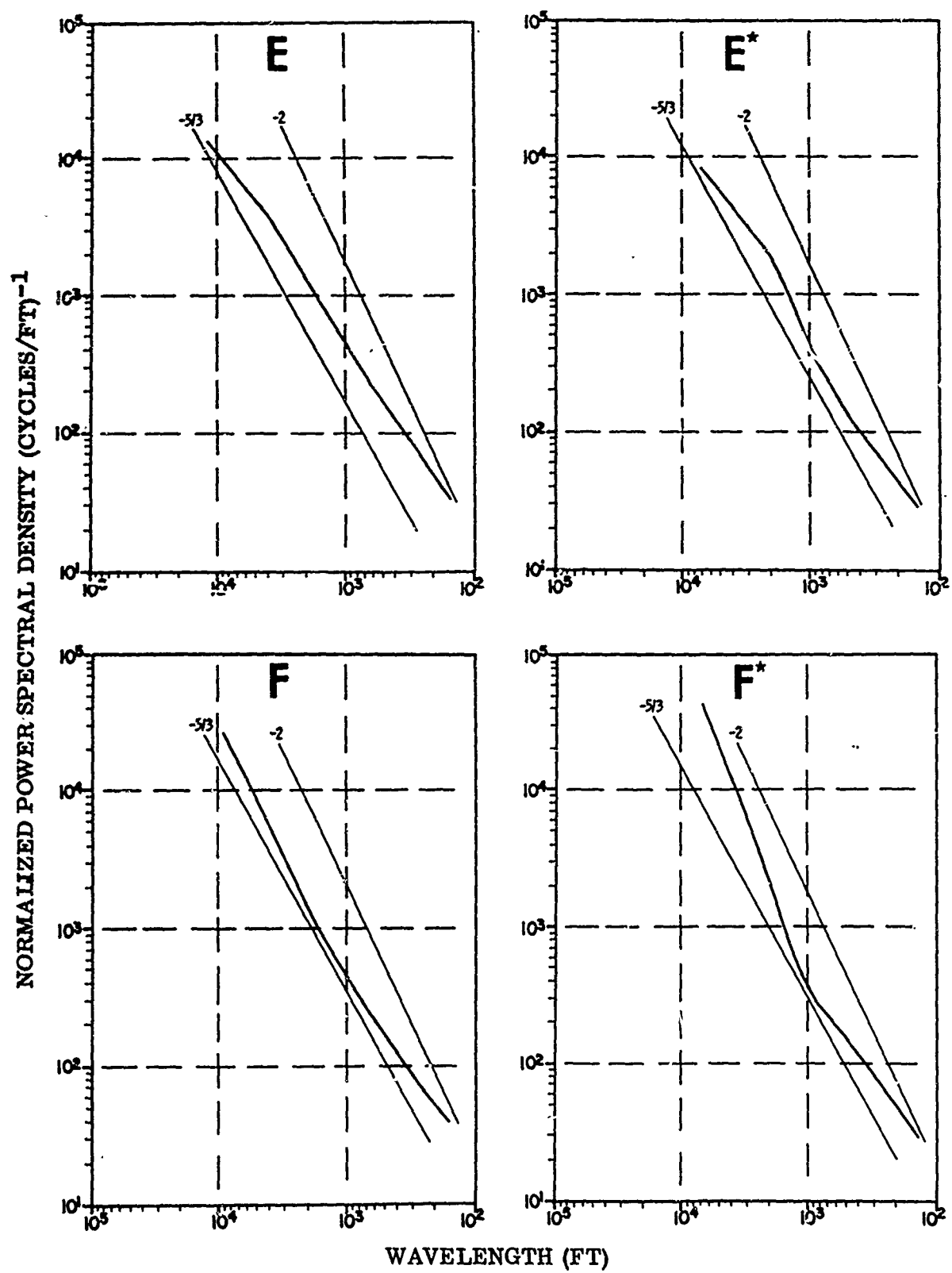


Figure 6.  $U_V$  Normalized Power Spectral Classes E Through F\*

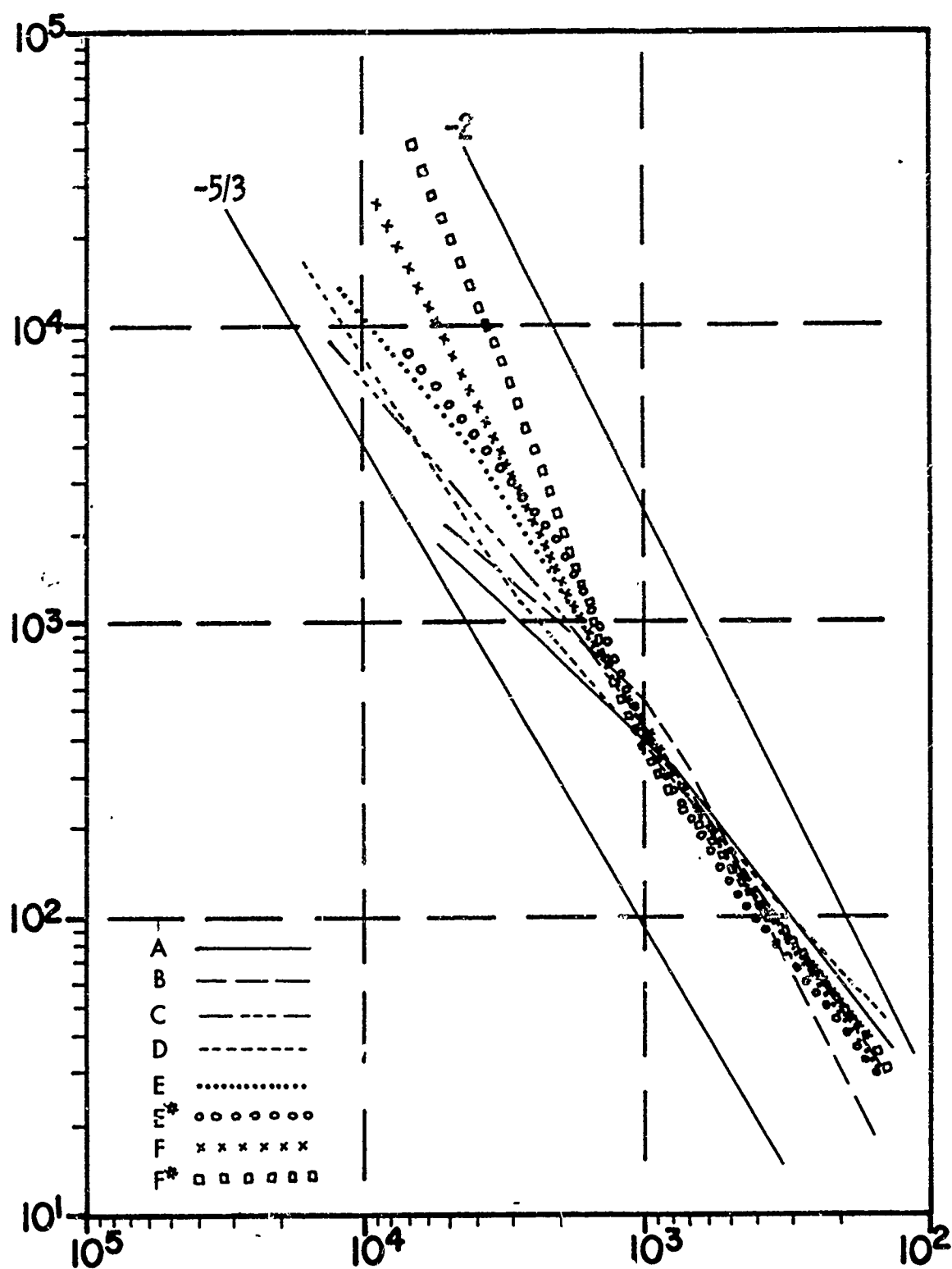


Figure 7. Composite of  $U_V$  Normalized Power Spectral Cassettes A Through F\*

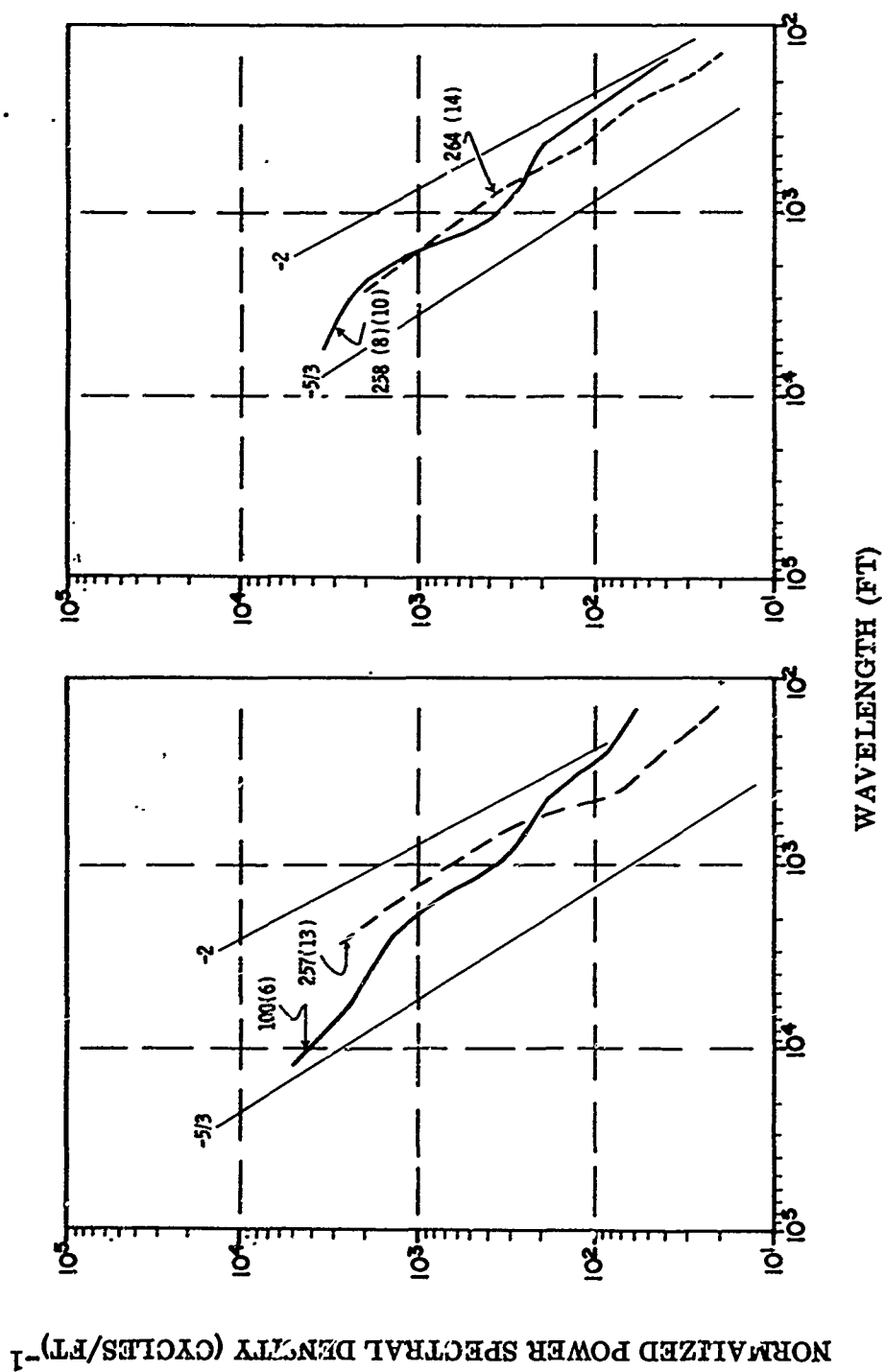


Figure 8a, Unclassified  $U_V$  Normalized Power Spectral Density

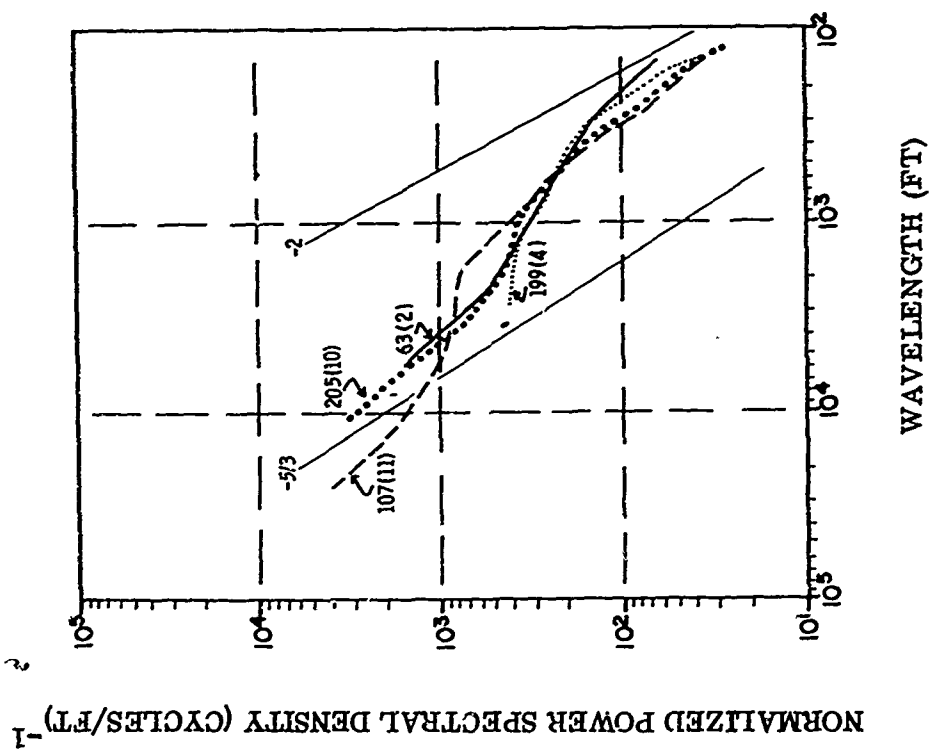


Figure 8b. Unclassified U<sub>V</sub> Normalized Power Spectral Density

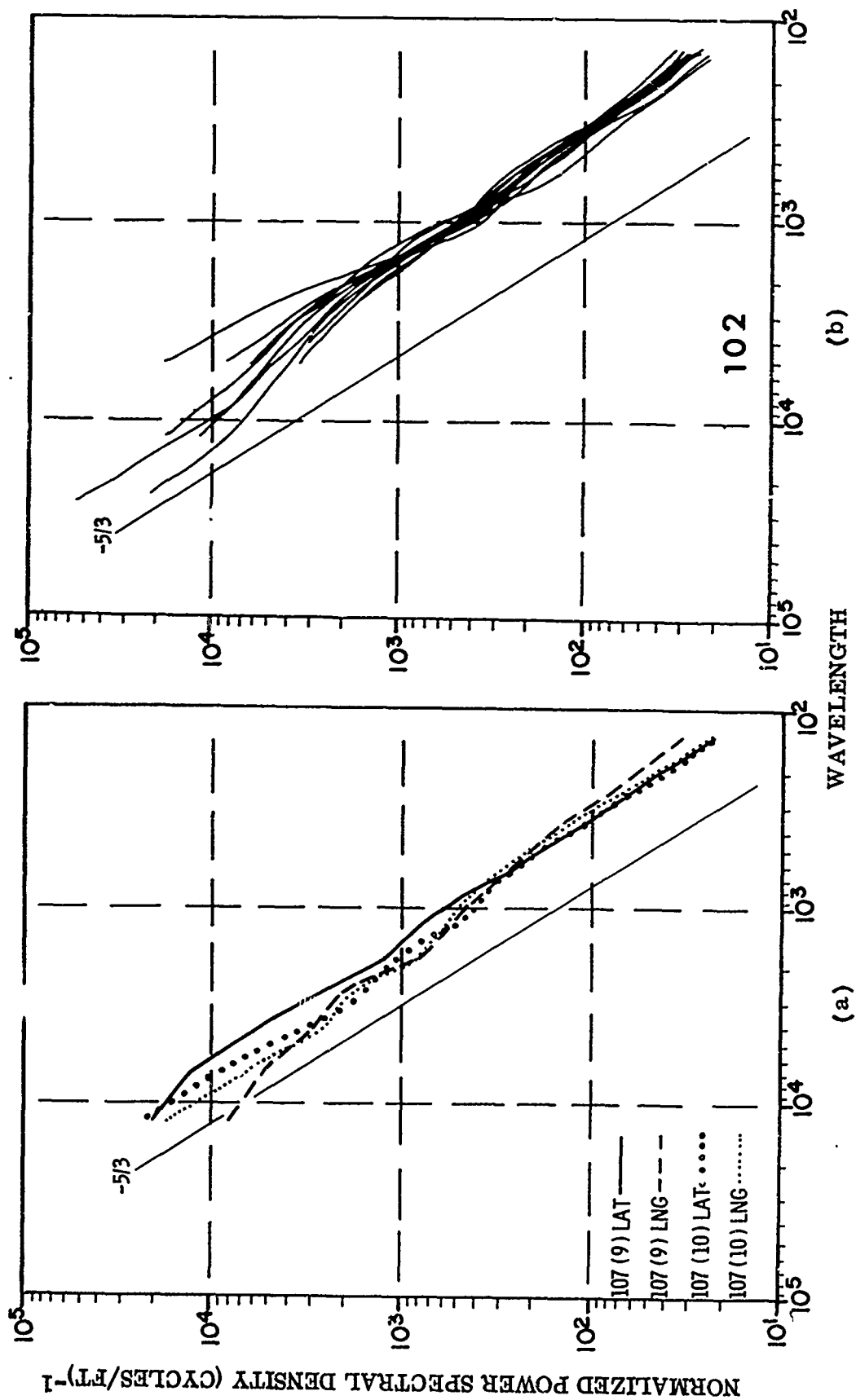


Figure 9. Normalized Power Spectra for Flight 107, Runs 9 and 10 ( $U_F$ ,  $U_L$ ) and Flight 102 ( $U_V$ )

The lateral ( $U_L$ ) and longitudinal ( $U_F$ ) gust velocity components show a tendency towards less variation in their spectral shapes and are not considered in detail. They appear to possess, on the average, slightly steeper slopes than the  $U_V$  spectra. A comparison between the three components is shown for two flights in Figures 10a-b. Flight 76 is over water, near the Hawaiian Islands, flight 114 is on the lee side of the Sierra Nevada range in California-Nevada. The spectra agree in shape reasonably well for both cases, following the  $-5/3$  law.

### Terrain

From a total of 126  $U_V$  spectra, 15% were over water, 30% over relatively flat plains, and 55% over or reasonably close to mountainous terrain. The distribution of classes by terrain (Table II) shows

TABLE II  
NUMBER OF CASES FOR EACH  $U_V$  SPECTRA AND TERRAIN  
CLASSIFICATION FOR FLIGHTS 54-265 (126 CASES)

Class	A	B	C	D	E	E*	F	F*	Unclassified	Total
Water	4	1	2	2	4	2	2	1	1	19
Flatland	11	3	7	9	2	0	3	0	3	38
Mountain	6	4	4	4	24	8	12	2	5	69

Grouping classes A through D into one category and E through F\* into a second category, the distribution by terrain shows 86% of the flatland spectra in the A through D class and 72% of the mountain spectra in the E through F\* class. The water spectra are divided equally between the two classes. However, the sample size in this case is small.

### Meteorological Conditions Associated with Spectral Classes

The analysis of the meteorological conditions associated with the various spectral classes is limited to flights 54 to 164 because of incomplete data analysis for later flights. For these flights, investigation indicated that there was no significant relationship between the spectral classes and various categories of stability, wind shear, jet strength, Richardson number, and proximity to thunderstorms. No conclusive evidence could be drawn from the data. The reasons for this are as follows:

1. The original sample size is too small.
2. Radiosonde and rawinsonde data are lacking in many cases at the heights flown.
3. It is difficult to resolve scale size differences between the meteorological variables and turbulence samples.
4. There appears to be an overlap between the effect of terrain and of various meteorological conditions on the spectral shapes.

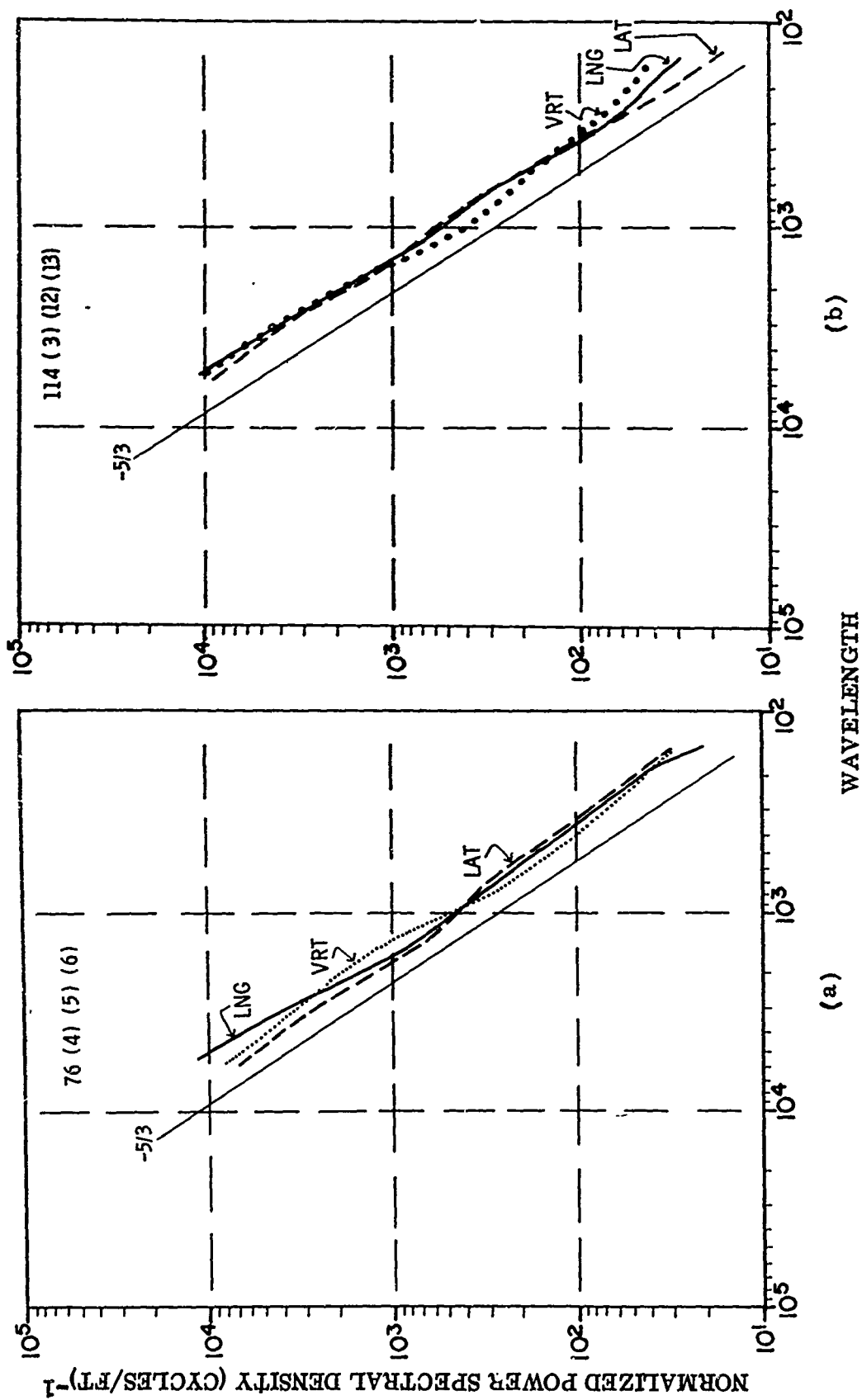


Figure 10.  $U_F$ ,  $U_L$ , and  $U_V$  Normalized Power Spectra for Flight 76, Runs 4, 5, and 6 and Flight 114, Runs 3, 13, and 14

5. Turbulence samples are limited in their geographical extent. Also, the method of pattern flying has resulted in several turbulence samples for very few types of synoptic situations.
6. An individual spectrum represents an average of the eddy conditions over the length of the run and its shape varies depending on the time period selected for the run. Consequently, spectra derived from data obtained within an area associated with a specific synoptic situation can exhibit diverse shapes.

## SECTION IV

### UPPER AIR DATA

Two principal sources of meteorological data were used in the present study. One source was the records of the ambient temperature presented in the time histories for the WU-2 flights. In these time histories the ambient temperature is shown as a function of time by 12.5 points for each second along the time axis. The response of the thermometer was such that temperature variations slower than one cycle per second could be followed. The second source of meteorological information was the twice daily (once daily in Australia and New Zealand) temperature, pressure and wind measurements reported by the various national meteorological organizations. The number of observations made per unit area and the type of instruments used varied from one HICAT search area to another. Specifically, the areas around the Hawaiian Islands and around the Panama Canal Zone have relatively few upper air observations at altitudes of 40,000 to 70,000 ft. In general, the national meteorological organizations make their observations of the upper atmosphere near 00Z and 12Z times. The time and space interval between the routine meteorological observations and the turbulence encountered by the WU-2 aircraft varied significantly. Only rarely was high altitude turbulence reported over a meteorological station within an hour of the measurement made by an instrument carried aloft by a balloon.

Figures 11-17 illustrates the relative numbers and locations of the meteorological stations at which temperatures, pressures, and winds are measured at WU-2 flight levels for each of the HICAT search areas.

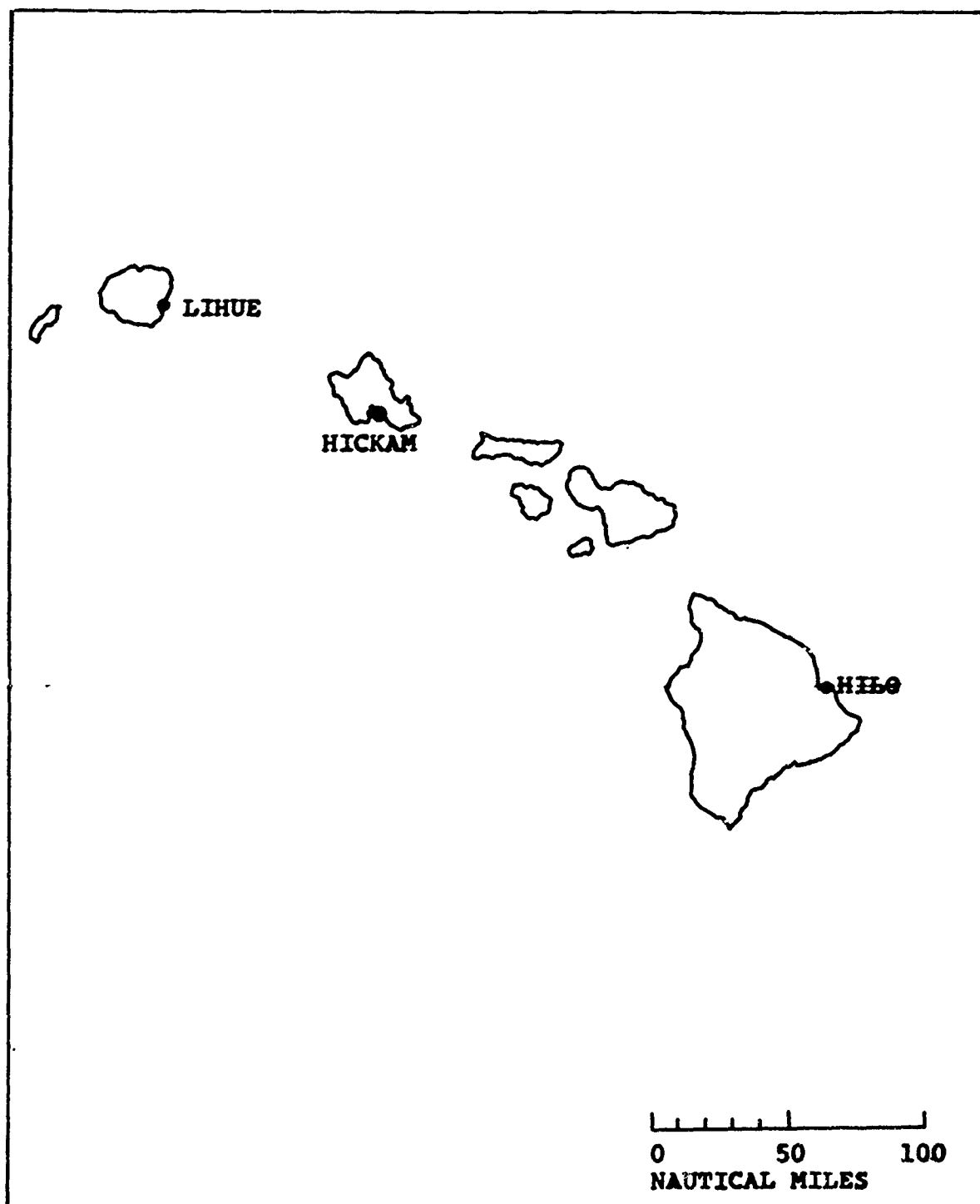


Figure 11. Upper Air Stations Locations. Hawaii

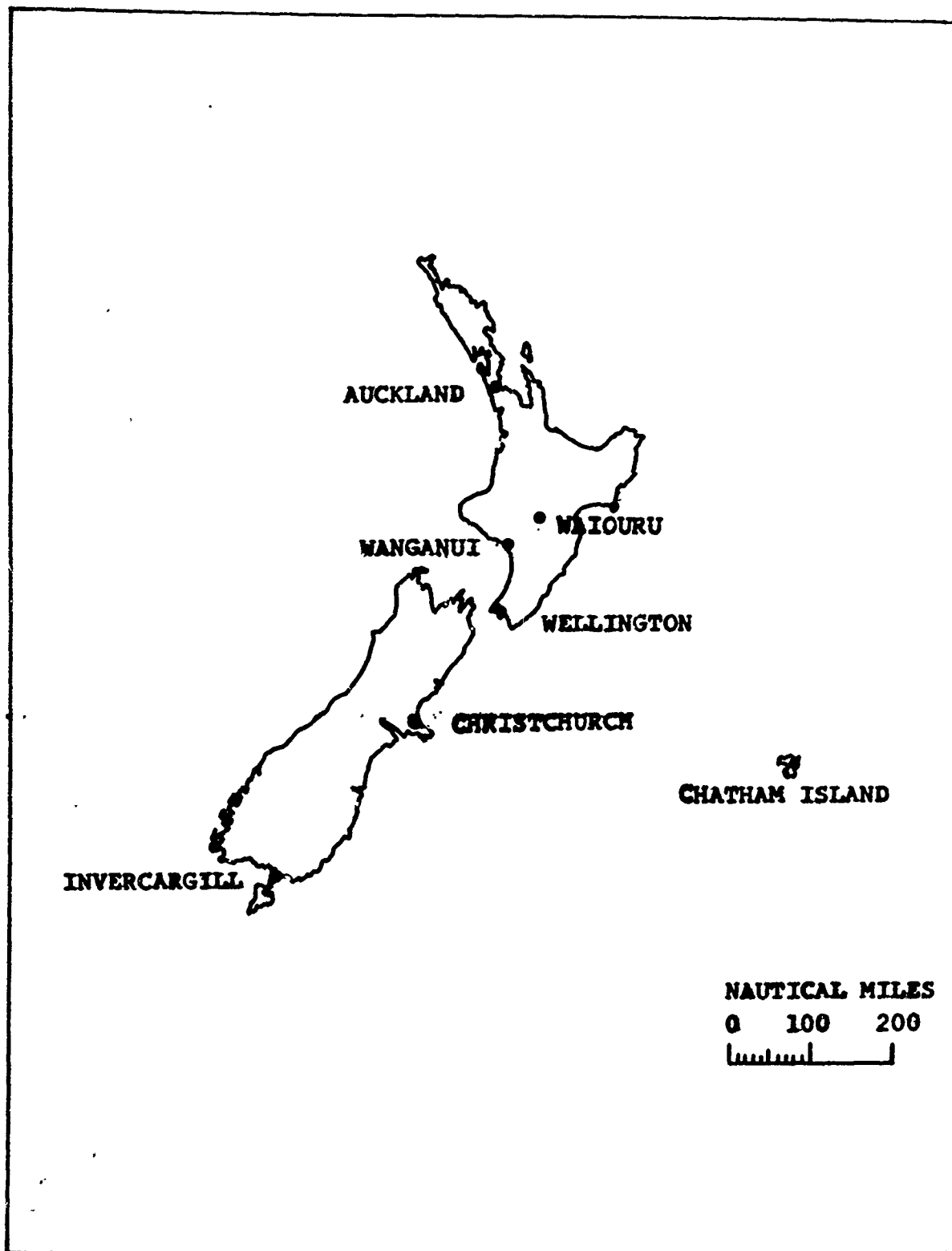


Figure 12. Upper Air Station Locations. New Zealand

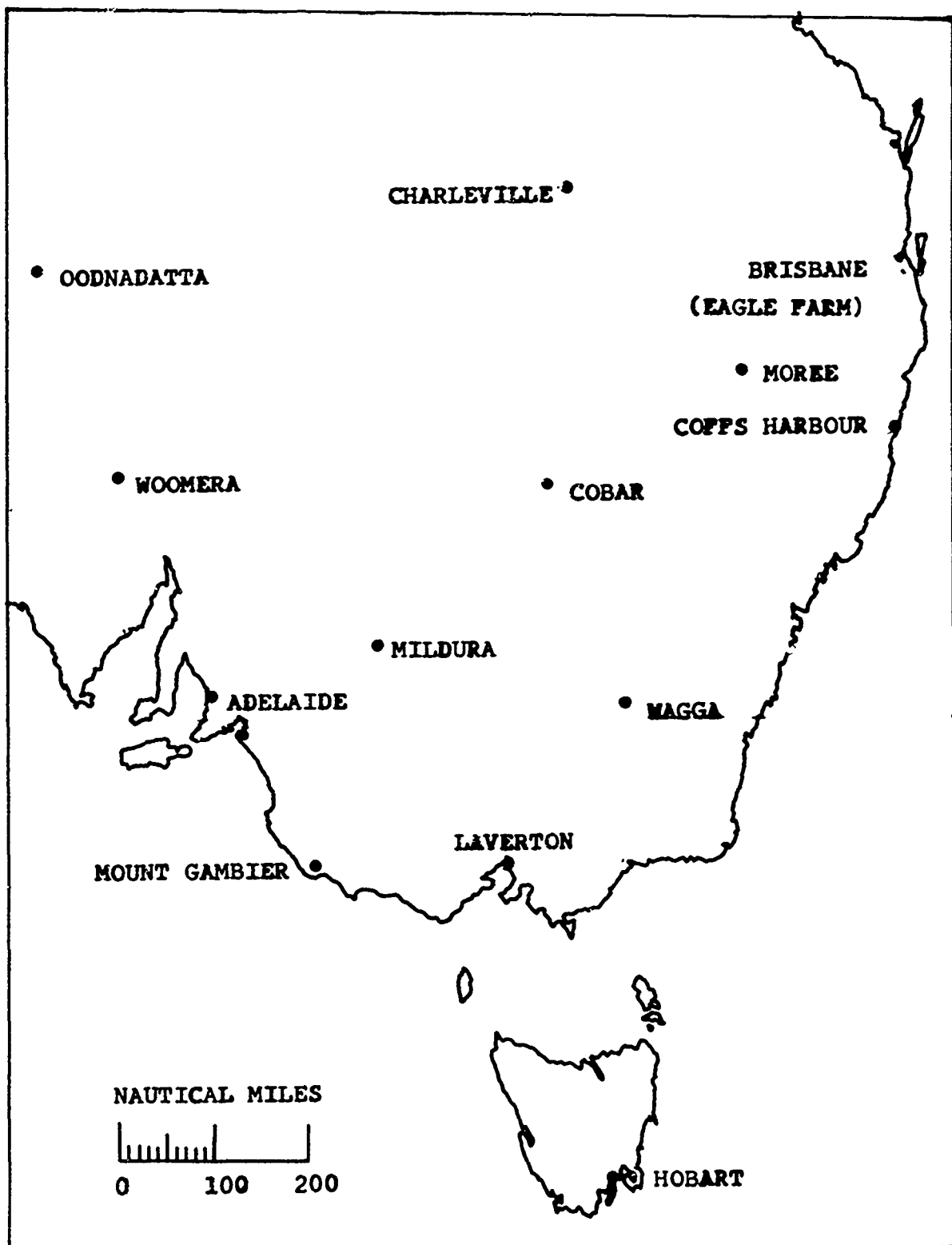


Figure 13. Upper Air Stations Locations. Australia

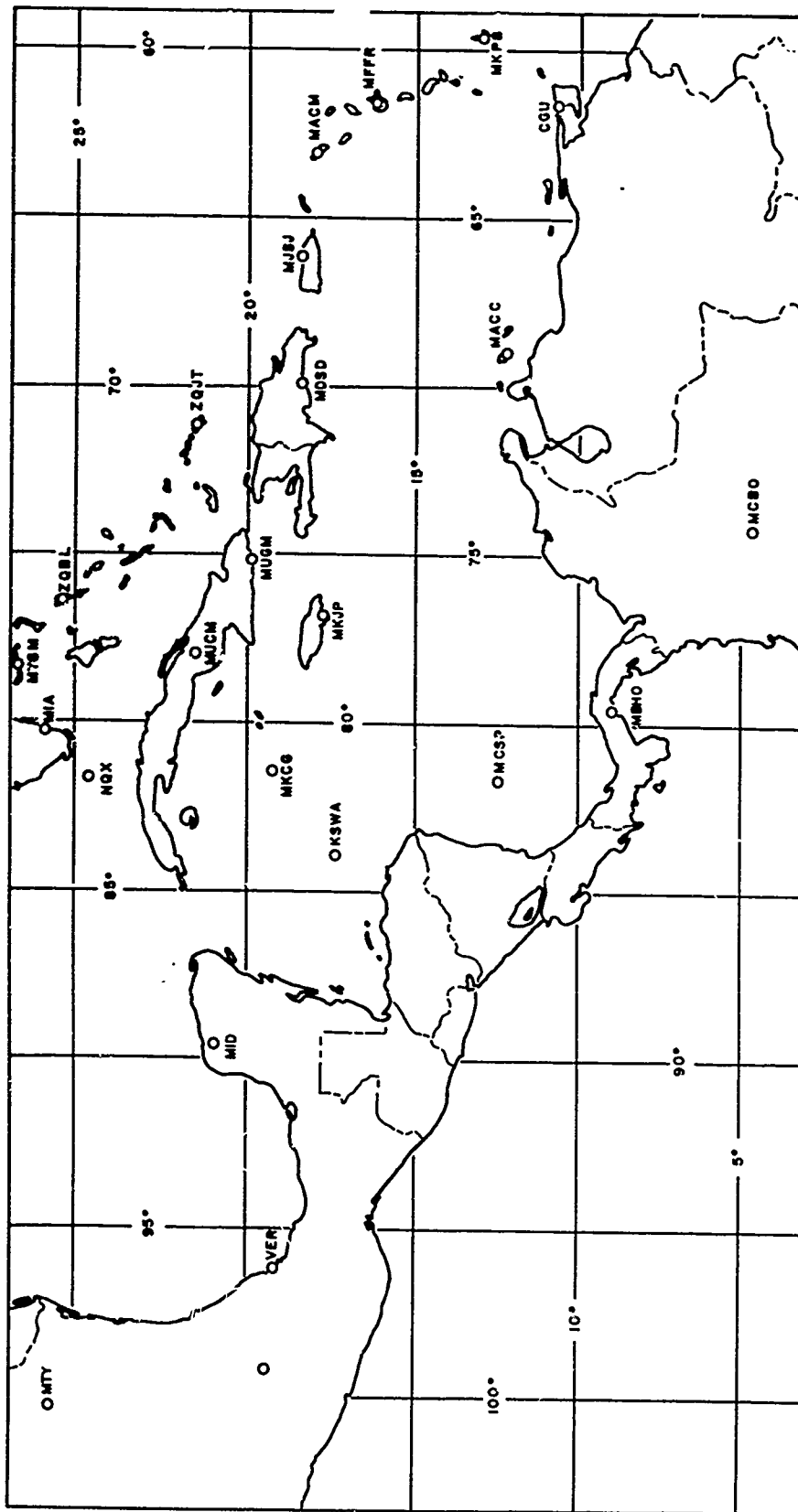


Figure 14. Upper Air Station Locations, Central America

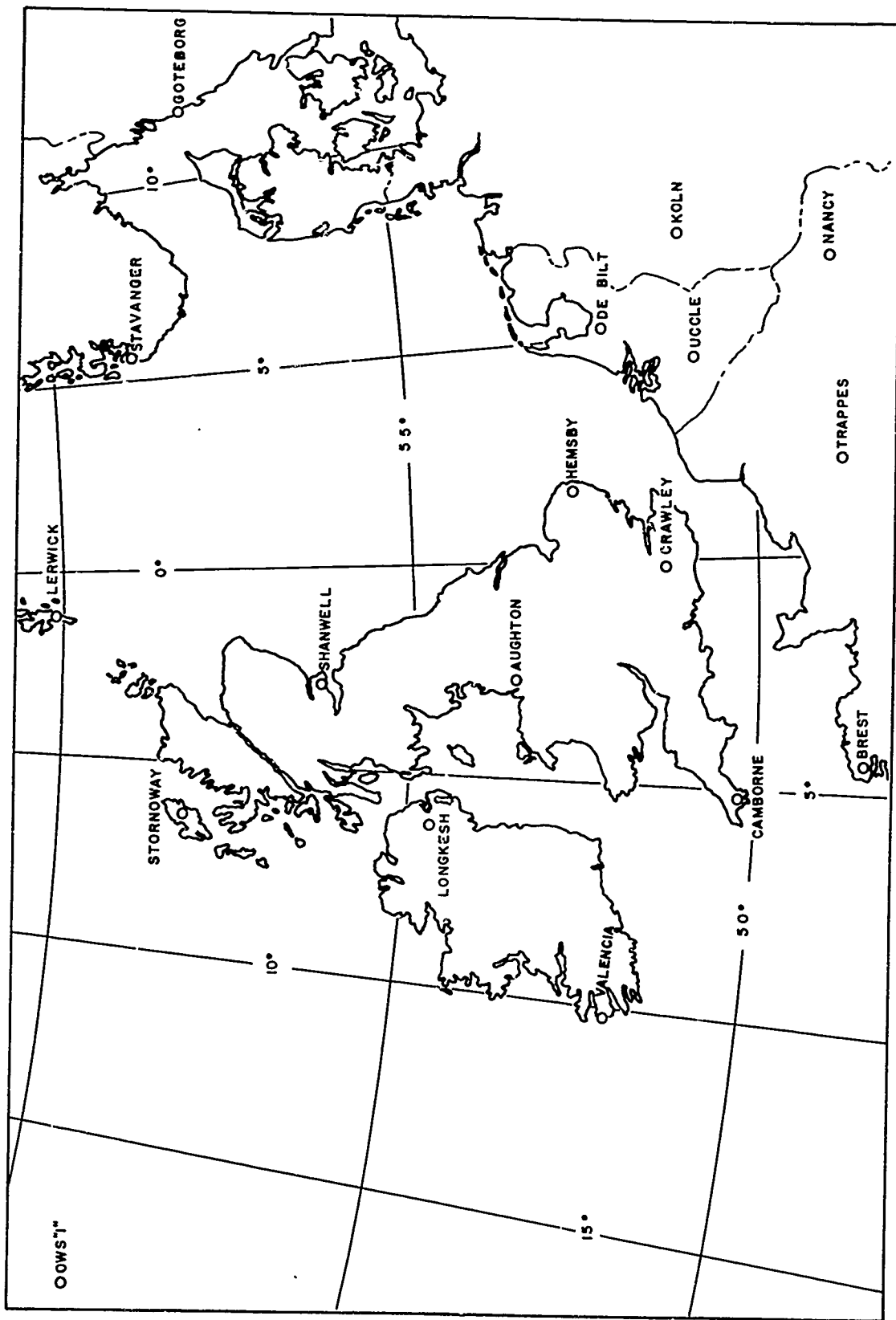


Figure 15. Upper Air Station Locations. Great Britain



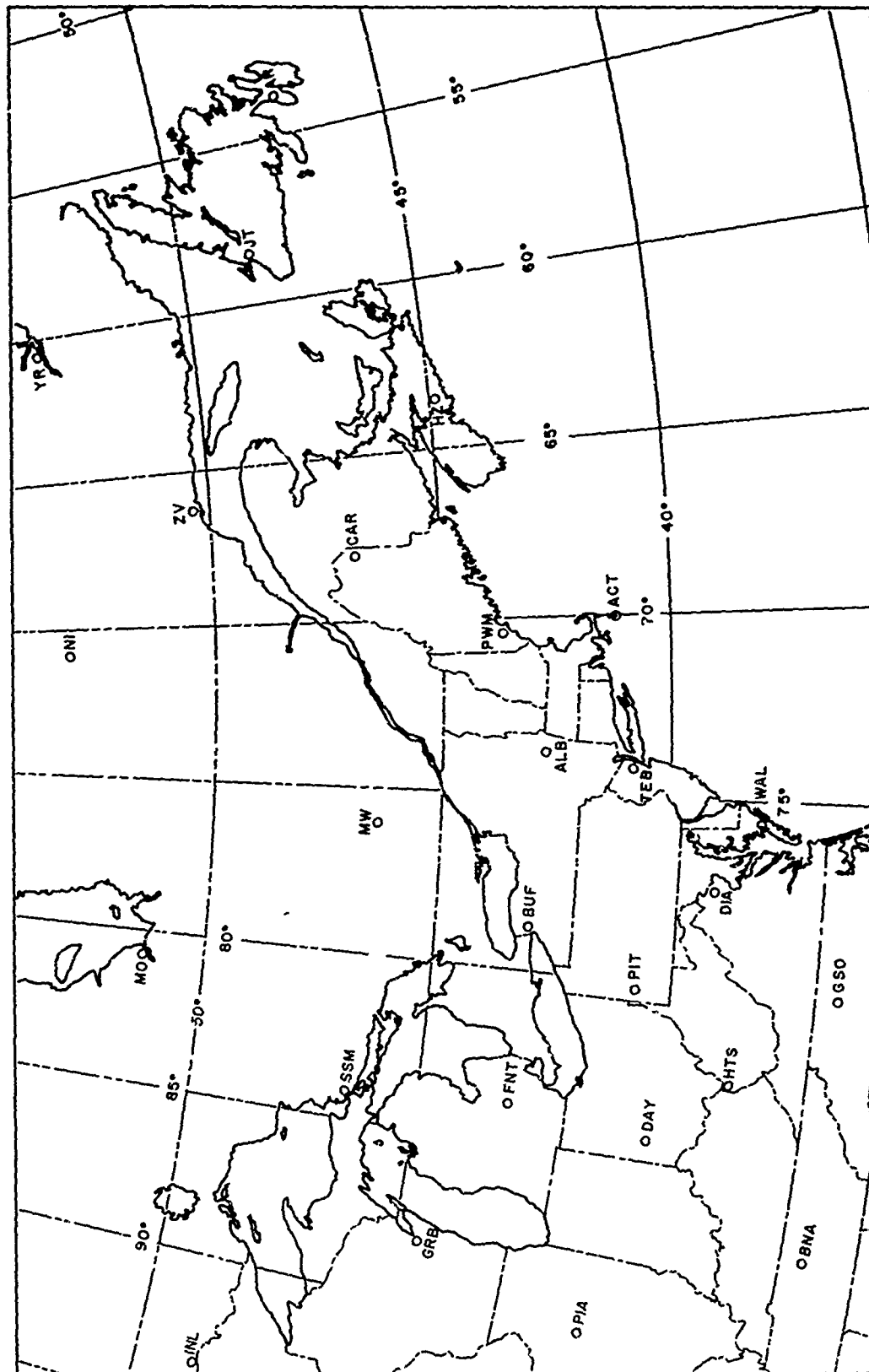


Figure 16b. Upper Air Station Locations, Northeastern United States

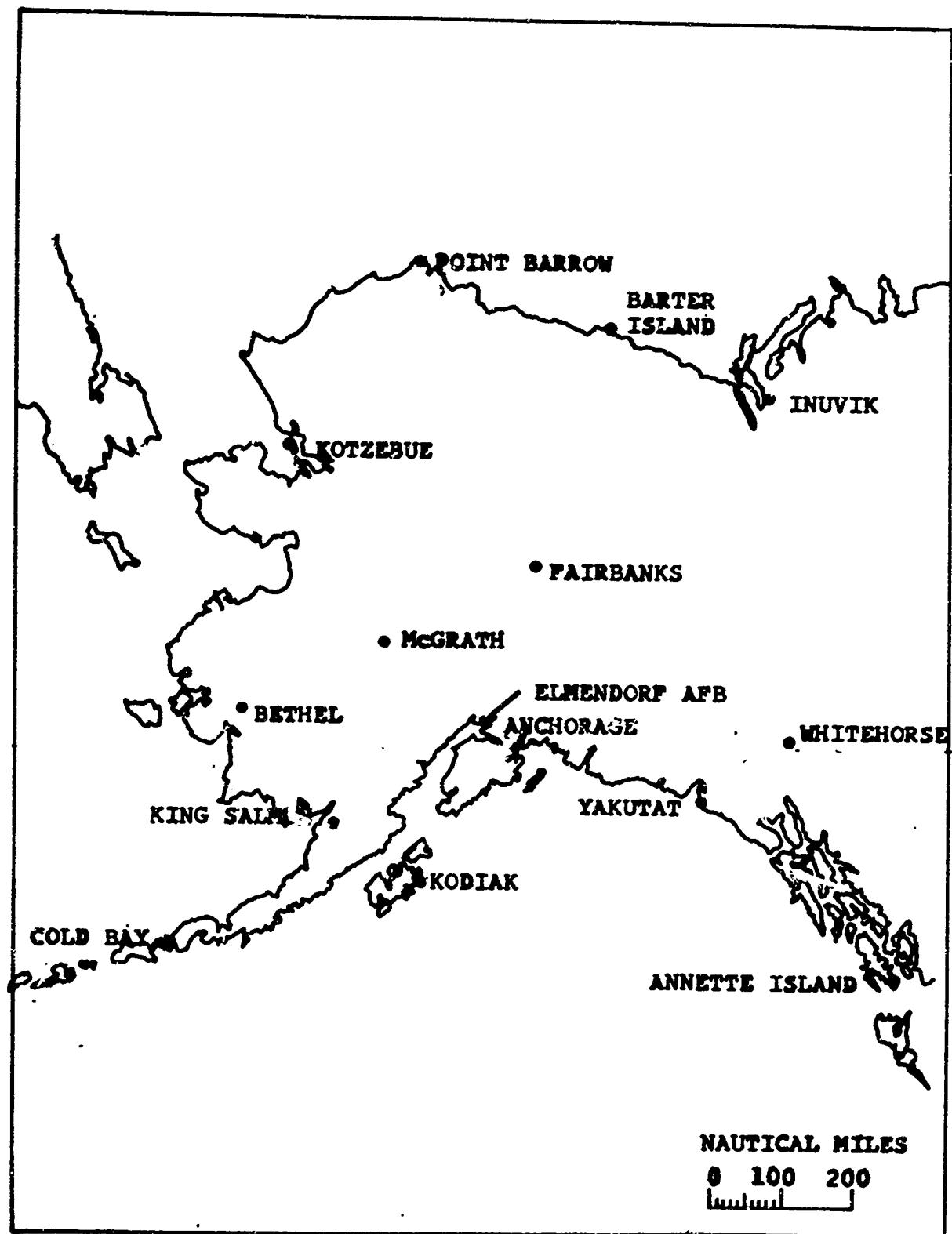


Figure 17. Upper Air Station Locations. Alaska

## SECTION V

### DISCUSSION

#### AN INTERPRETATION OF THE RADIOSONDE TEMPERATURE PROFILES IN TERMS OF VERTICAL WAVE MOTION IN THE ATMOSPHERE

Radiosondes are carried aloft by balloons and the balloons have a horizontal component of motion that is associated with the wind. Hence, the temperature-height profiles obtained from radiosonde data are actually temperature profiles along a three dimensional curve that is, in general, not a vertical line extending through the point of origin. For many purposes it suffices to assume that the radiosonde record provides an adequate approximation to a vertical sounding. In the following discussion it will be shown that under certain conditions, the departure of the radiosonde path from the vertical may result in a temperature profile that shows significant changes in lapse rate which would not be indicated if the radiosonde rose vertically. It will be shown that these changes in lapse rate may be interpreted in terms of wave motion in the atmosphere. Such an interpretation of the radiosonde temperature profiles provides a physical explanation of the apparently conflicting statements found in the literature relative to the correlation between high altitude clear air turbulence and temperature lapse rate.

The analysis that follows is an amplification of a discussion given by Scorer (18). Briefly, Scorer considered the case of a balloon-borne radiosonde rising at a constant rate relative to the air and also moving horizontally through a stationary wave in the atmosphere (mountain wave). He pointed out that the temperature indicated by the radiosonde sensor at any given height would be a function of position, i.e., the phase angle of the atmospheric wave at that particular height. The radiosonde traveling through the wave would indicate the existence of temperature inversions that would not be present for a sounding that had followed a truly vertical path. This may be illustrated by a hypothetical case presented in Figures 18a and 18b. In this case, it is hypothesized that a stationary wave motion of constant amplitude and wavelength is initiated in an isothermal layer. Due to the wave motion, the position of the potential temperature surfaces might be as illustrated in Figure 18a. If a radiosonde enters the wave at point "A" and follows the path ABCD, the temperature profile as indicated by the radiosonde would then be a nearly sinusoidal curve which in a teletype transmission would be approximated by the straight lines given in Figure 18b. A true vertical sounding would indicate an isothermal atmosphere with temperatures varying from a minimum in the ridges (maximum adiabatic cooling) to a maximum in the troughs (maximum adiabatic heating). Of course, if the wave were moving, then even a true vertical sounding would indicate layers of varying lapse rate.

It is proposed here that the simple stationary wave model provides a physical explanation for the apparent relationship between the occurrence of high altitude clear air turbulence and the presence of temperature inversions in the radiosonde temperature profiles as described in the literature. Further, this simple model may be used to

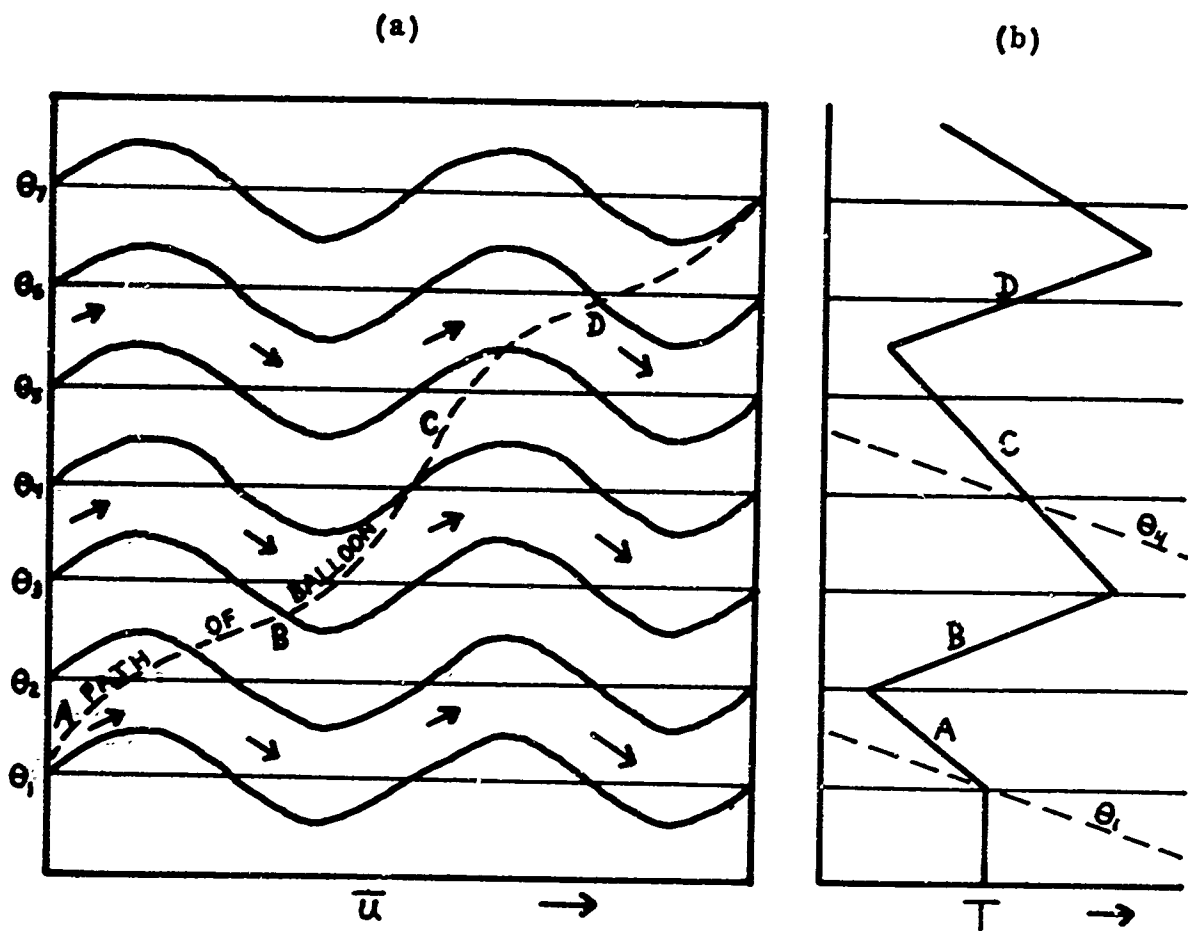


Figure 18. Hypothetical Case of Balloon Ascent Through a Wave and Resulting Temperature Sounding

explain the disagreements on the relative position of the observed turbulence with respect to the inversion. For example, Haymond (19) claims that the turbulence occurs in an inversion layer and others claim that turbulence occurs between inversion layers. The analysis outlined above indicates that the height of an inversion layer on the radiosonde temperature profile may simply be a function of the balloon's position, and that the observed clear air turbulence may be the result of wave motion in the atmosphere.

#### CALCULATION OF MEAN SQUARE VERTICAL ACCELERATION FROM RADIO-SONDE DATA

The mean square vertical accelerations associated with clear air turbulence were calculated starting with the postulate:

- a. The wave motion in a stably stratified atmosphere layer has constant phase and amplitude with altitude.
- b. Only dry adiabatic thermodynamic processes are significant.
- c. The balloon rises with a constant speed of 5.08 m/sec (1000 ft/min) relative to the air.
- d. The wind is normal to the crest and trough lines and for a stationary wave is equal to  $\bar{u}$ , the mean speed in the layer.

Under these conditions the horizontal distance that the radiosonde will travel in going from a minimum to a maximum temperature (maximum to a minimum) is given by

$$x = \lambda/2 = \bar{u} \Delta z / w_0 \quad (7)$$

where  $\lambda$  = wavelength of the wave in the atmosphere  
 $\bar{u}$  = horizontal component of the wind relative to the wave  
 $\Delta z$  = altitude interval between observed minimum and maximum temperature  
 $w_0$  = rate of rise of balloon with respect to air

For a sine wave the vertical displacement,  $z$ , may be expressed by

$$z = \Delta h \sin 2\pi (t/\tau_1) \quad (8)$$

where  $\Delta h$  = amplitude of the wave  
 $\tau_1$  = wave period  
 $t$  = time

The expression for the vertical velocity is obtained by differentiating Eq. (8) with respect to time:

$$dz/dt = w = \frac{2\pi\Delta h}{\tau_1} \cos 2\pi \frac{t}{\tau_1} \quad (9)$$

If an airplane were to fly horizontally through such a wave it would be subjected to vertical motions of the atmosphere given by

$$w = \frac{2\pi\Delta h}{\tau_1} \cos 2\pi \frac{t}{\tau_2} \quad (10)$$

where  $\tau_2$  is the period of the wave as experienced by the aircraft or

$$\tau_2 = \lambda/v_s \quad (10a)$$

and  $v_s$  is the speed of the aircraft relative to the speed of the wave.

The acceleration of the air through which the aircraft is flying is obtained by differentiating Eq. (10)

$$dw/dt = - \frac{4\pi^2 \Delta h}{\tau_1 \tau_2} \sin (2\pi \frac{t}{\tau_2}) \quad (11)$$

Squaring both sides we have

$$(dw/dt)^2 = \frac{16\pi^4 (\Delta h)^2}{\tau_1^2 \tau_2^2} \sin^2 (2\pi \frac{t}{\tau_2}) \quad (12)$$

To obtain the mean square acceleration both sides of Eq. (12) are integrated over the limits  $t = 0$  and  $t = \tau_2/4$  and divided by  $\tau_2/4$  yielding

$$\overline{(dw/dt)^2} = \frac{8\pi^4 (\Delta h)^2}{\tau_1^2 \tau_2^2} \quad (13)$$

and taking the square root to obtain the root mean square acceleration

$$\text{RMS} = \sqrt{\overline{(dw/dt)^2}} = \frac{\sqrt{8} \pi^2 \Delta h}{\tau_1 \tau_2} \quad (14)$$

Substituting  $\tau_1 = \lambda/\bar{u}$  and  $\tau_2 = \lambda/v_s$

$$\text{RMS} = 2 \sqrt{2} \pi^2 \frac{\Delta h \bar{u} v_s}{\lambda^2} \quad (15)$$

or since  $\lambda = \frac{2\bar{u} \Delta z}{w_0}$  from Eq. (7)

$$\text{RMS vertical acceleration} = \pi^2 / \sqrt{2} \frac{\Delta h v_s w_0^2}{\bar{u} (\Delta z)^2} \quad (16)$$

This equation implies that the RMS vertical acceleration of the atmosphere with respect to the aircraft is directly proportional to the speed of the aircraft relative to the speed of the wave and to the amplitude ( $\Delta h$ ) of the wave but inversely proportional to the square of the depth of the layer between the observed maximum and minimum temperature. Hence, with other things being equal, a sounding depicting fluctuations in the temperature gradient over relatively shallow layers implies more severe turbulence than when the same temperature changes take place through deeper layers.

A sample computation is given for flight test 114 (29 Aug. 1966). On this day extensive light to moderate turbulence was found on the lee side of the Sierra Nevada mountains from just south of Reno to Las Vegas. The Las Vegas radiosonde observation for 30 Aug. 1966 0000Z is shown for in Figure 19. The turbulence was reported between 53 to 57,000 ft, corresponding well with the fluctuations on the radiosonde temperature profile. A stationary wave is assumed. The following calculation was made from the sounding for the three layers A, B, and C.

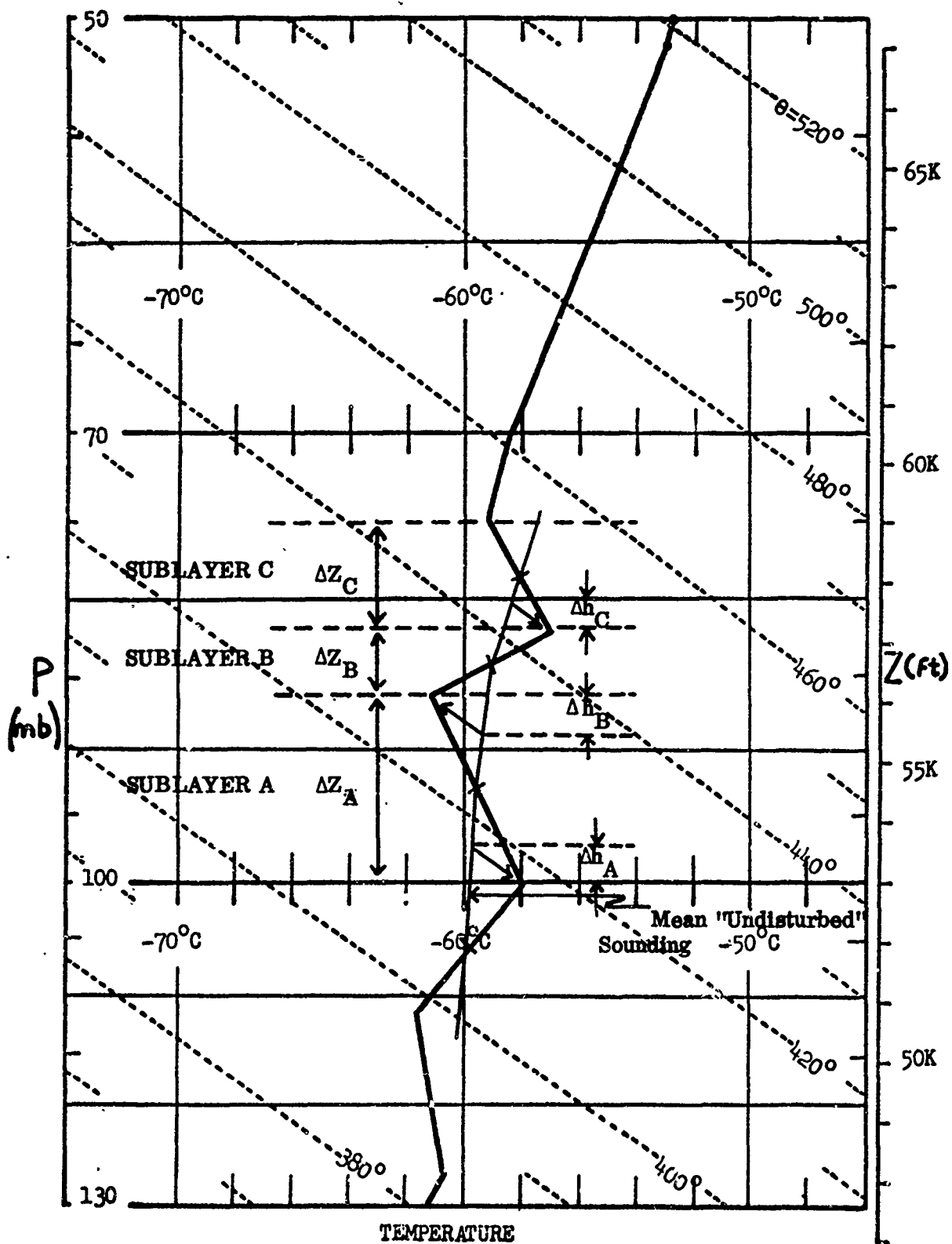


Figure 19. Temperature Sounding, Las Vegas, Nevada, 30 Aug 1966, 0000Z (Flight 114)

$$\begin{aligned}\bar{\Delta}h &= 483 \text{ ft (147 m)} \\ \bar{\Delta}z &= 1840 \text{ ft (564 m)} \\ \bar{u} &= 25 \text{ knots (12.5 m/sec)} \\ v_s &= 400 \text{ knots (206 m/sec)} \\ \lambda &= \frac{2\bar{u}\bar{\Delta}z}{w_0} = 9106 \text{ ft (2776 m)}\end{aligned}$$

$$\text{RMS vertical acceleration} = \frac{2\sqrt{2}\pi^2(147)(12.5)(206)}{(2776)^2} = 1.37 \text{ m/sec}^2$$

Assuming the aircraft responds to all vertical air motion, then this RMS vertical acceleration can be compared with the observed RMS incremental cg normal acceleration,  $\Delta a_N$ , of the aircraft which, when expressed in terms of the acceleration of gravity, is computed to be

$$\text{RMS } \frac{\Delta a_N}{g} = \frac{1.37}{9.8} = 0.14$$

The observed RMS  $\Delta a_N/g$  mean values, RMS  $\Delta G$  in Crooks, Hoblit and Prophet (2) near Las Vegas ranged from .051 to .078.

The aircraft did not fly near any other radiosonde stations on this day, but on the following day, Test 115 30 Aug. 1966, in addition to finding turbulence over the Sierra Nevada Mountains, light turbulence was also found at 61 thousand feet over Ely. The Ely sounding nearest this time is shown in Figure 20. However, no turbulence was found from just west of Ely to Reno. The nearest radiosonde to this no turbulence area is Winnemucca shown in Figure 21. Note the contrast compared to the Ely sounding.

Sample calculations for other areas have also been made. On 16 May 1966 (Test 76) widespread light and moderate turbulence occurred around the large island of Hawaii at about 58,000 ft. The Hilo sounding at this time is shown in Figure 22 and according to the proposed theory, indicates that turbulence is likely from 50,000 ft to just above 60,000 ft. The RMS  $\Delta a_N/g$  value calculated from the sounding is .075. The observed mean values for all runs in the Hilo area ranged from .024 to .051.

On 15 Apr 1966 (Test 58), no turbulence could be found anywhere in the Hawaiian area over the altitude range 50 to 68,000 ft. The Hilo and Lihue soundings at this time are shown in Figures 23 and 24, respectively. As may be noted, no wave motion is indicated at any altitude from 50 to 68,000 ft.

On 28 Jul 1966 (Test 102), moderate turbulence was quite widespread to the lee of the great dividing range in Australia while no turbulence was encountered to the west of the range. An extensive area of moderate turbulence was found at 60,000 ft over

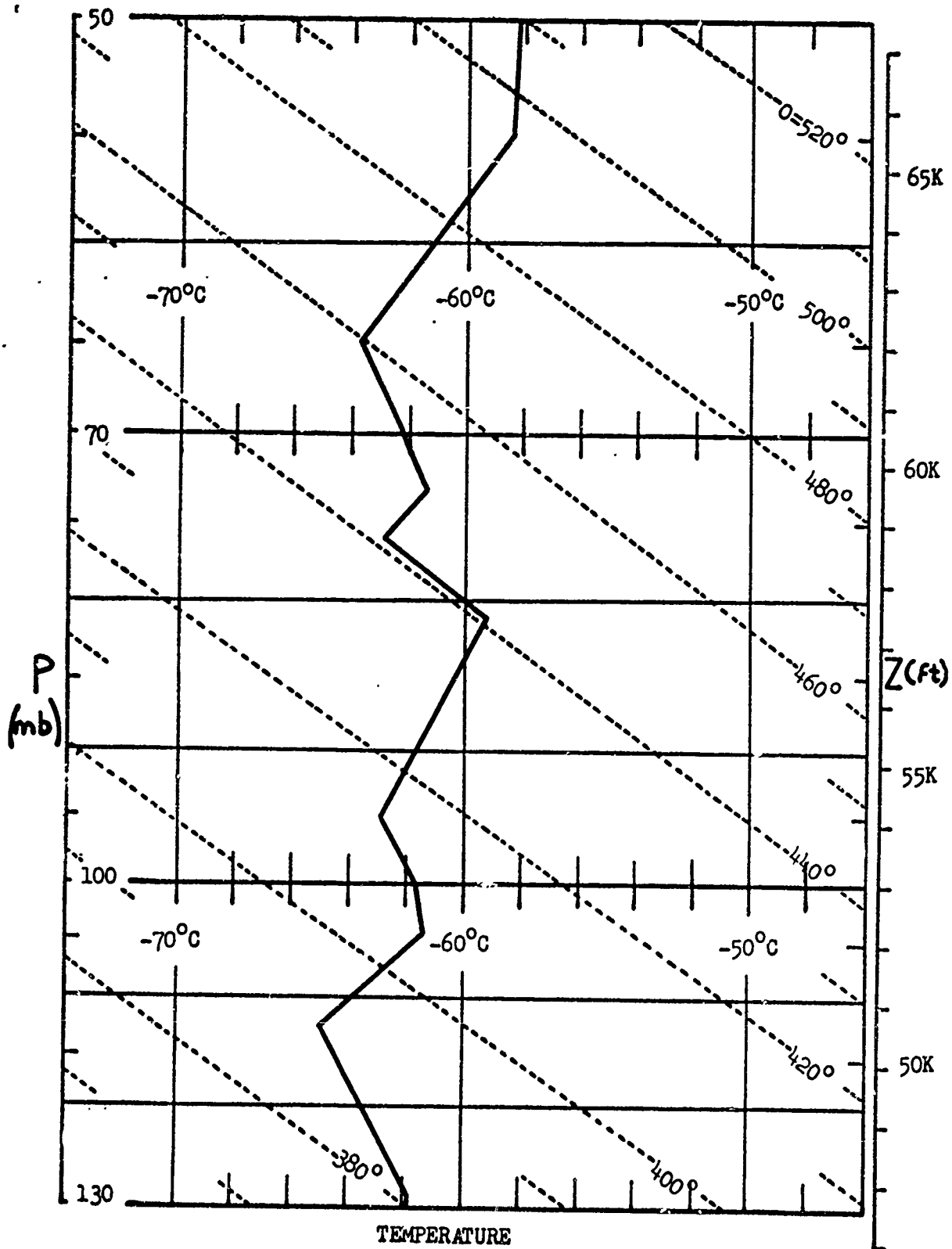


Figure 20. Temperature Sounding, Ely, Nevada, 31 Aug 1966, 0000Z (Flight 115)

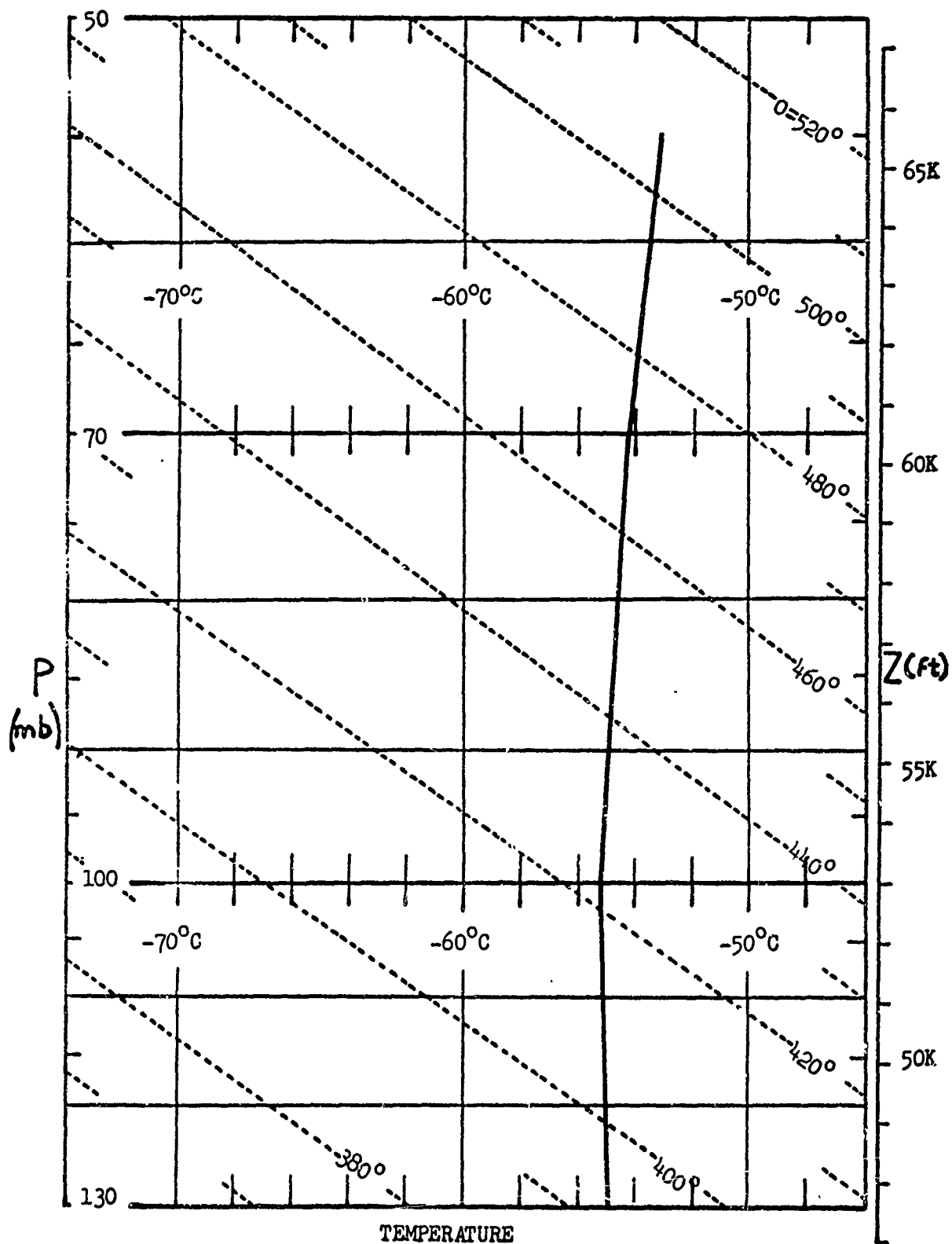


Figure 21. Temperature Sounding, Winnemucca, Nevada, 31 Aug 1966, 0000Z (Flight 115)

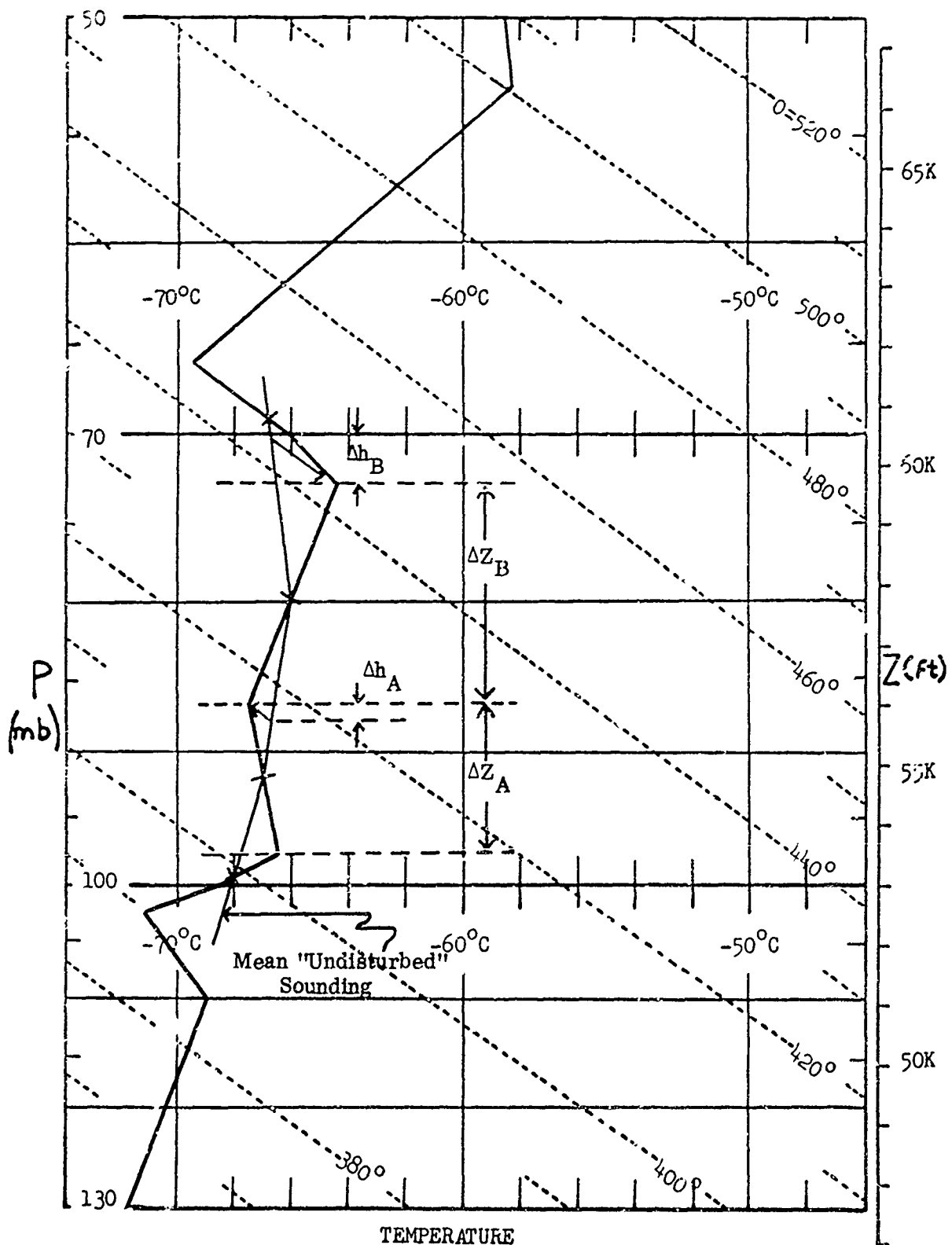


Figure 22. Temperature Sounding, Hilo, Hawaii, 17 May 1946, 0000Z (Flight 76)



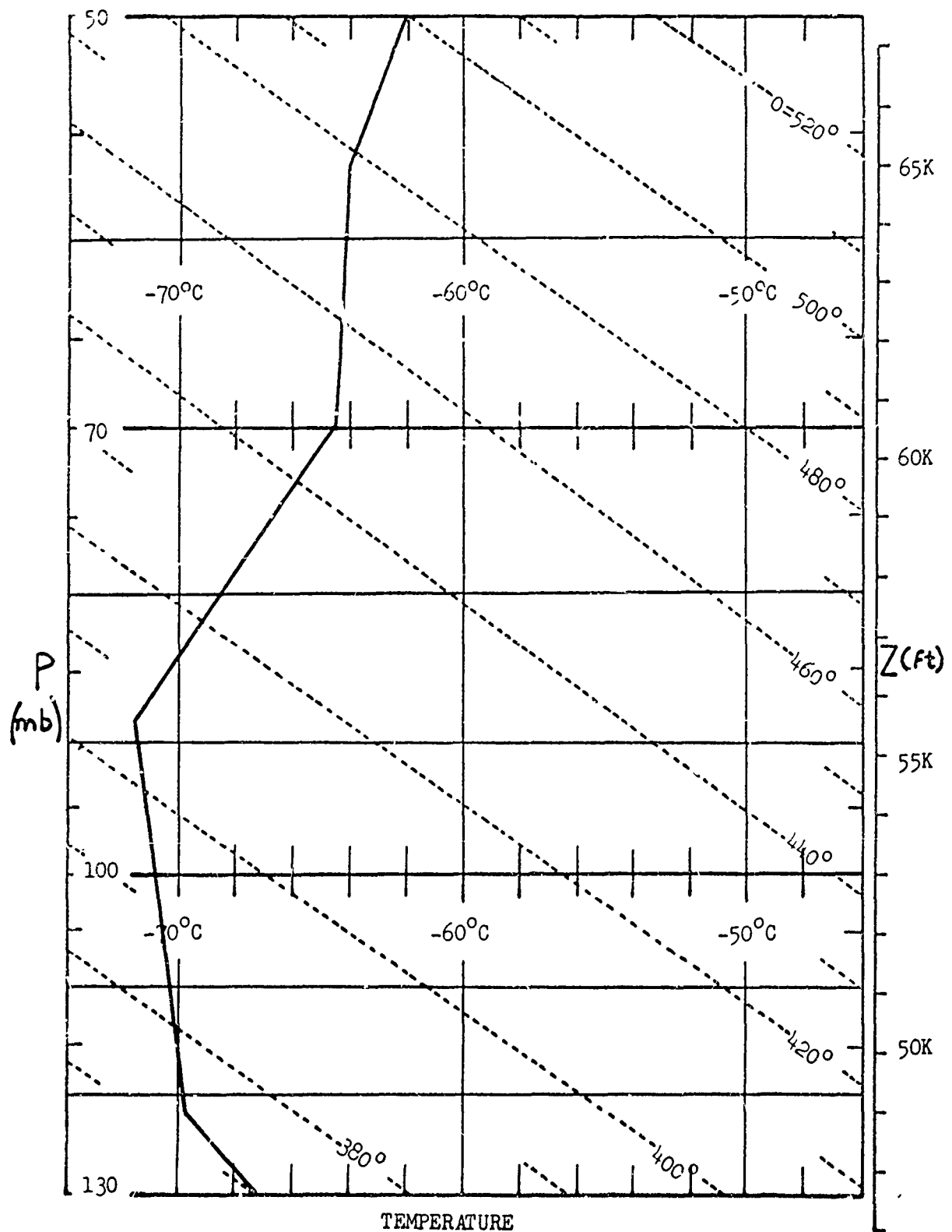


Figure 24. Temperature Sounding, Lihue, Hawaii, 16 Apr 1966, 0000Z (Flight 58)

Brisbane. The radiosonde at this time, shown in Figure 25 indicates probable wave motion over the interval 56 to 65,000 ft. For the layer 58.5 to 62.5 thousand feet, the computed RMS  $\Delta a_N/g$  value is .115. The observed mean values for all runs in the Brisbane area range from .038 to .095.

On the same day an area of moderate turbulence was found at about 63,000 ft just north of Williamstown and patches of lighter turbulence at 65 to 66,000 ft to the south. The Williamstown sounding, shown in Figure 26 indicates probable wave motion from 57 to 66,000 ft. The RMS  $\Delta a_N/g$  value calculated from the sounding for the layer 62 to 66,000 ft was .082. The observed mean values for all runs in the Williamstown area ranged from .050 to .059.

No turbulence was found to the west of the range. The soundings for Cobar and Wagga, shown in Figures 27 and 28 respectively, indicate no wave motion at flight altitudes, although moderate turbulence was found over the mountains less than 100 miles east of Wagga.

It appears from these examples, summarized in Table III, pg. 64, that when the radiosonde observations are taken fairly close to the time of flight good estimates of mean turbulence intensity can be obtained from the meteorological data. In the few rare instances, notably in Australia, when special radiosonde observations were taken six hours apart, it is evident that the temperature structure can change quite drastically. Hence, in areas where only the regular 12-hourly observations are made and the flight time is midway between, lower correlations between observed and calculated values can be expected. The distance to which a particular radiosonde might be applicable will undoubtedly be greater in areas of uniform terrain, whether rough or smooth, as compared to an area in which there is an abrupt change in terrain profile, as was noted in Eastern Australia.

The assumptions used in deriving this simple wave model should act to maximize the computed values for RMS  $\Delta a_N/g$ . For instance, if the wave train is not stationary but moving downwind at some speed less than the mean wind, the vertical velocities and accelerations would be smaller. If the depth of the layer or the relative wind speeds are so small that the balloon does not have time to travel downwind relative to the wave a distance equal to half a wavelength while passing up through the wave layer, the computed values for  $\Delta h$  and  $\Delta z$  in Eq. (16) will be too small, and since  $\Delta z$  is squared and in the denominator, the computed RMS  $\Delta a_N/g$  would again be on the large side. Moreover, it is assumed that the aircraft responds to all vertical air motion, i.e., there is no vertical motion of the air relative to the aircraft. Actually, due to inertia, the aircraft response is usually less.

#### A MODEL FOR CLEAR AIR TURBULENCE BASED ON SLOPING ISENTROPIC SURFACES

The model for identifying turbulent layers and computing approximate values for root mean square vertical accelerations presented in the previous section, is applicable only to situations when the turbulence happens to be occurring at the time and place of radiosonde ascent. Turbulence will sometimes occur within the relatively

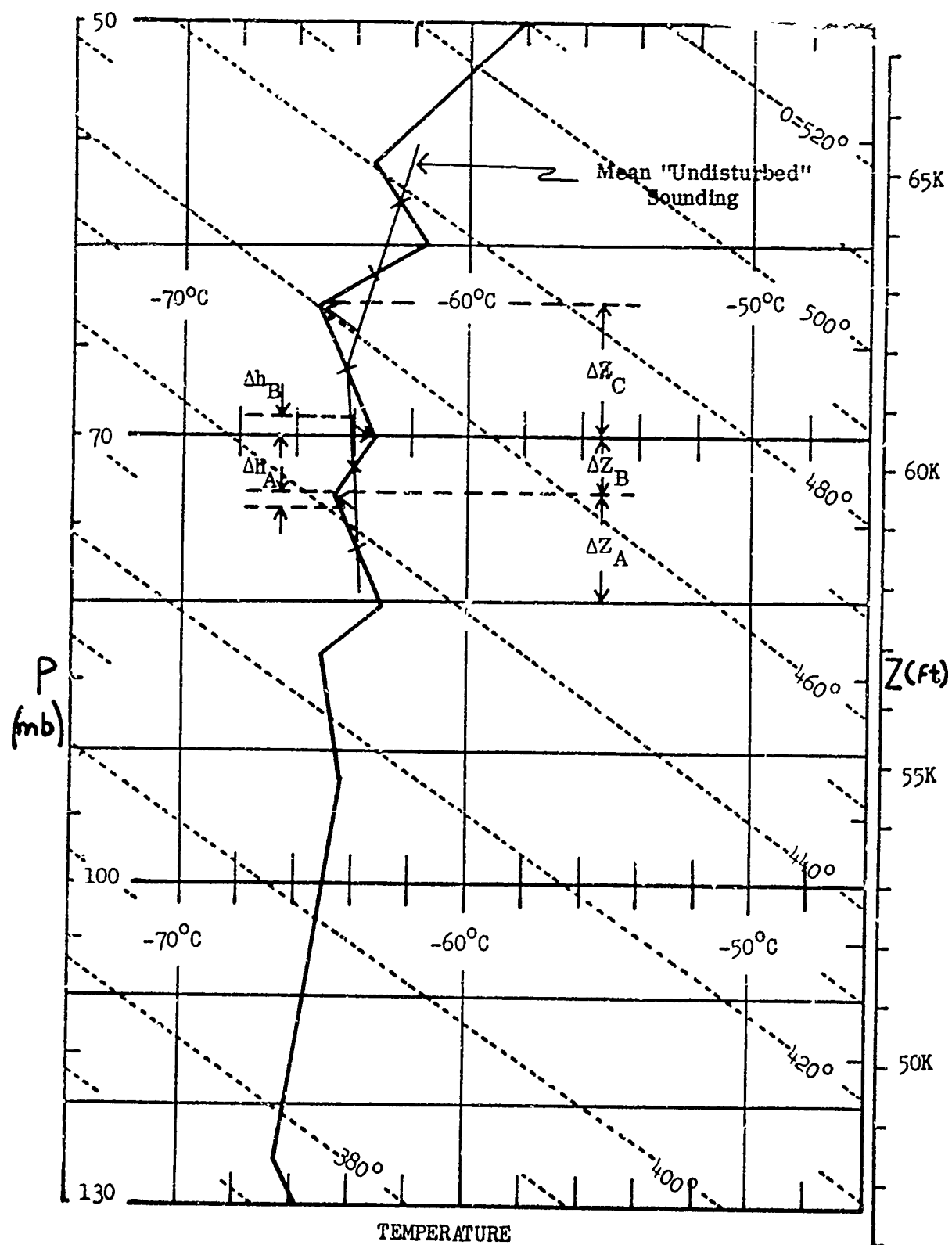


Figure 25. Temperature Sounding, Eagle Farm, Australia, 27 Jul 1966, 2800Z (Flight 102)

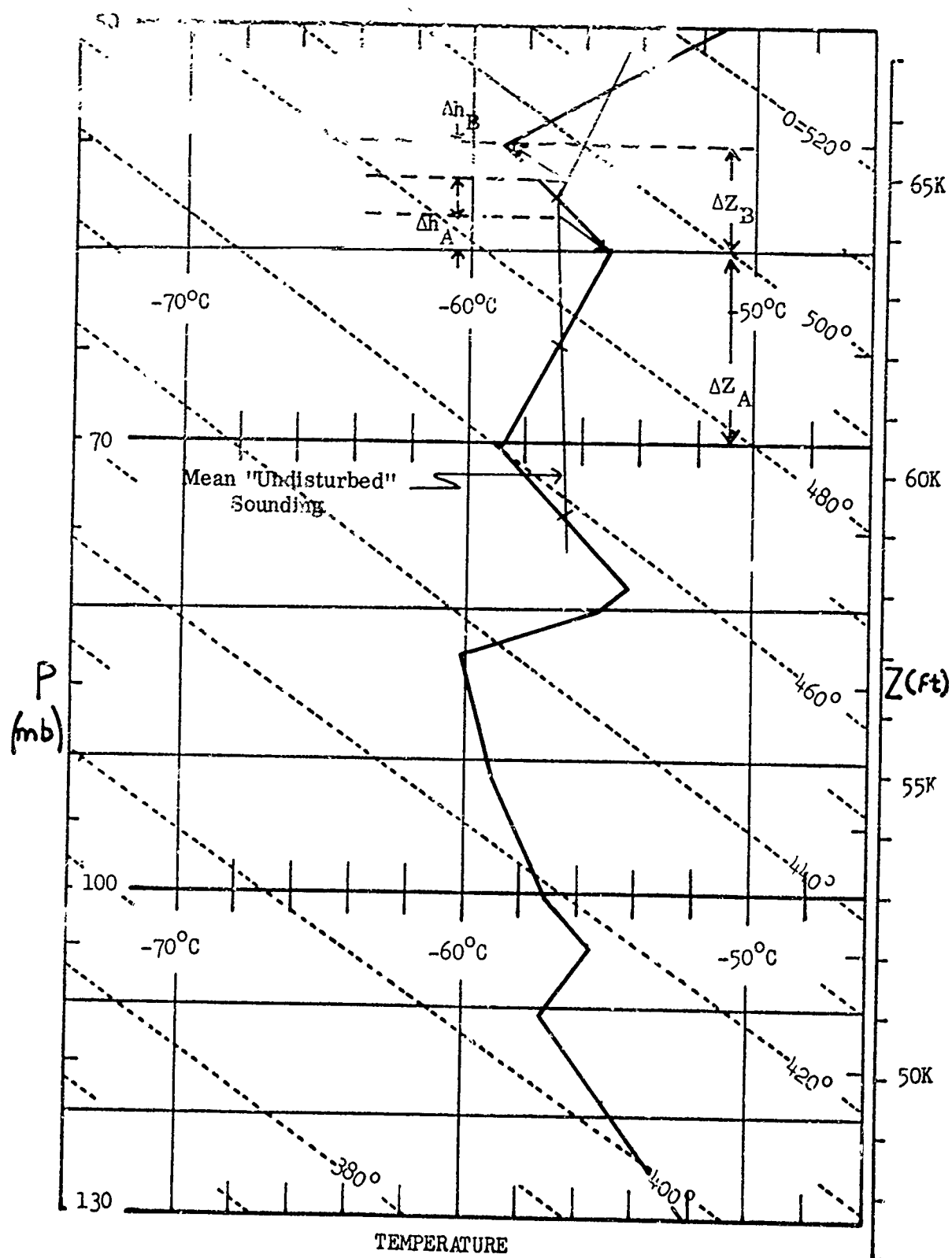


Figure 26. Temperature Sounding, Williamstown, Australia, 27 Jul 1966, 2300Z (Flight 102)

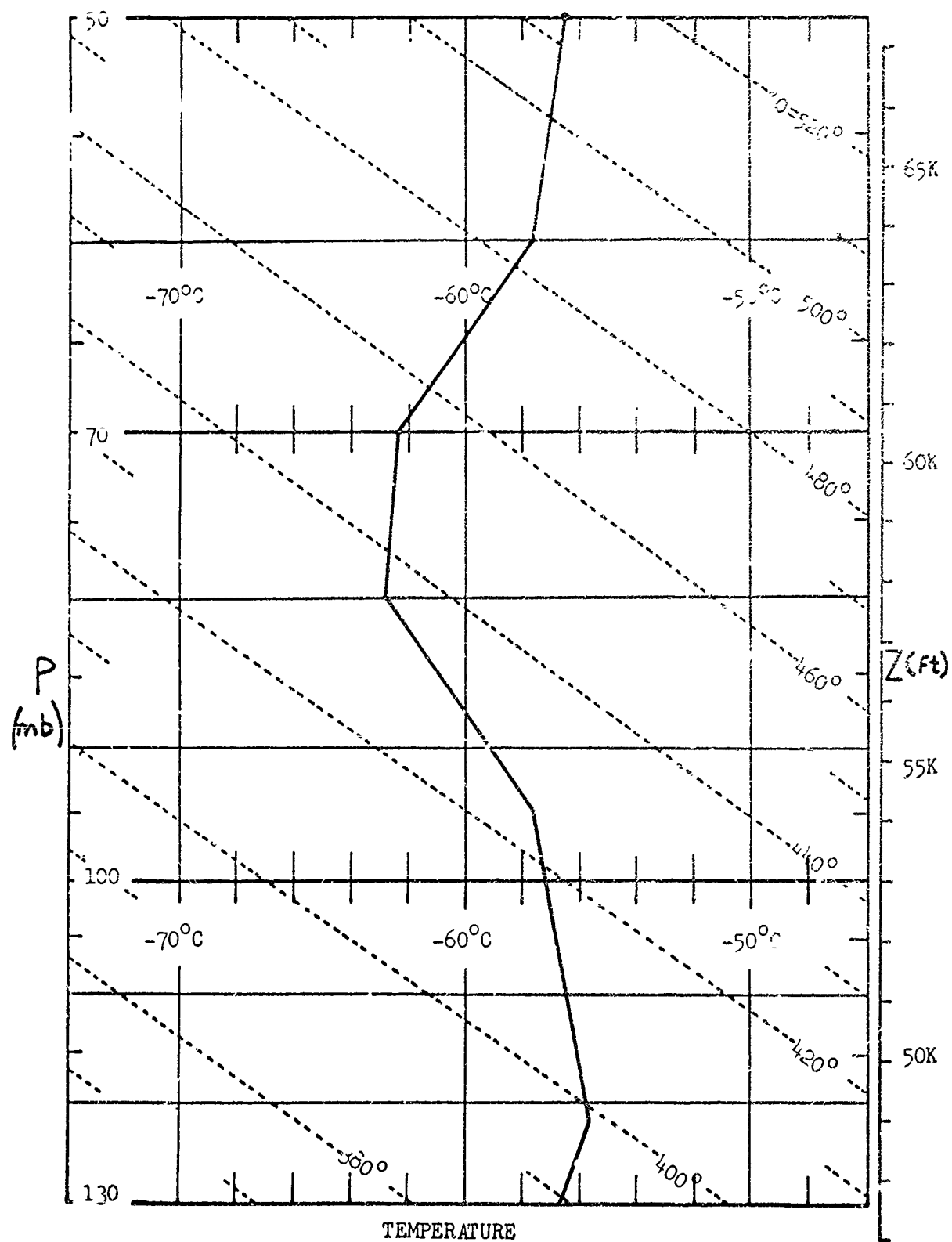


Figure 27. Temperature Sounding, Cobar, Australia, 27 Jul 1966, 2300Z (Flight 102)

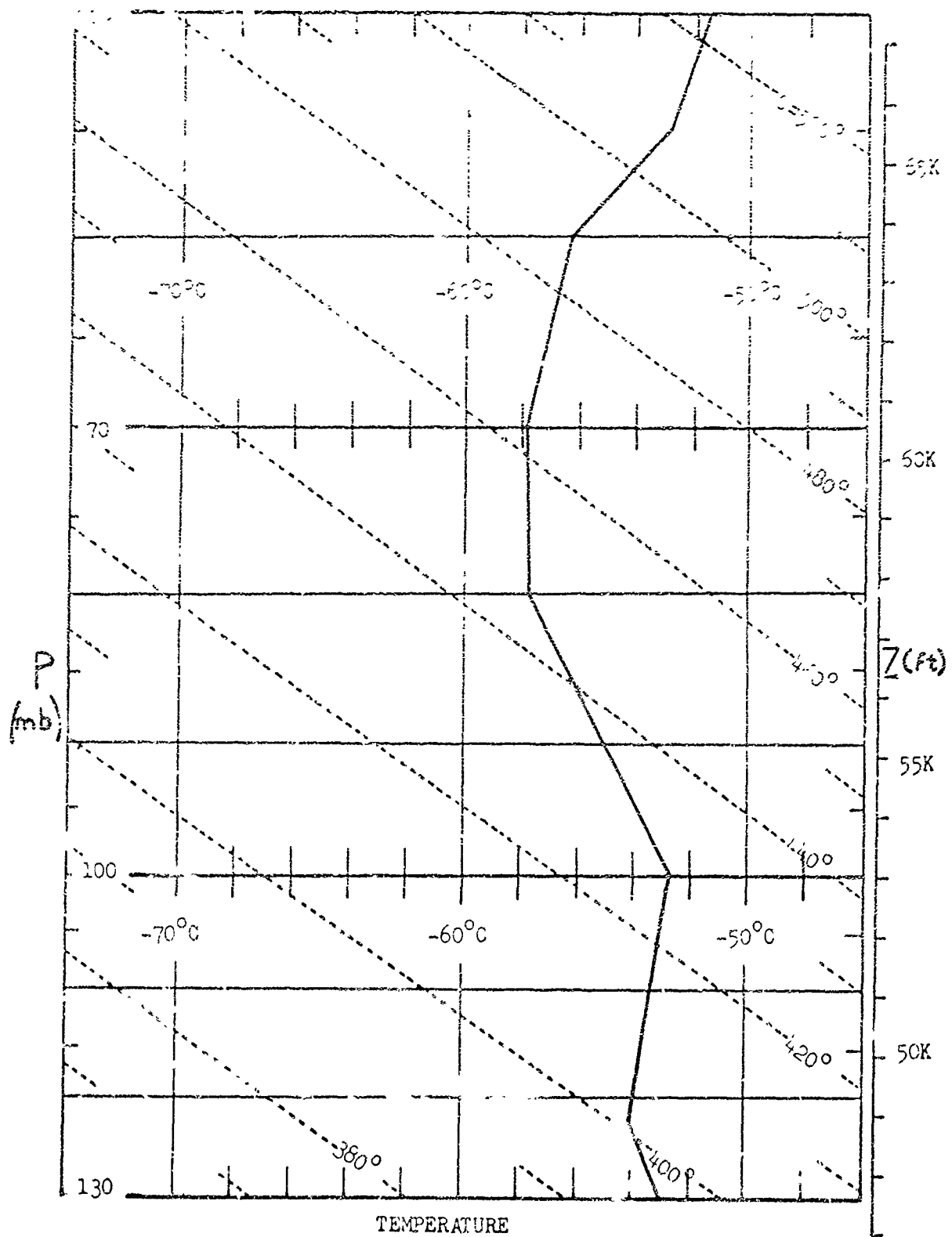


Figure 28. Temperature Sounding, Wagga, Australia, 27 Jul 1966, 2300Z (Flight 102)

widely spaced radiosonde network but not necessarily near enough to any station to be analyzed from the sounding. Therefore, there appeared to be a need to develop a model for identifying potential turbulence from the analyzed fields of temperature and pressure over relatively large areas as depicted on upper air synoptic charts.

It is assumed that turbulence in the stratosphere is associated with vertically rising and descending air and, due to the stable stratification, any vertical motion must be forced, i.e., energy consuming. Examples of mechanisms which could cause forced vertical motion are convection, mountains, fronts, and mass divergence associated with synoptic pressure systems. In the case of convection, we are concerned with the so-called negative buoyancy region above active convective cells. The role of frontal systems and mountains are similar in that both obstruct the air flow and may cause it to rise on the windward and descend on the leeward side. Synoptic pressure systems may involve large-scale horizontal mass divergence that is associated with vertical adjustment of air masses, and the more intense systems extend upward into the stratosphere. Continuity considerations require that diverging or converging horizontal wind fields be associated with vertical motion. As the jet stream itself may be subjected to vertical displacements as it passes around a trough or ridge aloft, the jet appears to play no direct role in producing vertical motion.

The proposed model is one in which an initial perturbation imparts a vertical component to the air motion. This perturbation is presumed to be produced by some intermediate to large-scale phenomena ranging from a few miles in diameter in the case of forced convective activity to 100 miles or more in the case of synoptic scale phenomena. As adiabatic temperature changes are assumed, then perturbations of vertical displacement should be associated with perturbations in the temperature field along the direction of flow. Methods of analyzing these perturbations can therefore be based on the pattern of isotherms on a constant pressure surface or from a height contour analysis of an isentropic surface.

As a consequence of the vertical displacement of air masses affected by the initial perturbations, buoyancy and inertial forces produce secondary perturbations or waves. The period of these secondary perturbations is a function of the vertical stability and also vertical wind shear. The resulting wavelengths, being of the order of a few miles, are short enough to produce significant vertical accelerations on aircraft flying through. In the event the period of the initial perturbation corresponds to wavelengths of this size, as is likely in convective activity, then the initial perturbation itself can cause vertical accelerations. However, for the larger scale phenomena, the wavelengths would be much too long to cause significant vertical acceleration on aircraft. It should be noted that according to this model the energy does not cascade down from the large scale initial perturbations to the smaller scale secondary perturbations and thereby yield a continuous spectrum of wavelengths. On the contrary, it is hypothesized that the secondary perturbations which contain the maximum vertical component of turbulent energy occur at discrete frequencies depending upon the vertical stability and wind shear.

### The Model

In a stably stratified layer, air which is forcibly displaced in the vertical will be subjected to deceleration due to buoyance forces. The air eventually stops rising or descending and is accelerated back toward the level of origin or equilibrium level. However, inertia carries the air past this level and, assuming no loss of energy, the air oscillates about the equilibrium level with amplitude  $h$  and frequency  $\nu$ .

The frequency is related to the period  $\tau$ , defined as the time required for one complete oscillation, by

$$\nu = 2\pi/\tau \quad (17)$$

and the period is related to the mean wind speed and wavelength by,

$$\tau = \lambda/\bar{u} \quad (18)$$

Assuming only adiabatic temperature changes, the amplitude  $h$  will equal the maximum vertical displacement of a potential temperature surface from its equilibrium level. The vertical displacement  $z$  in a sine wave is related to amplitude and time by

$$z = h \sin \frac{2\pi t}{\tau} \quad (19)$$

An expression for vertical velocity is obtained by differentiating Eq. (19) with respect to time,

$$dz/dt = w = \frac{2\pi}{\tau} h \cos \frac{2\pi t}{\tau} \quad (20)$$

from which

$$w^2 = \frac{4\pi^2}{\tau^2} h^2 \cos^2 \frac{2\pi t}{\tau} \quad (21)$$

Integrating both sides of Eq. (21) with respect to time

$$\int_{t=0}^{t=\tau/4} w^2 dt = \frac{4\tau^2 h^2}{\tau^2} \int_{t=0}^{t=\tau/4} \cos^2 \frac{2\pi t}{\tau} dt$$

and dividing both sides by  $\tau/4$ , the expression for the mean square vertical velocity becomes

$$\overline{w^2} = \frac{2\pi^2 h^2}{\tau^2} \quad (22)$$

The equation for root mean square vertical velocity is then

$$\sqrt{\overline{w^2}} = \frac{\sqrt{2} \pi h}{\tau} \quad (23)$$

Expressions for  $h$  in terms of the slope of an isentropic surface and for  $\tau$  in terms of stability and wind shear will now be derived.

In a turbulent source region, energy for wave motion is continually being produced at a constant rate. As the air passes downwind beyond this region, the wave energy may be gradually dissipated by mixing with air outside the turbulent layer, but any such dissipation will not be considered here. An expression for the rate of production of wave energy per unit mass can be defined by

$$\frac{dE}{dt} = \frac{1}{\tau/4} \int_{t=0}^{t=\tau/4} d/dt (w^2/2) dt$$

Substituting in the right hand side from Eq. (21),

$$w^2/2 = \frac{2\pi^2}{\tau^2} h^2 \cos^2 \frac{2\pi t}{\tau} \quad (24)$$

we find

$$\overline{dE/dt} = \frac{8\pi^2 h^2}{\tau^3} \quad (25)$$

Hence the resulting wave amplitude, and from Eq. (22) the mean square vertical velocity, depend upon the mean rate at which energy becomes available. This energy for wave motion must be supplied by the initial perturbation.

In fluid mechanics, it is known that a submerged object, such as a weir, may disturb the flow by producing a standing wave over the object. When the wave amplitude is large relative to the depth of the fluid, the familiar hydraulic jump occurs. Upon approaching the submerged object, the flow is subjected to contraction and acceleration. This is followed by a rapid expansion and deceleration in the standing wave to the lee of the obstruction, e.g., see King (20). Air flowing over a mountain range or mound of cold air appears to behave similarly, e.g., see Queney et al. (21).

In general, any change in conditions of flow which is accompanied by contraction or expansion of the depth of fluid produces a series of waves on the sloping fluid surface. If the change occurs suddenly, such as when the fluid passes over a fixed submerged object, an abrupt standing wave usually occurs. In a stably stratified compressible fluid of great depth, contraction or expansion would be associated with mass divergence and hence vertical motion. Assuming adiabatic temperature changes, vertical motion would produce horizontal temperature gradients and hence sloping isentropic surfaces. Therefore, energy for wave formation might be a function of the mass divergence which is related to the horizontal gradients of both density and velocity. An expression which takes into account both mass divergence and vertical motion is the pressure tendency equation, Homboe, et al. (22) which may be written as,

$$(\partial P / \partial t)_z = -g \int_z^\infty \nabla_H \cdot (\rho V) \delta z + (g \rho w)_z \quad (26)$$

In Eq. (26), the local pressure tendency at any height  $z$  can be represented explicitly as the change in weight of the vertical air column above. This change is caused in part by the horizontal divergence in mass above the level and in part by the vertical transport of mass through the level. The horizontal mass divergence is defined by

$$\nabla_H \cdot (\rho V) = \partial/\partial x (\rho u) + \partial/\partial y (\rho v) \quad (27)$$

and so is dependent upon the horizontal gradients of velocity and density.

In a stationary system, such as a mountain wave, the horizontal density and velocity gradients are fixed and the local pressure tendency term in Eq. (26) is zero. An expression for the rate of energy production per unit mass  $dE/dt$  can be obtained by dividing the remaining two terms in the pressure tendency equation by the mean density, hence

$$dE/dt = g/\bar{\rho} \int_{z_1}^{z_2} \nabla_H \cdot (\rho V) \delta z = g w \quad (28)$$

where the integration is taken over the thickness of the layer with horizontal density gradients, i.e., the layer undergoing vertical motion. The inference is made that whenever a perturbation in the flow causes a vertical displacement of a stably stratified layer, energy for wave motion is produced, and according to Eq. (28) the mean rate at which this energy becomes available is directly proportional to the vertical velocity associated with the initial perturbation.

For an adiabatic process, an estimated value for vertical velocity can be obtained from the product of the horizontal wind speed and the vertical slope of the isentropic surfaces in the direction of the wind. Of course, for air to move vertically along such a sloping surface, it must be moving relative to the surface, i.e., moving faster or slower than the apparent forward motion of the isentropic surfaces. In a stationary system, such as a standing wave, the isotherms remain stationary and the sloping isentropic surfaces define the trajectories of the air passing through the system. If  $s$  is the vertical slope of an isentropic surface and  $u_r$  is the component of the mean wind speed in the direction of the slope, then the absolute value of the vertical velocity can be represented by

$$|w| = |u_r s| \quad (29)$$

In the special situation where the isotherms on a constant pressure level are oriented at right angles to the height contours and are stationary in time, then  $u_r$  is simply equal to the mean wind speed  $\bar{u}$ .

Upon substituting this expression for  $w$  in Eq. (28), we find,

$$dE/dt = g |u_r s| \quad (30)$$

where  $u_r$  and  $s$  are mean values taken over the layer of interest. Upon equating this expression to the rate of wave energy production in Eq. (25), we find

$$g |u_r s| = \frac{8\pi^2 h^2}{\tau^3} \quad (31)$$

and upon rearranging terms, the expression for amplitude  $h$  is

$$h^2 = \frac{g}{8\pi^2} |u_r s| \tau^3 \quad (32)$$

Substituting for  $h^2$  from Eq. (22), the expression for mean square vertical velocity becomes

$$\bar{w}^2 = g \frac{\tau}{4} |u_r s| \quad (33)$$

Substituting for  $\tau$  from Eq. (18), we find

$$\bar{w}^2 = \frac{g\lambda}{4\bar{u}} |u_r s| \quad (34)$$

This expression states that for a given set of initial conditions, i.e., given values for  $u_r$ ,  $s$  and  $\bar{u}$ , the mean square vertical velocity associated with the wave can be expressed as a function of wavelength only.

An expression for wavelength in terms of local stability and wind shear will now be postulated. In a stable atmosphere, the frequency  $\nu$  is defined by

$$\nu^2 = \frac{g}{T} (\gamma - \gamma_d) = \frac{g}{\theta} \partial \theta / \partial z \quad (35)$$

where  $\theta$  is the potential temperature. Substituting from Eqs. (17) and (18), the expression for wavelength is found to be

$$\lambda = \frac{2\pi \bar{u}}{\sqrt{g/\theta \partial \theta / \partial z}} \quad (36)$$

However, this equation does not take into account the possible effects of vertical wind shear. It is well known that shear acts to restrict the vertical dimensions of turbulent eddies even in the absence of stability. One method of introducing the effect of shear into the model is to modify Eq. (36) to read

$$\lambda = \frac{2\pi \bar{u}}{B} \quad (37)$$

where  $B^2 = \frac{g}{\theta} \frac{\partial \theta}{\partial z} + \left( \frac{\partial \vec{u}}{\partial z} \right)^2$ . The term  $\frac{\partial \vec{u}}{\partial z}$  is the vector wind shear.

Upon substituting Eq. (37) for  $\lambda$  in Eq. (34), the expression for root mean square vertical velocity becomes

$$\sqrt{\overline{w^2}} = \sqrt{\frac{\pi}{2} \frac{g}{B} |u_r s|} \quad (38)$$

The slope of the isentropic surfaces can be calculated from three dimensional fields of temperature and pressure, or by analyzing the height contours of an isentropic surface. The difficulty here is the tendency to equally space the height contours between points of observation where actually they may be crowded somewhere in between. The thermal wind equation may prove helpful in deciding whether the mean temperature gradient through a layer is concentrated near a point of observation. The thermal wind equation may be written

$$\partial \rho / \partial n = \frac{f \rho}{g} \frac{\partial \vec{u}}{\partial z} \quad (39)$$

where  $f$  is the coriolis parameter and equals  $2 \Omega_e \sin \phi$  or about  $10^{-4}$  at mid-latitudes. The  $n$ -direction is a horizontal vector oriented perpendicularly to the wind shear vector. The expression for the slope is

$$s = \frac{\partial \rho}{\partial n} / \frac{\partial \theta}{\partial z} \quad (40)$$

and of course,  $u_r$  in Eq. (38) is the component of the mean layer wind in the  $n$ -direction. Substituting Eq. (39) in this expression for  $S$ , we get

$$s = \frac{f \theta}{g} \frac{\vec{\Delta u}}{\Delta \theta} \quad (41)$$

where  $\Delta \vec{u}$  is the magnitude of the vector wind shear and  $\Delta \theta$  is the difference in potential temperature through the same vertical layer, e.g., a layer between standard wind reporting levels.

When computing RMS vertical velocities, Eq. (38) could be used. However, in order to determine whether the computed value is reasonable,  $\lambda$  may be computed from Eq. (37) and it should have a value, on the average, of a few thousand meters. Next  $S$  can be computed from Eq. (41), or in areas between data stations from an isentropic height analysis.  $S$  should have an average value of the order of  $10^{-3}$ . Then a value for  $h$  can be obtained from Eq. (32) upon substituting  $\tau = \lambda / \bar{u}$ . It should average around one to a few hundred meters. Finally, the RMS vertical velocity can be obtained from Eq. (23).

#### Examples of World Wide Application of Both Models

In order to test the applicability of both models, it was decided to analyze data for a sample of the HICAT turbulence tests which met the following criteria:

1. The radiosonde and rawinsonde data were concurrent with the aircraft flights.
2. The observed turbulence occurred over or very near a radiosonde station.
3. The tests include at least three geographical areas.
4. The tests include observed turbulence intensities ranging from light to severe.

The tests chosen are listed in Table III along with the particular runs and geographical areas. The areas are Western United States, Hawaii and Eastern Australia. In the Australian Test 102, there were two altitude bands with turbulence - at 60 K ft near Brisbane and at 66 K ft near Williamstown - so both are treated as separate samples. As shown in Figures 29 and 30, two isentropic height analyses were made corresponding approximately to these two altitudes. In the other geographical areas, the slope term was obtained from the thermal wind equation.

For several of these tests, no RMS vertical velocity data were obtained. However, RMS incremental cg normal acceleration data are available. These data are based on acceleration of the aircraft and hence do not include the component representing the acceleration of the air relative to the aircraft. Nevertheless, the acceleration of the aircraft should be highly correlated with the intensity of turbulence so that computed RMS accelerations based on the proposed model should correlate well with the aircraft acceleration data if the models are applicable. In the previous section, an equation was derived for RMS vertical acceleration which an aircraft would experience if it responded completely to all changes in vertical motion of the air. As the aircraft response is usually less, the computed RMS acceleration should tend to be high. The derived Eq. (15) expressed in terms of the acceleration of gravity is

$$\text{RMS } \Delta a_N/g = \frac{2\sqrt{2} \pi^2 h \bar{u} v_s}{g \lambda^2} \quad (42)$$

where  $v_s$  is the aircraft speed<sup>2</sup>.

As shown in Table III, the wavelengths, amplitudes and RMS  $\Delta a_N/g$  values are computed using both models. The observed RMS  $\Delta a_N/g$  values are given in the last columns in terms of the average value for all runs in the area and the range of average values experienced over all the individual runs.

---

<sup>2</sup>Actually  $v_s$  is the speed of the aircraft relative to the wave pattern. In a stationary wave,  $v_s$  is the ground speed, i.e., the speed relative to the air passing through the wave. Since the speed of the aircraft is always much greater than the wind speed and in most instances any possible progression of the wave pattern will be unknown, any correction for the value of  $v_s$  does not seem justified at this time. Nevertheless, it may account for the occasional differences in intensity of turbulence noted by pilots between downwind and upwind runs. These differences were especially prevalent in Australia where the wind speeds were generally greater than in other areas.

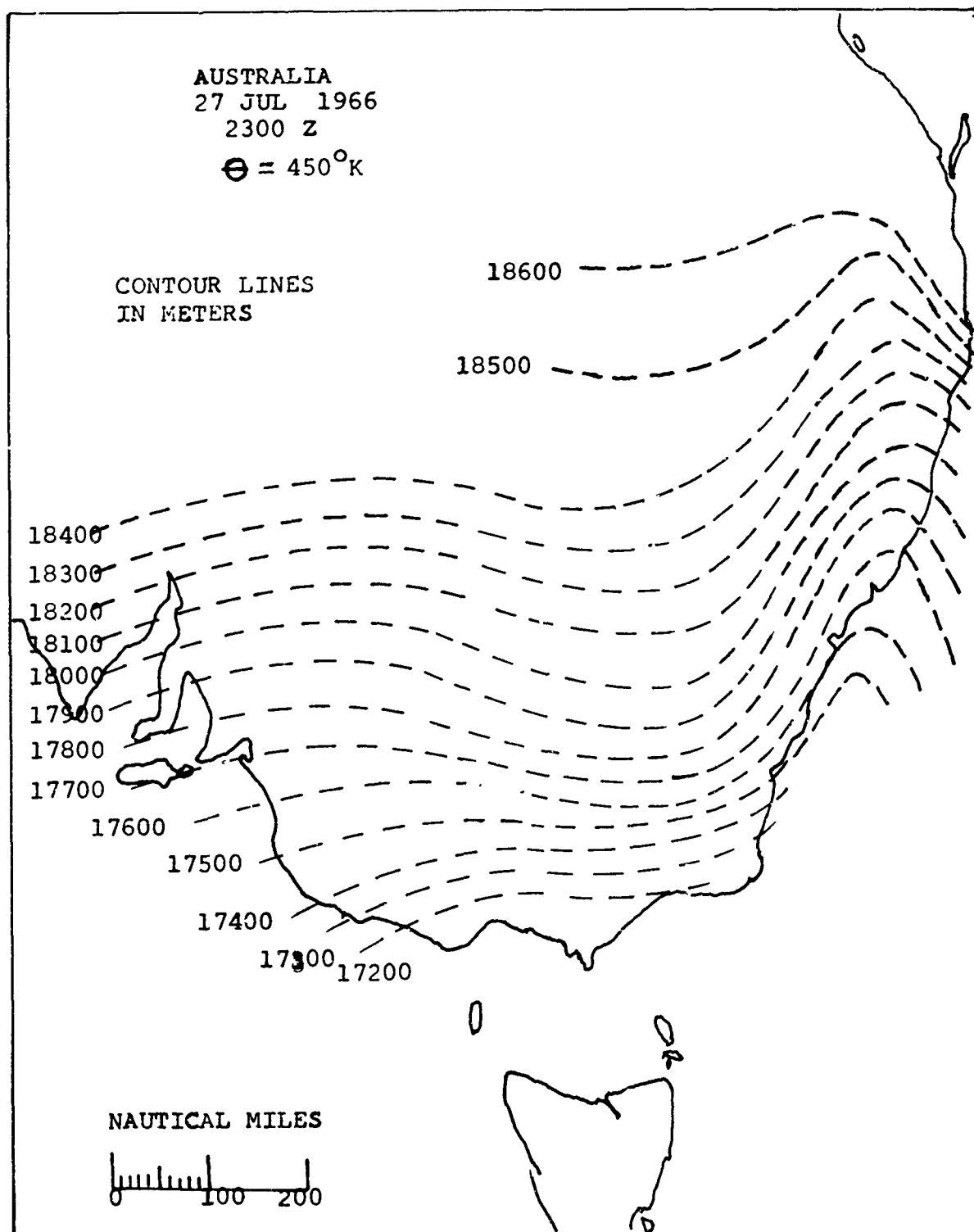


Figure 29. Isentropic Height Analysis for  $\Theta = 450^{\circ}\text{A}$ , Southeastern Australia.  
27 Jul 1966. 2300Z (Flight 102)

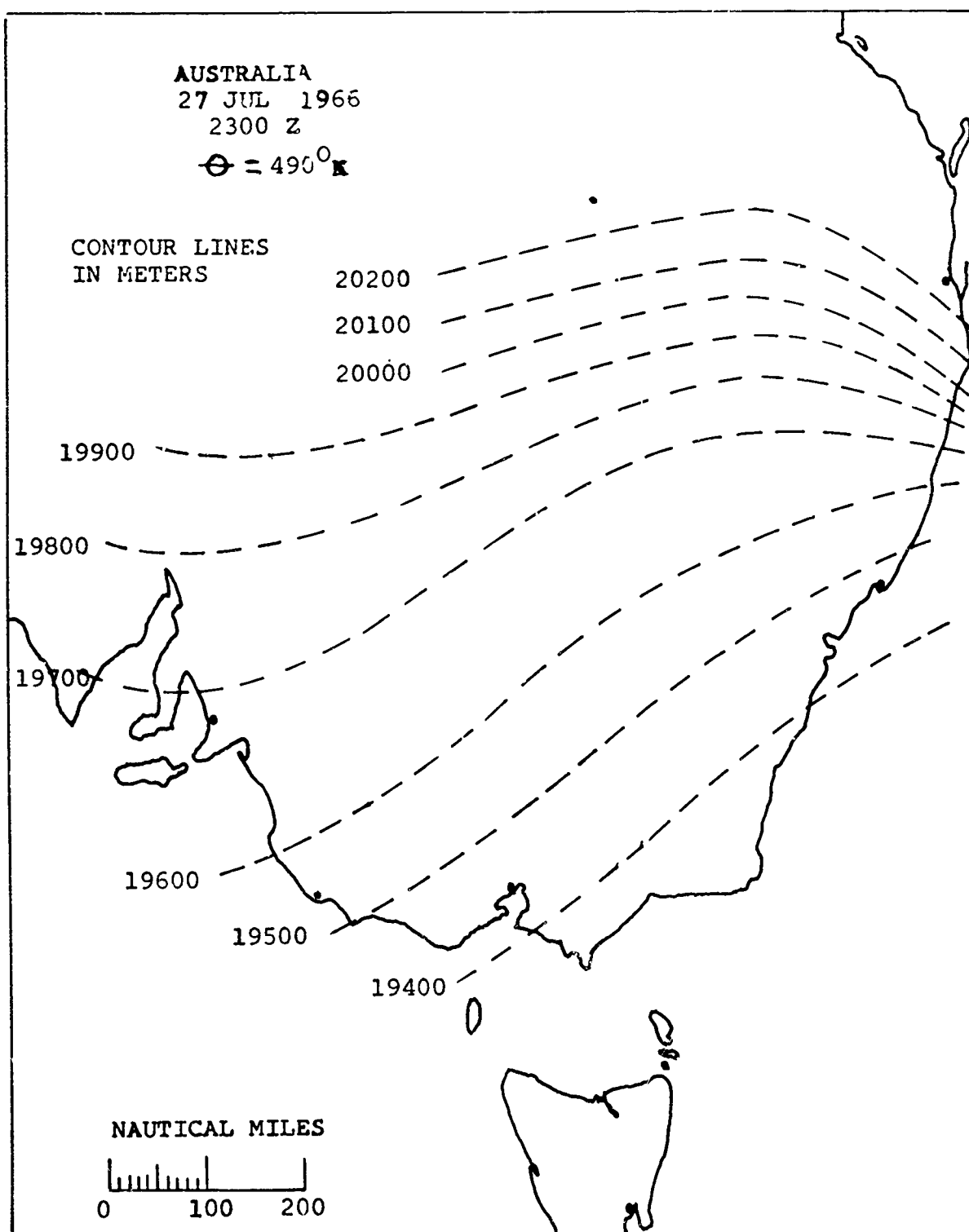


Figure 30. Isentropic Height Analysis for  $\Theta = 490^{\circ}\text{A}$ , Southeastern Australia, 27 Jul 1966, 2300Z (Flight 102)

TABLE III  
COMPARISON OF COMPUTED AND OBSERVED RMS  $\Delta a_N/g$  VALUES

Test No. and Area	Model	Wave Length (M)	Amplitude (M)	RMS $\Delta a_N/g$	Average Observed RMS $\Delta a_N/g$	
					Average of Runs	Range over all Runs
77 Hawaii	I	7248	213	.043	.036	.027-.050
	II*	4355	144	.081	(Light)	
102 Runs 12-14 Williamstown Australia	I	4933	183	.082	.056	.050-.059
	II**	4605	135	.069	(Light to Moderate)	
114 Las Vegas Nevada	I	2776	147	.140	.060	.051-.078
	II*	3665	129	.068	(Moderate)	
102 Runs 2-9 Brisbane Australia	I	1882	69	.115	.063	.038-.095
	II**	3044	85	.060	(Moderate)	
267 Albuquerque New Mexico	I	3638	178	.169	.083	.034-.162
	II*	3851	235	.138	(Severe)	

\*Slope determined from geostrophic thermal wind shear

\*\*Slope determined from isentropic height analysis

The general agreement between corresponding computed quantities for the two methods is good considering the fact that the two models involve entirely different data. In Model I, the data are obtained directly from the radiosonde temperature-height curve; while in Model II, the computations are based upon an assumed rate of vertical ascent along a sloping isentropic surface.

In general, it appears that the range of values calculated by Model I yields RMS  $\Delta a_N/g$  values which correlated slightly better with the indicated intensities of turbulence, i.e., light to severe. They are also greater than the average, as was expected,

but within a factor of two of the observed value for the most turbulence run in each area. On the other hand, Model II yields RMS  $\Delta a_N/g$  values which are in general closer to the observed average values of all the runs in each area but generally less than the observed maximum average value.

## STATISTICAL STUDIES

The literature describing the results of statistical and case history studies of relationships between meteorological conditions and high altitude clear air turbulence is summarized in Table I, pg. 3-5. Generally, the meteorological conditions have been expressed explicitly as functions of the atmospheric temperature, pressure, and wind fields. The temperatures, pressures, and winds at HICAT flight levels are measured at stations that are spaced two or more hundreds of miles apart. Temperatures, heights of pressure surfaces, and winds are reported for specific intervals. The observations are made at 00Z and 12Z time except in some areas in which only the 00Z observations are made. Horizontal and vertical temperature gradients and wind shears are derived quantities. With few exceptions the horizontal temperature gradients and the horizontal wind shears are obtained by drawing isolines on charts. This method introduces a subjective element into the analysis. In the following discussion an attempt has been made to keep the subjective element to a minimum.

The criteria used for selecting the cases for study are as follows:

A "run" as given by Crooks, Hoblit and Prophet (2) was designated as a sample of turbulence if the run was within 100 miles of a RAOB or RAWIN station. A sample was designated "non-turbulent" if no "run" was shown within 150 miles of a station and the flight track was within 100 miles of a station.

All such "turbulence" and "no turbulence" cases from HICAT flights 54-179 were used in the study. These flights were made in Australia, New Zealand, Hawaii, Alaska, California, Massachusetts and Puerto Rico. Frequency distributions for eight functions of the temperature and wind fields are shown in Figures 31 through 32. The interval limits were chosen to produce approximately the same number of cases in each interval. Chi-square tests with four degrees of freedom and Kolmogorov-Smirnov tests were used to indicate the degree to which the turbulence and no turbulence cases may be considered to come from differing populations.  $\chi^2 = 9.49$  is the critical value for  $\chi^2$  with 5 degrees of freedom. Degrees of freedom are determined by the number of class intervals. For a  $\chi^2$  value calculated from the observed data greater than 9.49, the hypothesis that the two frequencies are from the same population is rejected at the 95% confidence level. In the Kolmogorov-Smirnov test,  $K-S = 1.36$  is the critical value above which the null hypothesis that the two frequencies come from the same population is rejected at the 5% level. If the critical statistic obtained from the observed data is less than 1.36, the null hypothesis is accepted (the two frequencies are assumed to come from the same distribution). The results of the two tests differ mainly because of the greater power of the Kolmogorov-Smirnov test which, unlike the Chi-square test, considers sample size. The tests are an estimate of by how much

the two distributions differ. In both the Chi-square and Kolmogorov-Smirnov tests larger numbers for the critical value indicate less chance that the distributions were drawn from the same population.

The results obtained by applying the Chi-square and the Kolmogorov-Smirnov tests are presented in Table IV.

TABLE IV

CHI-SQUARE ( $\chi^2$ ) AND KOLMOGOROV-SMIRNOV (K-S) TESTS APPLIED TO METEOROLOGICAL VARIABLES FOR HICAT FLIGHTS 54 THROUGH 179

		$\chi^2$ (Deg. Freedom: 4)	K - S
Critical Values	Probability = .95	9.49	1.36
	Probability = .99	13.30	1.63
$\bar{V}$	Mean scalar wind speed (5000 to 10,000 ft layers)	28.8	1.08
$\Delta V / \Delta z$	Vertical scalar wind shear	86.3	2.30
$ \Delta \bar{V}  / \Delta z$	Magnitude of vertical vector wind shear	126.5	2.69
$\bar{V} ( \Delta \bar{V}  / \Delta z)$	Product mean scalar wind speed and vertical vector wind shear	89.8	2.27
$\partial T / \partial z$	Vertical temperature gradient at flight level	76.8	1.94
$ \Delta T  / \Delta z$	Absolute value of temperature change (layer $\pm$ 2000 ft of flight level)	65.1	2.05
$(\partial T / \partial z)^*$	Min vertical temperature gradient (layer $\pm$ 2000 ft of flight level)	90.4	2.11
Ri	$\frac{g}{\theta} (\partial \theta / \partial z) ( \Delta \bar{V}  / \Delta z)^{-2}$ , $\partial \theta / \partial z$ is min $\pm$ 2000 ft of flight level	144.1	2.89

Figure 31a and the first row in Table IV indicate that at the altitudes of the HICAT flights no significant distinction can be made between the population of turbulence and non-turbulence cases for scalar winds. The scalar winds at the flight altitudes were obtained by interpolating between the winds reported by the meteorological station. This was necessary because the altitudes for reporting the winds do not correspond with the flight altitudes. The data presented in Figure 31a does,

however, justify further study with a larger sample for the strong wind cases. See, e.g., Briggs and Roach (23).

Figures 31b and c and rows 2 and 3 of Table IV indicate the vertical vector or the scalar wind shear may be used to separate, to a significant degree, the populations of turbulence and non-turbulence. The use of the vector wind shear produces the greater success in the separation of the populations. This conclusion is derived from the values in Table IV for the Chi-square test and the Komolgorov-Smirnov test. In 51 cases of the vertical vector shear equal to or less than 2 kts/1000 ft 7 were turbulent and 44 non-turbulent. There were twenty instances of the vertical vector shear equal to or greater than 5 kts/1000 ft. Of these, eighteen were cases of turbulence.

The product of the scalar wind and the vertical vector shear (Figure 31d and row 4 of Table IV) has less value as an aid for the separation of turbulence and non-turbulence populations than the vector wind shear alone.

Several methods were employed in analyzing the vertical temperature gradient relationship to turbulence:

- a) The vertical gradient at turbulence level (Figure 32a);
- b) The absolute value of the average gradient over a layer  $\pm$  2000 ft above and below the level of turbulence (Figure 32b);
- c) The minimum gradient in any layer within  $\pm$  2000 ft of the level of turbulence (Figure 32c).

Results suggest a relationship exists between large decreases in actual temperature (small potential temperature gradients) with height and turbulence (Figure 32a), although several cases of turbulence were accompanied by large temperature increases (stable layers). Only 3% of the non-turbulent cases had vertical temperature gradients  $< -1^{\circ}\text{C}/1000$  ft, compared with 19% in turbulence. Changes greater than  $+1^{\circ}\text{C}/1000$  ft were associated with 14% of the non-turbulent and 22% of the turbulent cases. There is a definite trend towards the association of large fluctuations in vertical temperature gradients with turbulence. Conversely, uniform temperature gradients are more likely to be accompanied by smooth flying conditions.

Richardson's Number (Figure 32d) may be used relatively successfully to distinguish between turbulence and non-turbulence. Turbulence was recorded in 32 of 42 cases with  $Ri < 15$ . It is apparent, however, that small values of  $Ri$ , recommended by various authors as the necessary criterion for the occurrence of turbulence in the troposphere, are rarely observed in the stratosphere. There was but 1 case in 115 of  $Ri < 1$ , a turbulence criterion used by Briggs and Roach (23) and Endlich and Mancuso (24) but rejected by Reiter and Lester (25) due to lack in quality of wind and temperature measurements in the stratosphere.

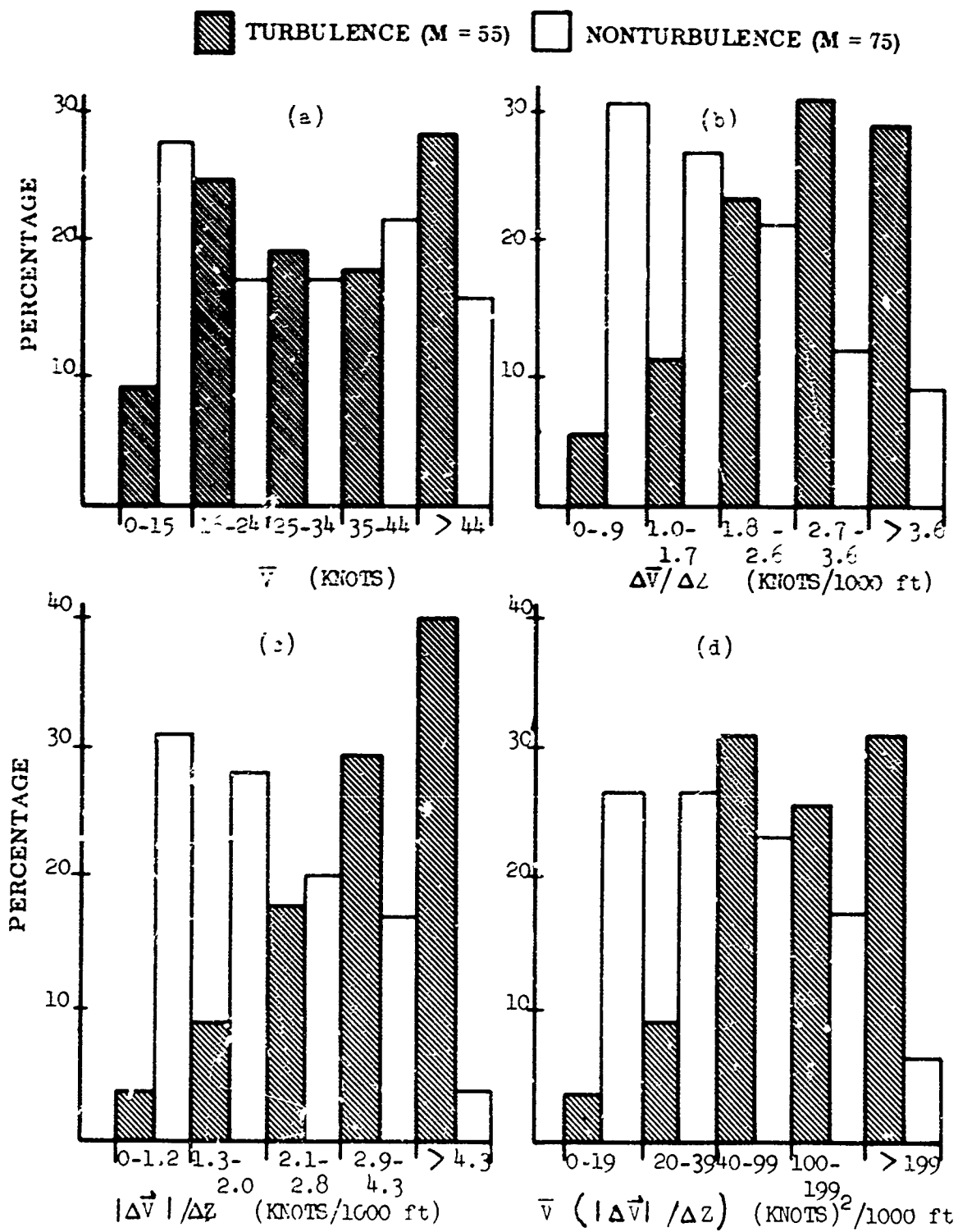


Figure 31. Frequency Distribution of Meteorological Variables for Turbulent and Nonturbulent Cases

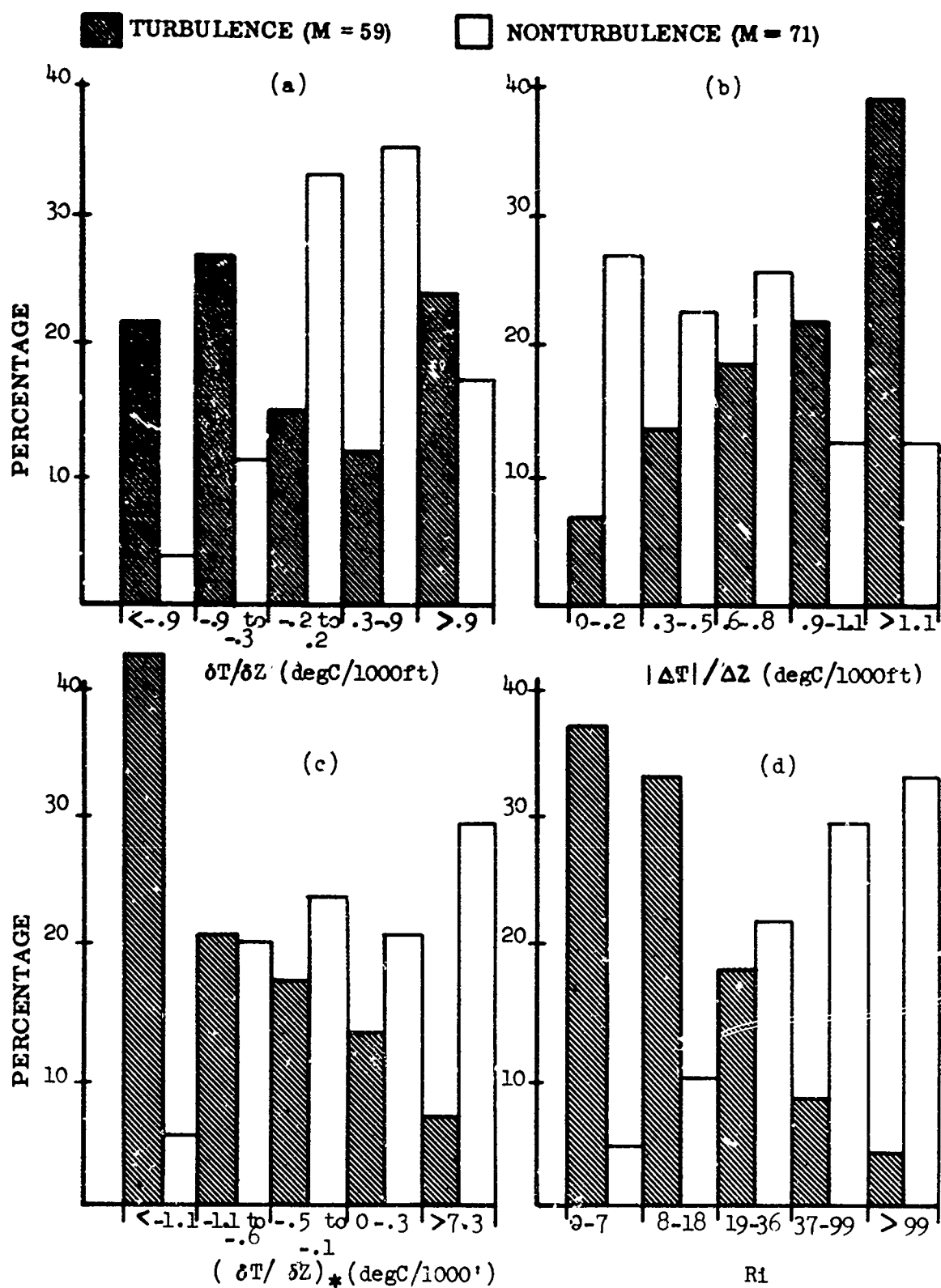


Figure 32. Frequency Distribution of Meteorological Variables for Turbulent and Nonturbulent Cases

## THE DEVELOPMENT OF A PRACTICAL PROCEDURE FOR FORECASTING HIGH ALTITUDE CLEAR AIR TURBULENCE

The problem of developing practical methods of forecasting high altitude clear air turbulence has been approached from three points of view; theoretical, statistical, and that of a synoptic meteorologist. The theoretical work was presented in Section V and the statistical work in Section V. In March 1967 a meteorologist was assigned to the WU-2 flight crew. This assignment provided an excellent opportunity for a meteorologist to work closely with the pilots in selecting the HICAT search areas, the search procedures, and to modify the search plan in mid-flight whenever this appeared to be desirable. In addition, the meteorologist obtained direct practical experience in operating under field conditions.

The method of preparing the forecasts of the HICAT have changed as the program progressed. These changes have been associated with differing communication and meteorological organizations at the various bases of operation and with meteorological conditions and added experience. The present state of development of a forecasting procedure is illustrated by two case histories described in detail below.

### Case of Severe Clear Air Turbulence

#### Synoptic Weather Patterns

The weather pattern generally believed to favor the production of CAT below the tropopause is typically that in which a well established low pressure center near the 500 mb level moves across the western states. The polar jet stream dips far to the south, bringing cold air at most levels from the surface to the tropopause. If the trough persists through the tropopause, the temperatures in the stratosphere over the southern station portion increase. At the 70 n level alternate north-south zones of relatively high and low temperatures are observed.

Synoptic patterns such as these, which are primarily a winter and spring phenomena, seem to be related to conditions that produce abundant clear air turbulence in both the troposphere and stratosphere.

These typically CAT producing synoptic patterns were observed to occur during two different periods in November and December over the western United States. The first period was from 12 to 23 November 1967 and the second from 29 November to 2 December 1967.

Moderate to severe CAT was encountered at approximately 50,000 feet over Santa Barbara, California, during flight number 257 on 17 November 1967. A post flight analysis of this mission provided clues that were utilized in refining forecast procedures. These procedures were applied at the beginning of the next favorable turbulent period. Results of the HICAT flights during this period were as follows:

<u>Test No.</u>	<u>Date</u>	<u>Place</u>	<u>Turbulence Rating</u>	<u>Incremental c. g. Acceleration</u>
262	29 Nov 1967	Albuquerque, N.M.	Moderate	(+ .40g)
264	30 Nov 1967	Grand Junction, Colo.	Severe	(+ .65g)
265	30 Nov 1967 (night)	Grand Junction, Colo.	Severe	(+ .65g)
266	1 Dec 1967	Albuquerque, N.M.	Severe	(+ 1.0g, -0.7g)
267	1 Dec 1967	Albuquerque, N.M.	Severe	(+ .60g)

#### Forecast Procedure

Prior to the beginning of HICAT operations on 16 November 1967 from Edwards Air Force Base, California, a number of meteorological analyses techniques had been tested with varying degrees of success. Analyses of tropopause slopes, horizontal and vertical wind shear, Richardson Numbers, isobaric surface, pressure height changes, and thickness patterns did not indicate a pattern of consistency insofar as a reliable forecast technique was concerned. One notable feature, however, did stand out in its relation to turbulence and this was a distinctive isothermal pattern. With this idea in mind it was decided to analyze three surfaces (100, 70, and 50 mb) for isotherms and wind streamlines only. These charts indicated that the gradient of temperature along the constant pressure surface varied to a significant degree.

It can be stated with a reasonable degree of confidence, that CAT will occur in an area where the temperature gradient is large. The critical value of the horizontal temperature gradient appears to be about 5°C per 120 nm. It is significant that the Meteorological Department of Trans World Airlines in their Technical Bulletin Number 61-2, observed such a horizontal temperature gradient to be associated with CAT in the tropospheric range of 15,000 - 40,000 feet. For gradients less than this turbulence should be light to non-existent. For gradients higher than this, moderate or severe CAT may be expected.

This is considered a good generalization but should be qualified to some extent. For example, it cannot be stated unequivocally that these criteria would apply to CAT associated with convective activity or a mountain wave although there may very well be a similar relation.

#### Constant Pressure Surface Analysis

Figure 33 shows the route of the flight made on 1 Dec 1967. The pilot flew to Albuquerque, New Mexico, located the turbulence directly over Albuquerque and began a vertical search pattern that a short time later resulted in the location of severe CAT. Figure 34 is the pattern at the 70 mb level that was associated with the severe turbulence.

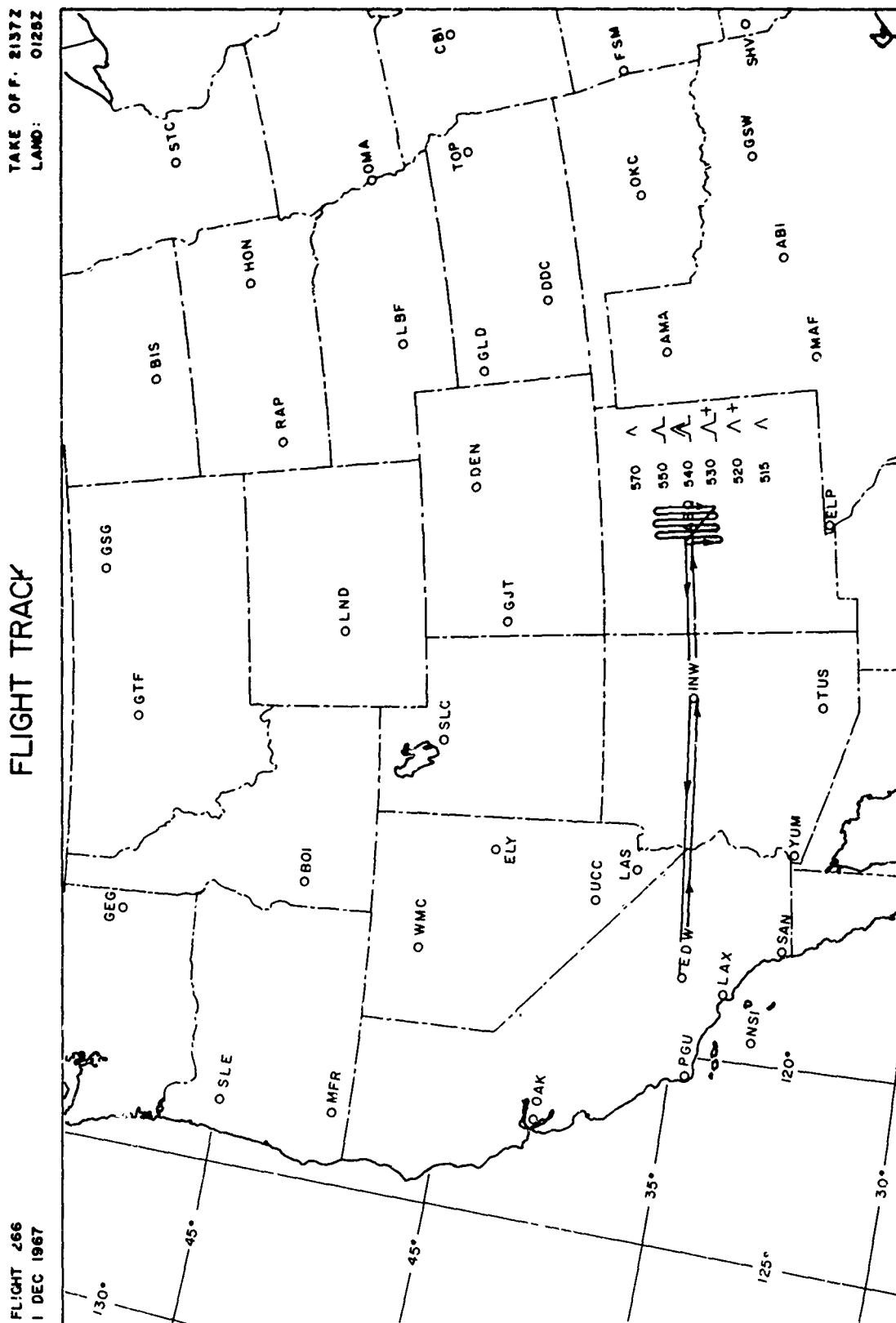
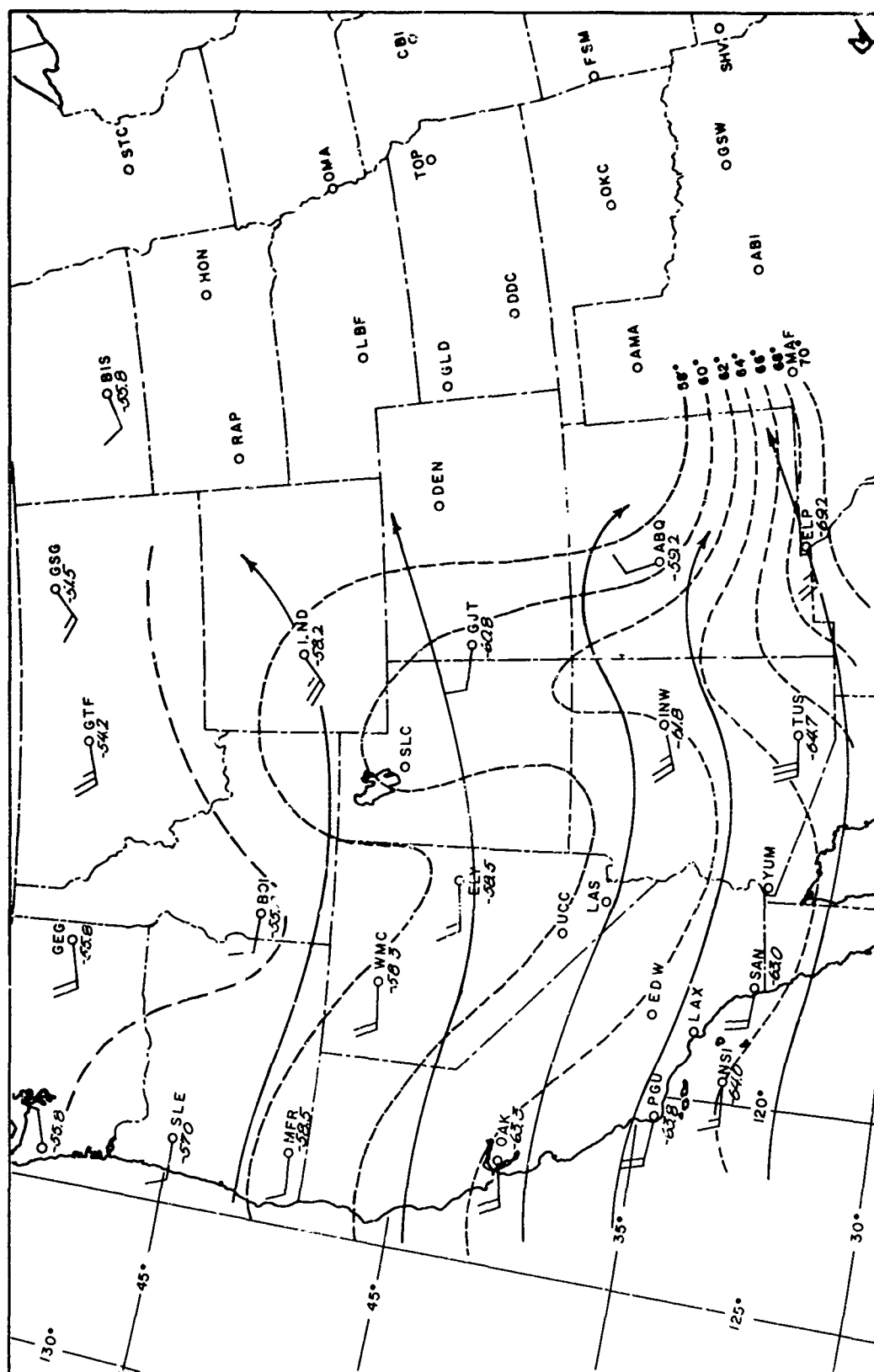


Figure 33. Flight Track, Flight 266, 1 Dec 1967



70 mb

00Z, 2 DEC 1967

**Figure 34. 70 mb Analysis, 2 Dec 1967, 0000Z**

The analysis of the 70 mb level in Figure 34 shows the strong horizontal temperature gradient that exists between Albuquerque, New Mexico, and El Paso, Texas, at 00Z 2 December 1967. These RAOB's were being taken at the same time severe CAT was encountered over Albuquerque on Test 266. The horizontal temperature gradient on the constant pressure surface of 70 mb was approximately  $10^{\circ}/180$  nm. This is considerably above the critical value of  $5^{\circ}/120$  nm mentioned above. It should be noted that the 70 mb chart in Figure 34 was not that used for the forecast for Test 266 but was the analysis nearest the actual time the aircraft was over Albuquerque. Twelve and twenty-four hour analyses, prior to the 00Z chart did show, however, a steady progression and intensification of the horizontal temperature gradient across Utah, Arizona and New Mexico.

Figure 35 shows a plot of temperature as a function of pressure over Grand Junction, Colo., Albuquerque, New Mexico, and El Paso, Texas for 00Z 2 Dec 1967 and corresponding to the time of the horizontal 70 mb surface analysis (Figure 34). The irregular appearance of the sounding is quite obvious as compared to that of Grand Junction, Colo., which Figure 34 shows to be in an area of small horizontal temperature gradient. The turbulence over Albuquerque was reported by the pilot to be light to severe at altitudes 51,000 to 57,000 feet. The altitudes reported were those read directly from the altimeter which was set at 29.92 inches.

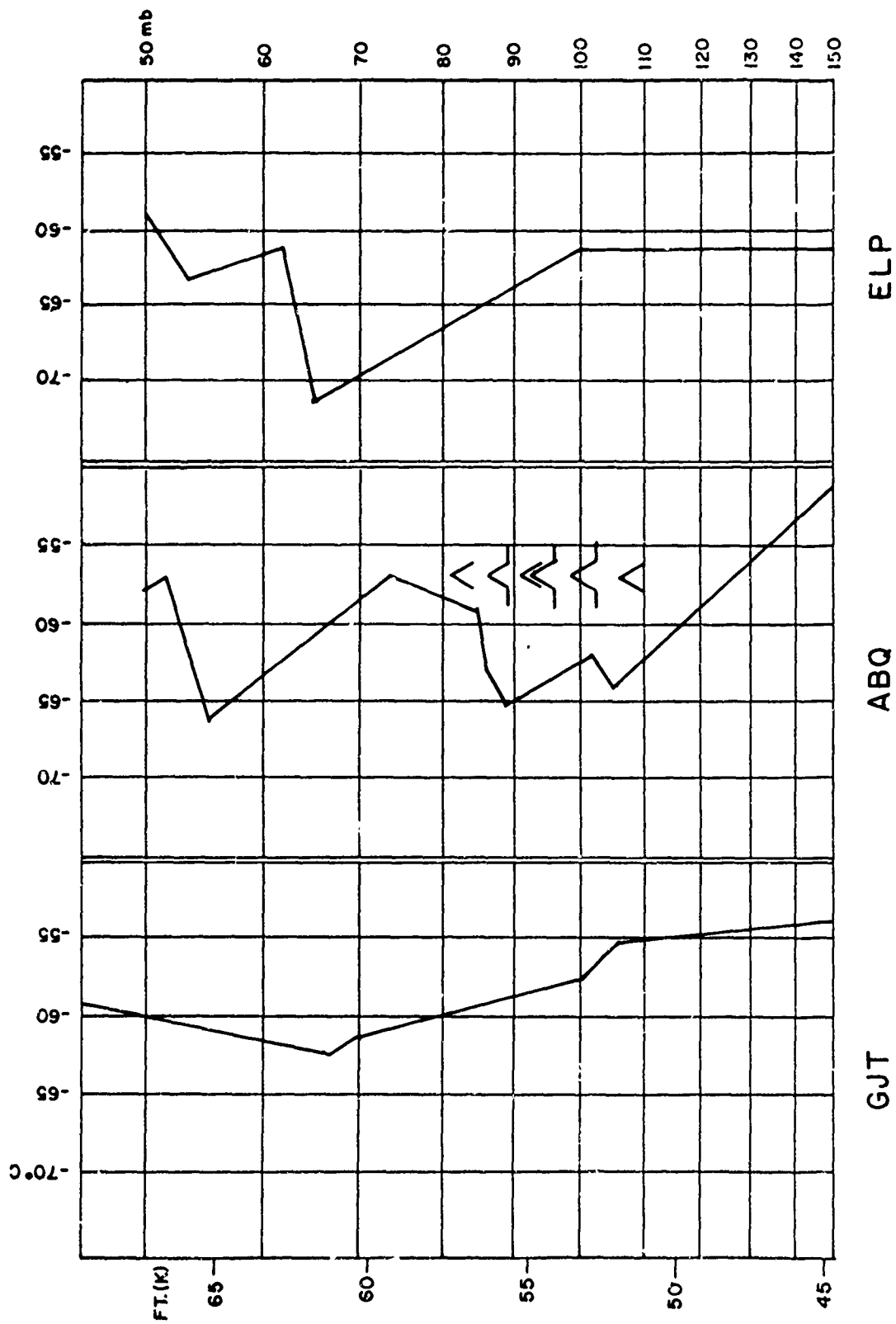
The fact that CAT is associated with a strong temperature inversion has been recognized for some time. S. M. Serebreny (26) stated "Turbulence is a result of an abrupt increase or decrease of wind velocity in the thermal gradient. The stronger the vertical shear the more stable the lapse rate". Frederick B. Haymond (19), in evaluating 953 forecasts for 110 U-2 flights out of Davis Monthan Air Force Base, Arizona, observed that excellent forecast verification was achieved by predicting CAT to occur in areas and near levels of inversions as follows:

1.5°C/1000 ft	No CAT
1.5°C to 2.5°C/1000 ft	Light CAT
2.5°C to 4.0°C/1000 ft	Moderate CAT
4.0°C/1000 ft	Severe CAT

#### Isentropic Analysis

Potential temperature is a function of pressure and temperature, hence charts of surfaces of equal potential temperature (isentropic surfaces) are simply an alternate method of indicating temperature gradients. Often isentropic cross-sections are the most convenient method of determining the extent of baroclinicity. Reiter and Hayman (27), commenting in the paper "The Nature of Clear Air Turbulence", stated "It became evident, however, that all cases of moderate and severe CAT were located in, or very close to, the axis of a drop of the isentropic surfaces - the isentrope trough".

Figure 36 is an isentropic cross-section through Salt Lake City, Utah, Grand Junction, Colorado, Albuquerque, New Mexico, and El Paso, Texas, as of 00Z



RAOB 00Z, 2 DEC 67  
Figure 35. Temperature Soundings, 2 Dec 1967, 0000Z

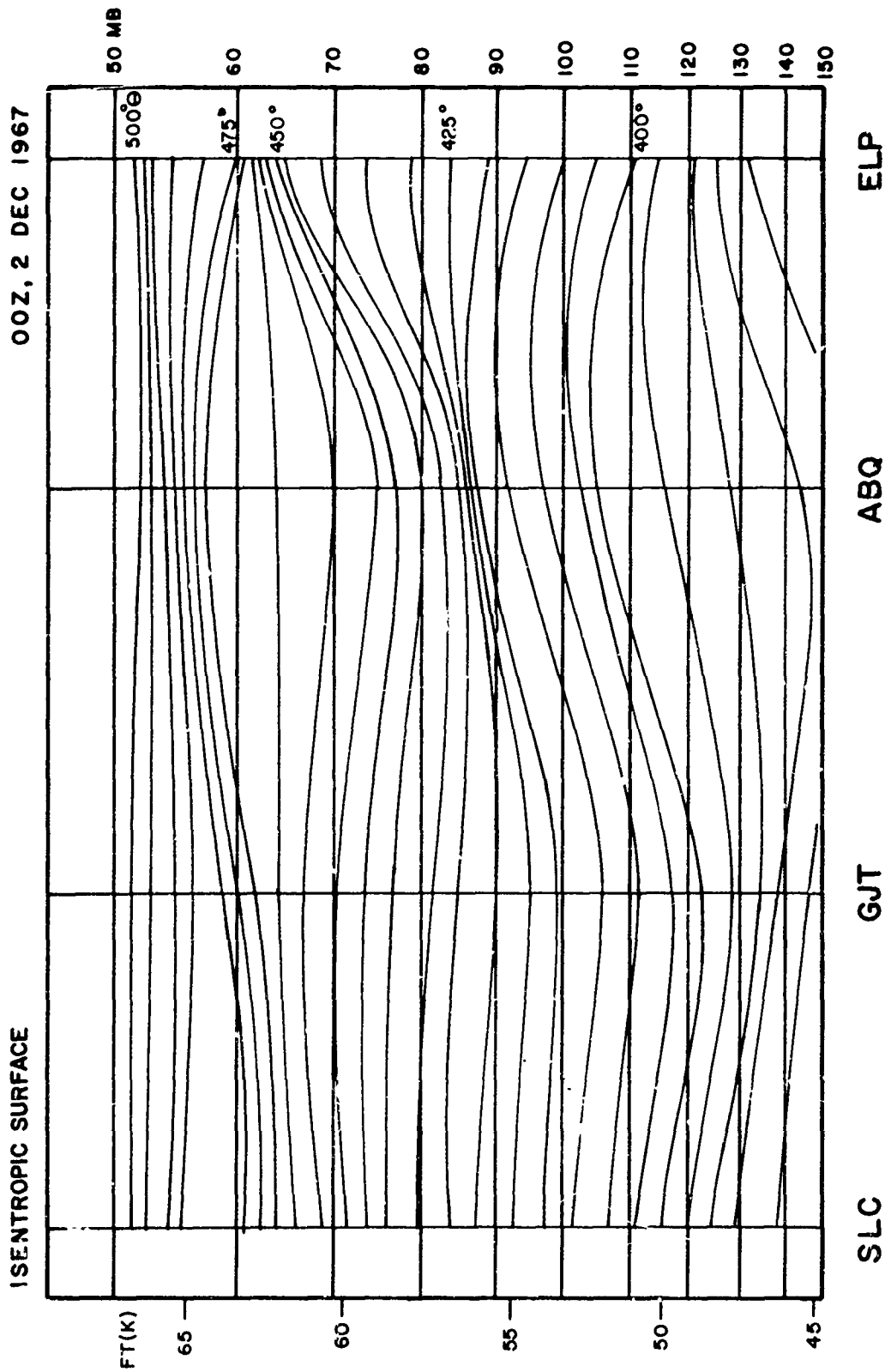


Figure 36. Isentropic Analysis, 2 Dec 1967, 0000Z

2 Dec 1967. It corresponds to the flight track in Figure 33 and the analyses in Figures 34 and 35.

The baroclinic zones are quite pronounced, particularly over Albuquerque and El Paso. As stated above by Reiter and Hayman, the turbulence was encountered near the axis of an isentrope trough. It should be noted however, that the turbulence had decreased to very light at 57,500 feet which was at the low point of the isentrope trough. The severe CAT was observed to be at about 54,000 feet which was slightly below the level of the inversion. Although the turbulence was, in fact, along the axis of the isentrope trough the severe turbulence was actually in an isentropic hump. It is perhaps more significant that the turbulence occurred near the vertical axis of a zone in which there was considerable packing and spreading of the isentropes.

One of the most difficult parameters to forecast in regard to clear air turbulence is the altitude at which it is likely to occur. If the turbulent area moves along, or close to the isentropic surface then the isentropic analysis should prove to be an aid in forecasting levels of turbulence.

#### No Turbulence Case

It is interesting to note that the bibliography in this report lists many titles of studies concerning clear air turbulence but no titles of studies devoted to smooth air or lack of turbulence.

To be able to closely define the limits of any problem is, of course, a distinct advantage. With this thought in mind numerous cases where CAT was not found have been analyzed. It can be stated that there are certain characteristics of synoptic patterns that are associated with conditions of no turbulence.

Figure 37 shows the route of flight on 30 June 1967. From Figure 38 it can be seen that the flight at the 70 mb level was in an area of weak horizontal temperature gradient. The  $-50^{\circ}\text{C}$  and  $-52^{\circ}\text{C}$  isotherms are approximately 300 nm apart. The isotherms are nearly parallel to the streamlines.

Figure 39 shows the RAOBS at Moosonee, Ont., Maniwaki, Que., and Caribou, Maine. The soundings are relatively straight as compared to those in Figure 35 indicating small temperature changes in the vertical.

The isentropic analysis in Figure 40 shows a smooth isentropic surface with a slight downward tilt towards the colder air to the north.

The obviously smooth surfaces of 30 June 1967 may be compared to the relatively steeply sloping isentropic surface of 2 Dec 1967. In short the analyses of 30 June 1967 reflect a pattern of weak thermal activity. Enough cases have been examined to indicate that when upper level synoptic conditions are similar to those in Figures 37, 38, 39, and 40, clear air turbulence was very light to nonexistent.

In summary then it may be said that, of the 108 cases examined since March 1967, if the flight of 30 June 1967 is typical of that of no-CAT and the flight of 1 Dec 1967

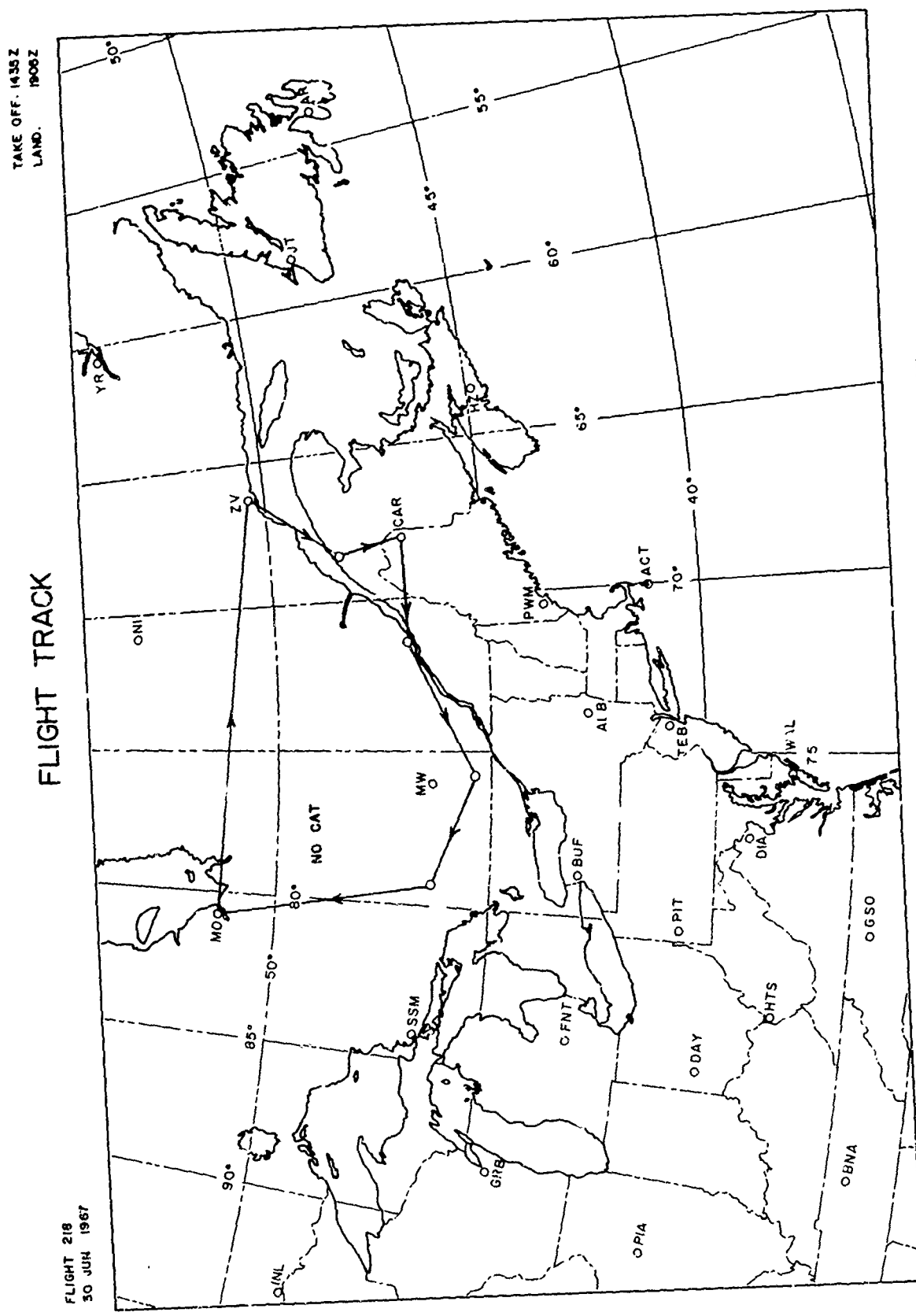
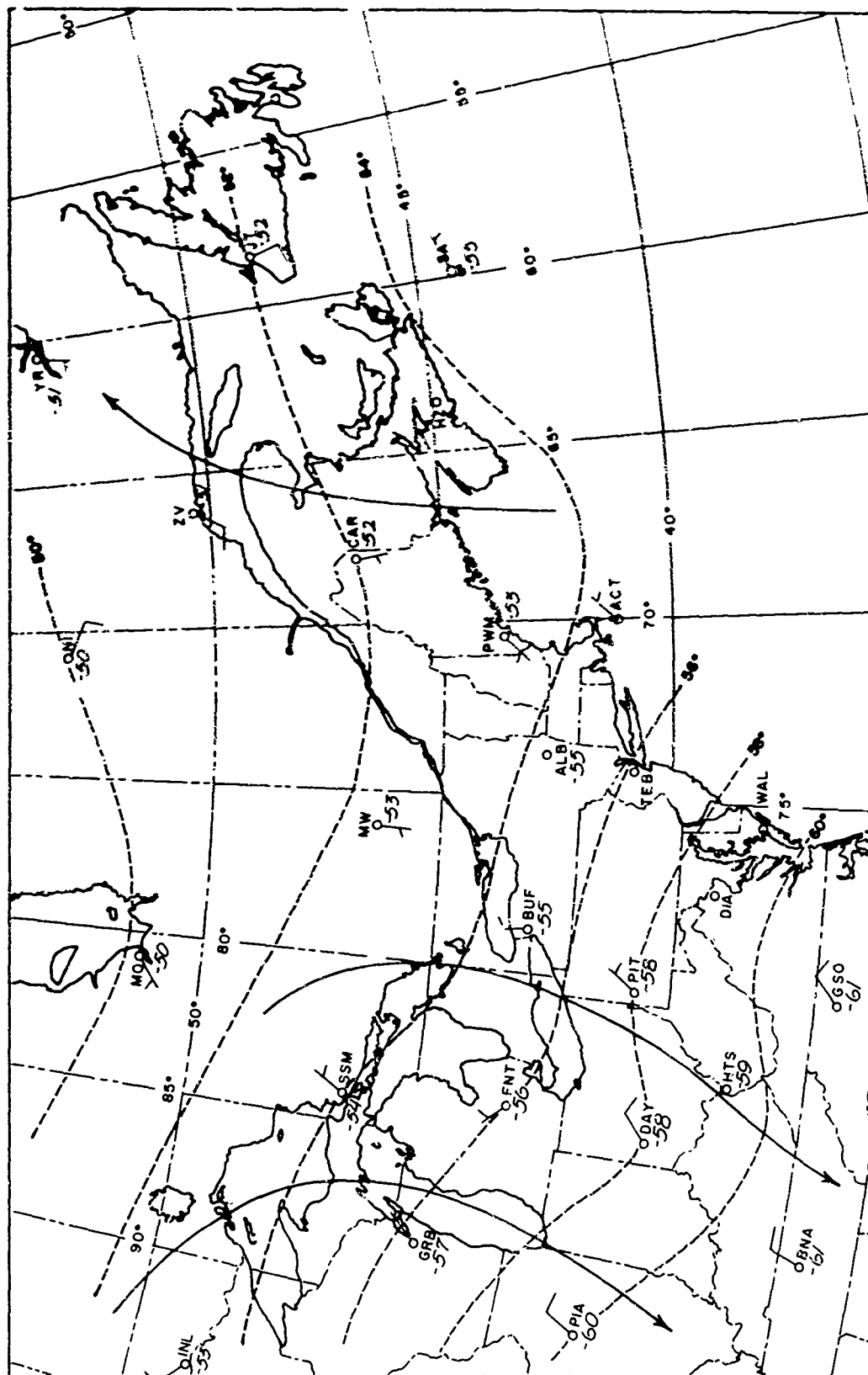


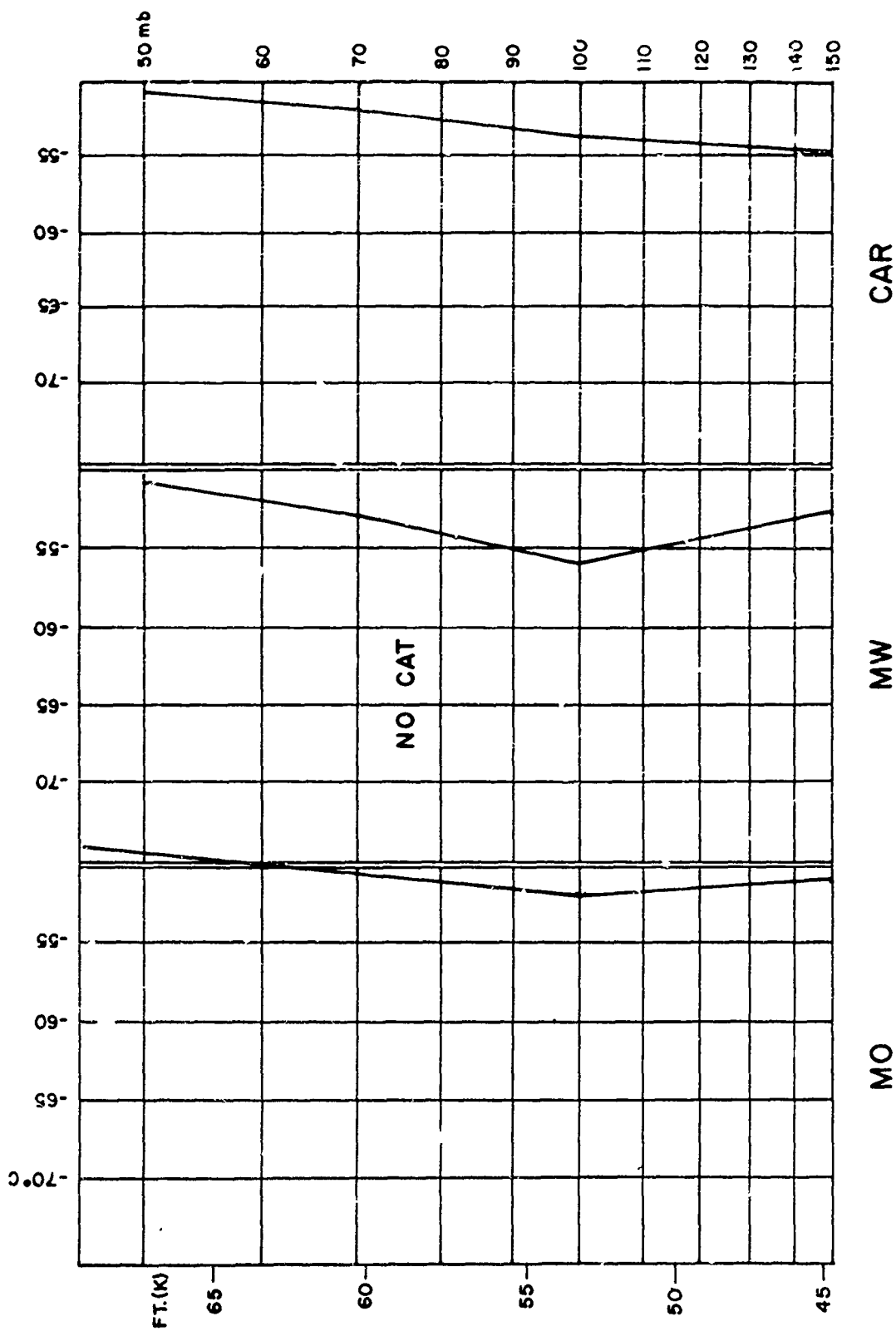
Figure 37. Flight Track, Flight 218, 30 Jun 1967



70 mb

12Z, 30 JUN 1967

Figure 38. 70 mb Analysis, 30 Jun 1967, 1200Z



RAOB 12Z, 30 JUNE 67  
Figure 39. Temperature Soundings, 30 Jun 1967, 1200Z

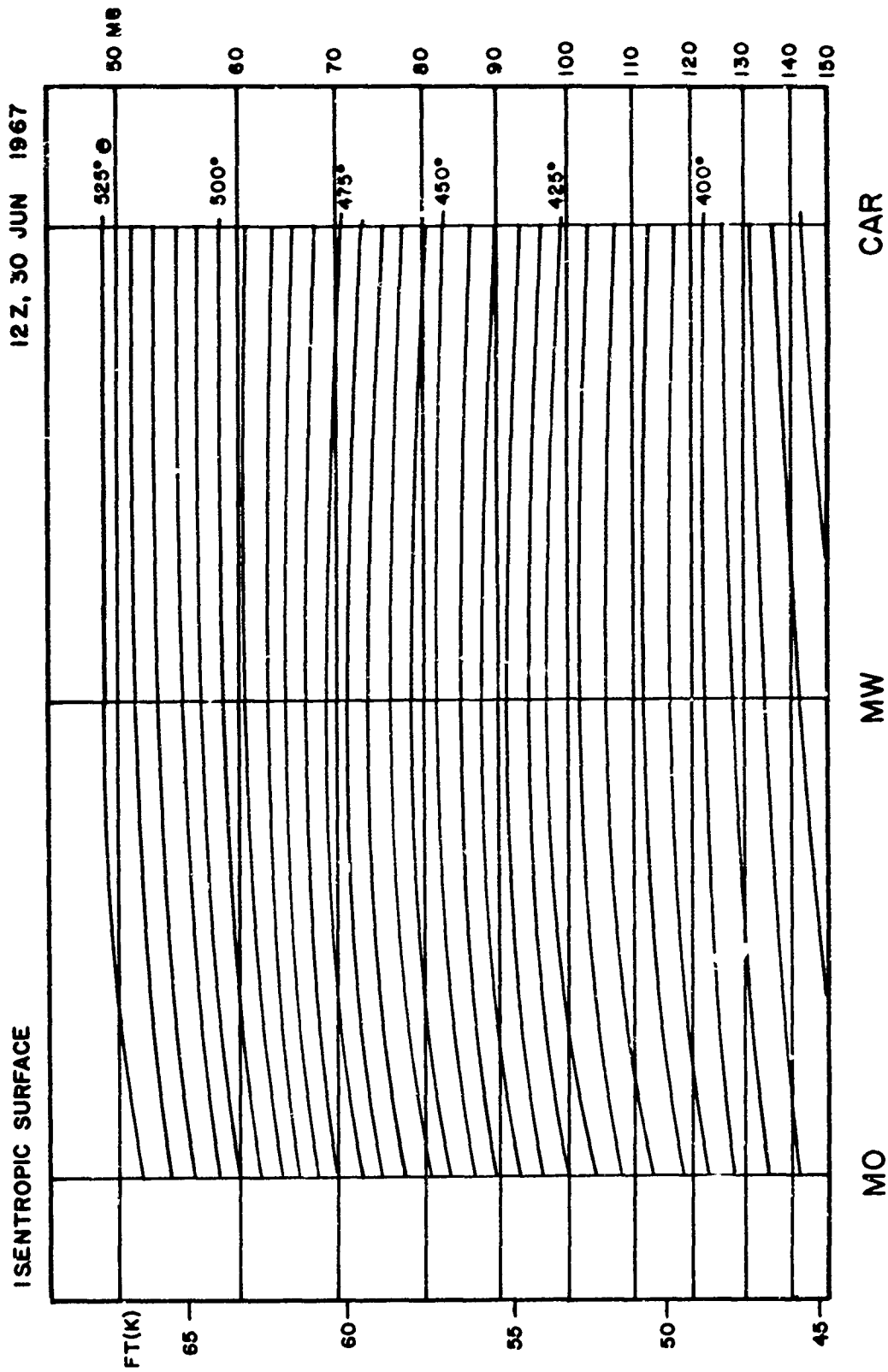


Figure 40. Isentropic Analysis, 30 Jun 1967, 1200Z

is representative of conditions associated with severe to extreme clear air turbulence significant progress has been made towards defining the limits of the problem of identifying meteorological parameters associated with turbulence.

#### HORIZONTAL TEMPERATURE GRADIENTS IN REGIONS OF CLEAR AIR TURBULENCE

Kadlec (28, 29), George (30), and Helvey (31) have discussed measurements of temperature changes that occurred in regions of clear air turbulence. Most of these measurements were made at the flight altitudes of commercial jet aircraft (25,000 to 35,000 ft). A few of the measurements were made in the 50,000 to 60,000 ft range of altitude. These measurements indicated that significant clear air turbulence is strongly correlated with temperature changes that often are as large as 3°C in 2 minutes of flight time.

Crooks, Hoblit, and Prophet (2) presented approximately 930 minutes of time histories of ambient temperatures that are synchronous with the turbulence observed in HICAT flights No. 54 to No. 178. An additional 543 minutes of time histories were available for the present study. The time histories of the ambient temperatures were displayed by plotting 12.5 points/sec. The sensitivity of the temperature measuring device is such that it does not adequately follow changes of temperature whose frequencies are greater than one cycle/sec. In the study described in the following paragraphs frequencies of temperature changes greater than one cycle per five seconds were eliminated by smoothing.

The study of the atmosphere temperature changes associated with clear air turbulence may be divided conveniently into two parts: The temperature changes observed within a region of turbulence, and the temperature changes observed within a few minutes preceding the entry into the turbulent region. This section will consist largely of a discussion of the temperature changes within the turbulent region only. Few data relevant to the non-turbulent region were received in time to be included in this report.

First, the definition of a turbulent region given by Crooks, Hoblit, and Prophet (2) was accepted. Their designation by flight number and run number was also accepted. Small sample calculations of the correlation coefficient between the temperature changes and the RMS values of the gust velocities (Figure 41a and b) indicated that the correlation coefficient was low. Further, the changes in aircraft altitude during the "run" made it difficult to distinguish between horizontal and vertical temperature gradients.

Selected time histories that illustrate the relationship between clear air turbulence and gust velocities are shown in Figures 42 to 46. A comparison of two time histories obtained from HICAT flights over the Cobar, Australia area is shown in Figure 42a and b. One without turbulence (flight 100, run 9) shows nearly isothermal conditions and one with moderate turbulence (flight 100, run 6) shows short time interval temperature changes of 2.5°C accompanying the turbulence. The runs are separated by a time interval of 1 1/2 hours.

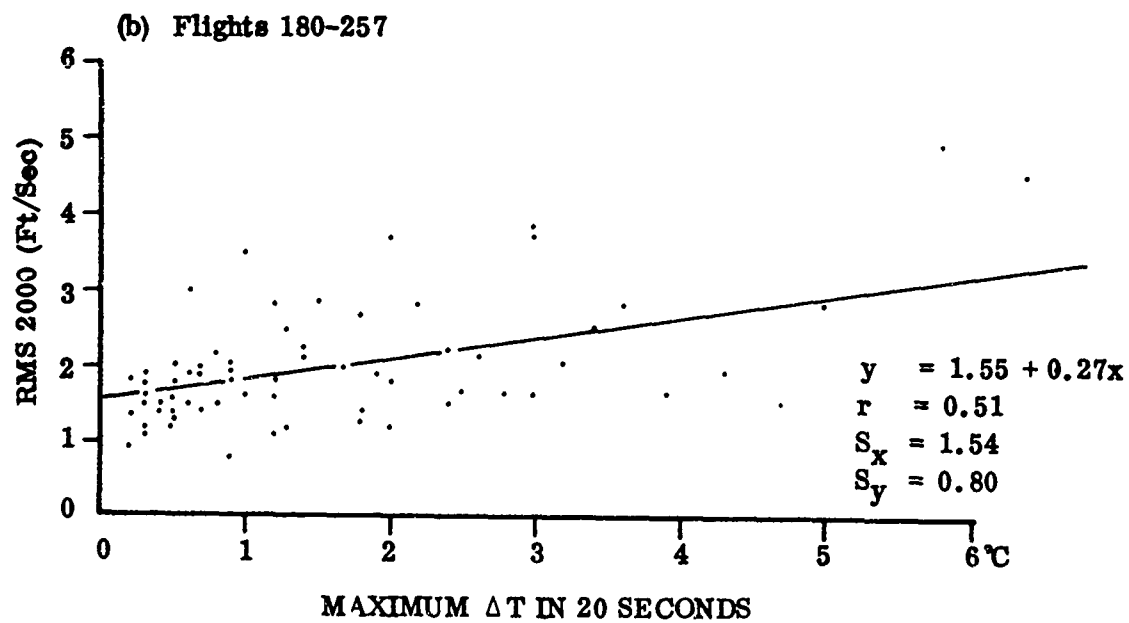
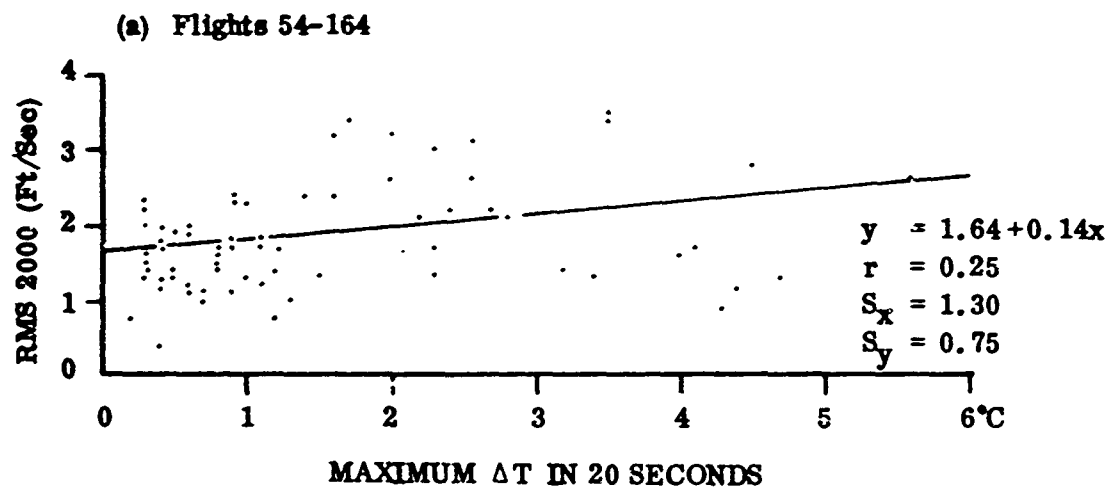


Figure 41. Correlation Between Temperature Changes and RMS 2000 Values

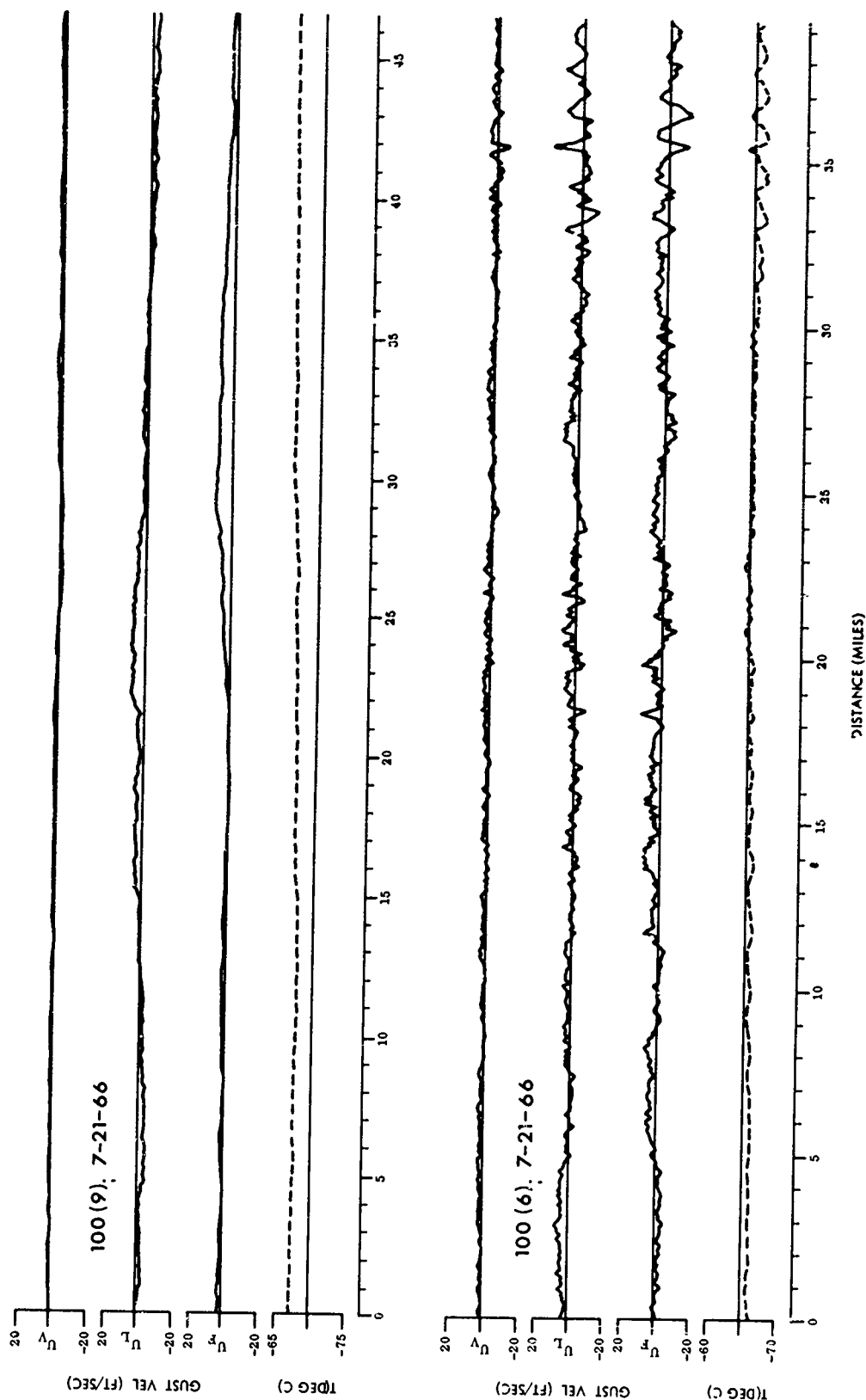


Figure 42. Time Histories of Gust Velocity and Temperature Variations for Flight 100, Runs 6 and 9

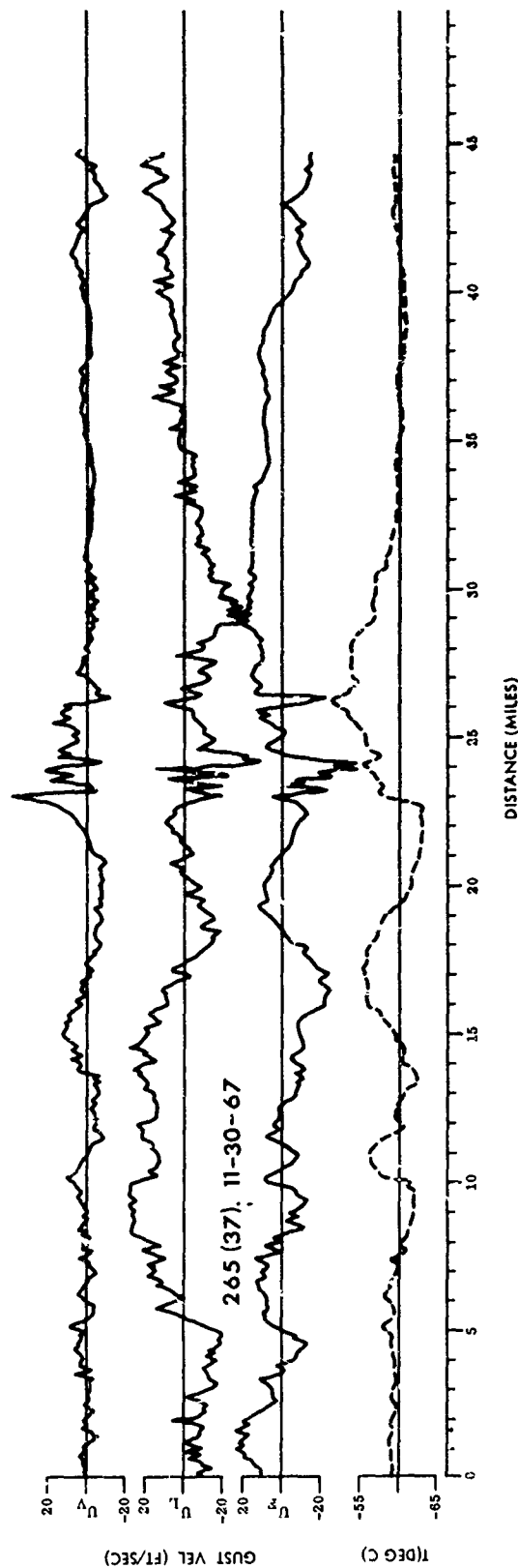
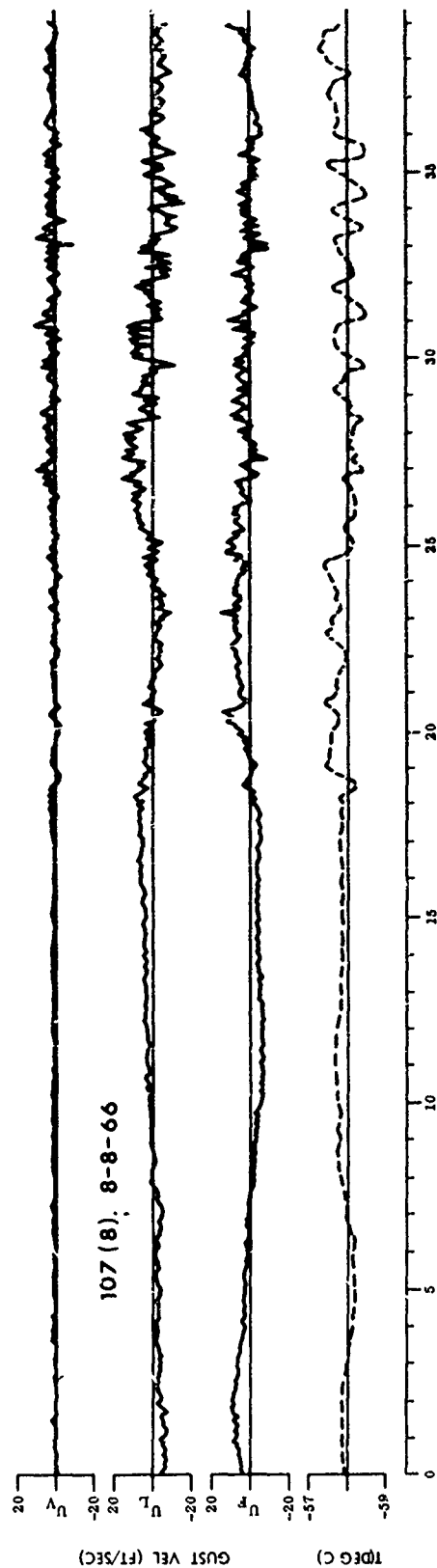


Figure 43. Time Histories of Gust Velocity and Temperature Variations for 107, Run 8 and Flight 265, Run 37

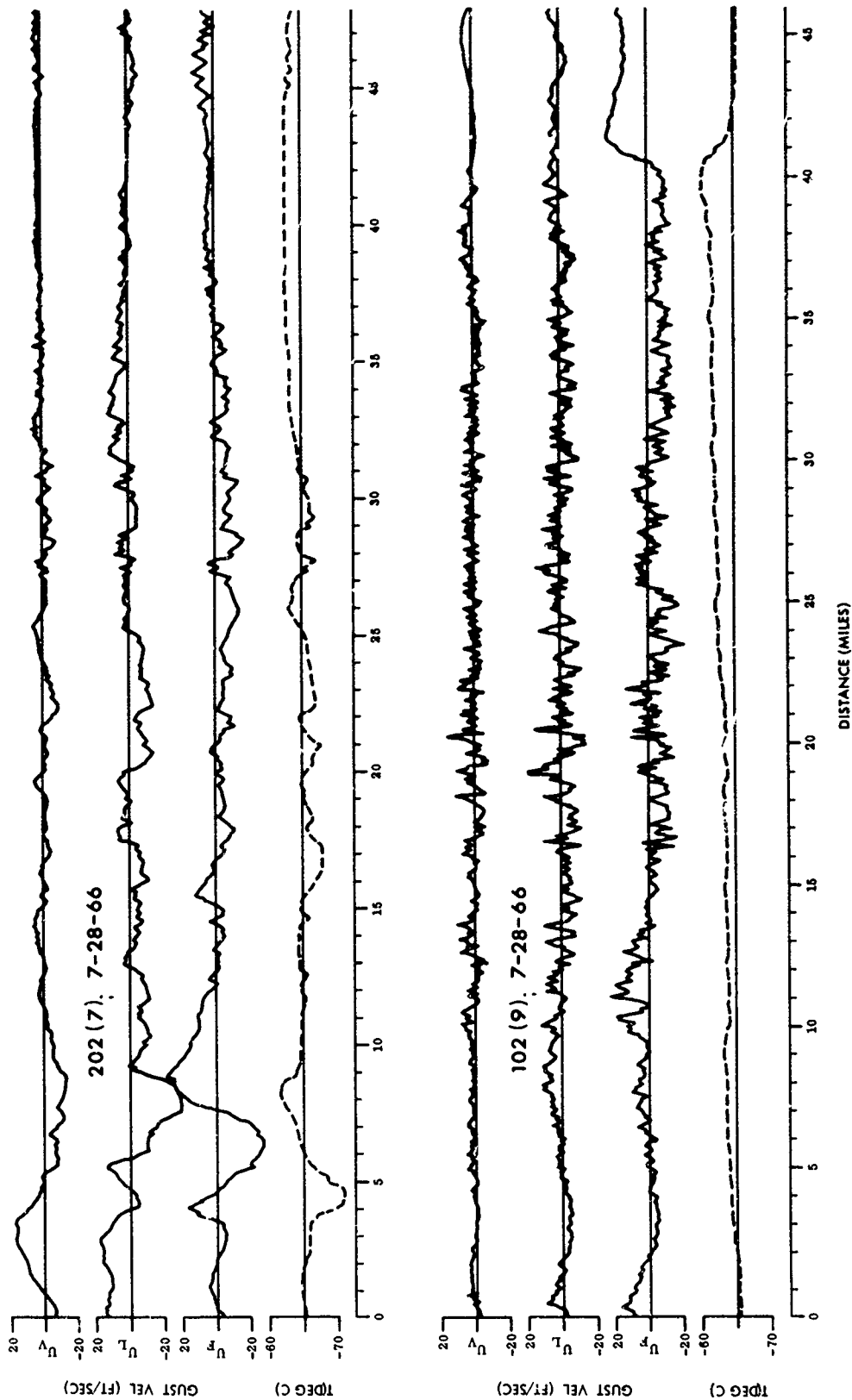


Figure 44. Time Histories of Gust Velocity and Temperature Variations for Flight 202, Run 7 and Flight 102, Run 9

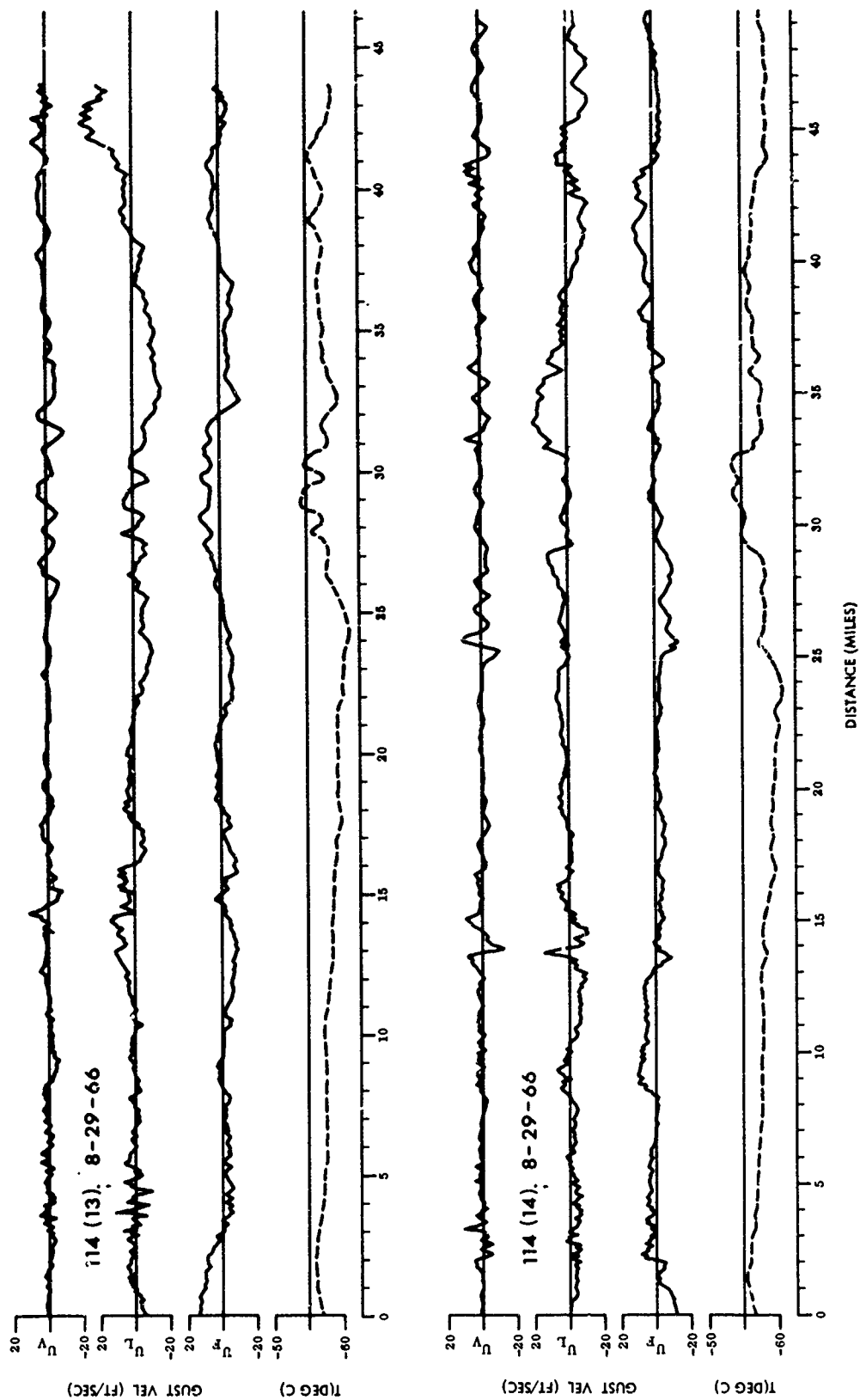


Figure 45. Time Histories of Gust Velocity and Temperature Variations for Flight 114, Runs 13 and 14

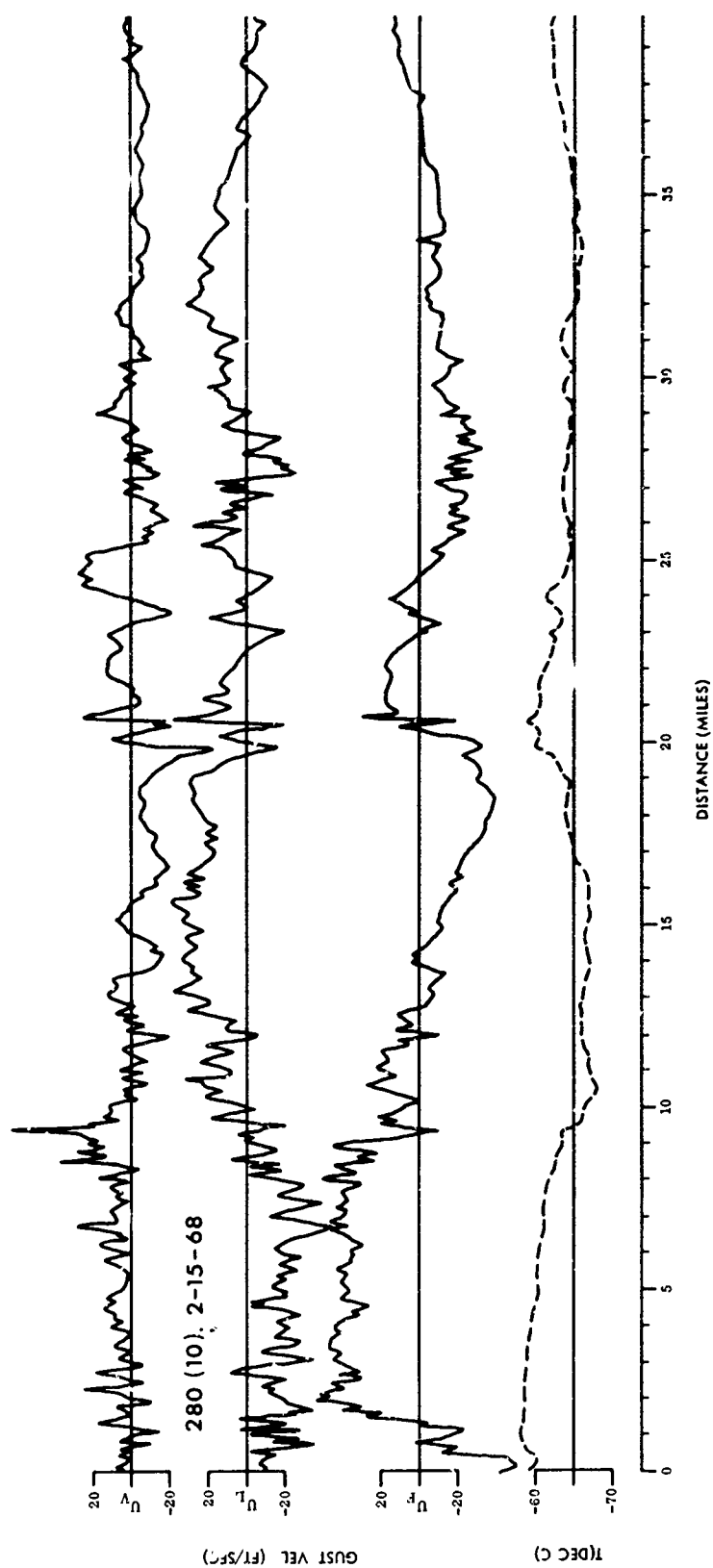


Figure 46. Time Histories of Gust Velocity and Temperature Variations  
for Flight 280, Run 10

The variability of temperature preceding turbulence contrasted to that within the turbulence is illustrated for flight 107, run 8, by Figure 43. These changes occurred above relatively flat terrain between Laverton and Cobar in southeast Australia. The temperature scale has been enlarged to emphasize changes during turbulence.

The largest temperature change for any flight occurred during flight 265, run 37 (Figure 43b) when an  $11.5^{\circ}\text{C}$  change in 4 miles was recorded along with severe turbulence. The flight was over mountainous terrain near Albuquerque, New Mexico.

Although statistical studies have suggested a strong relationship between turbulence and atmospheric temperature changes, the characteristic of the change varies considerably for any given case. For example, Figure 44a shows a temperature change of  $9^{\circ}\text{C}$  in 3 miles recorded during flight 202, run 7 above thunderstorm activity northeast of Little Rock, Arkansas. Flight 102, run 9 (Figure 44b) shows a gradual rise in temperature over a distance of several miles, although a drop in the temperature of  $5^{\circ}\text{C}$  in  $2\frac{1}{2}$  miles appears near the end of the run. The moderate turbulence accompanying this flight was at 61,000 ft on the lee side of the Great Dividing Range in southeast Australia. There was a strong jet at 36,000 ft with winds exceeding 150 knots. This case illustrates that the effectiveness of a remote sensing device may depend upon the relative flight direction. Had the aircraft flown at  $180^{\circ}$  to the actual heading the sharp temperature change would have probably preceded the turbulence. It is reasonable to assume this type of change could be detected more readily than a gradual one.

The temperature variations for flight 114, run 13 and run 14 (Figure 45a and b) east of the ridge line of the Sierra Nevada Mountains in California, are indicative of a mountain wave situation. The heading during flight 114, run 13 was towards the ridge and away from the ridge for flight 114, run 14. Both runs were at right angles to the ridge, nearly overlapping, and separated by only a few minutes. Time histories for flight 114, run 13, are plotted in reverse to correspond with the wind flow which is west-southwest and perpendicular to the ridge both at mountain top and flight levels.

A trough-ridge structure in the horizontal temperature field is discernible for both runs. The distance between crests is approximately 9 to 10 miles, with the exception of the first wave which has a wavelength about three times as large. In a detailed report on 1964 U-2 measurements in the same general area, Helvey (1967) concluded that the temperature troughs, or cold zones, were associated with crests in the mountain wave. Turbulence was found to be concentrated in the zone between the warm axis and the cold axis, the warm axis being oriented upwind from the cold. The present HICAT flights do not supply any conclusive evidence to verify this. There is, however, a case of severe turbulence in the Denver, Colorado area, flight 280, run 10 (Figure 46) where the greatest gusts occurred in the zone designated by Helvey. Flight 265, run 37 (Figure 43b) also verifies this.

The examples discussed in the preceding paragraphs illustrate that the gust velocities are not simple functions of the variations in the ambient temperature. The flights through the turbulent regions designated by Crooks, Hoblit and Prophet (2) had

time durations that varied from 20 seconds to 15 minutes. In the present study only those turbulence cases that had a duration of one minute or more were studied. Various methods of determining the degree of correlation between any or all of the components of the gust velocities and the variation of temperature were tried. The method that yielded the highest correlation coefficient was as follows:

- a) Each run was used as one sample. The largest temperature change for any 20 second period during which the altitude did not change by more than 100 ft was determined.
- b) The largest change in gust velocity during any 10 second period for each of the three components was determined.
- c) The temperature change and the gust velocity changes need not be synchronous nor have a fixed time lag.
- d) The quantity  $(\Delta U_F^2 + \Delta U_L^2 + \Delta U_V^2)^{1/2}_{\max}$  was computed.
- e) The correlation coefficient between this quantity and the temperature change described above was computed.

The results of the computations are illustrated in Figures 47a and b. For 73 cases selected from 16 flights from the records from flights 54 to 178 the correlation coefficient was 0.76. For 69 cases from 21 flights from flights 180 to 257 the correlation coefficient was 0.82. In only 10 of 52 cases was the maximum temperature change less than  $1.5^\circ\text{C}$  if  $(\Delta U_F^2 + \Delta U_L^2 + \Delta U_V^2)^{1/2}_{\max}$  was greater than or equal to 25 ft/sec, whereas 78 of 88 cases had temperature changes less than  $1.5^\circ\text{C}$  when  $(\Delta U_F^2 + \Delta U_L^2 + \Delta U_V^2)^{1/2}_{\max}$  was less than 25 ft/sec.

#### GEOGRAPHIC DISTRIBUTION OF TURBULENCE

In previous sections, evidence is presented that high altitude clear air turbulence is a function of, in part, relatively large horizontal temperature gradients at the flight level. The direct determination of the frequency of occurrence of these large horizontal temperature gradients for all the principal regions of the earth was beyond the scope of work for this report. However, an alternative approach to the problem was feasible. This approach was based upon the hypothesis that regions of strong horizontal temperature gradients are also regions in which the 24 hour temperature changes are relatively large. This presented an opportunity to use the Northern Hemisphere upper atmosphere temperature data collected during the International Years of the Quiet Sun (1964-1965). These data were available on magnetic tape. Data from the 100 mb level for the western portion of the Northern Hemisphere were selected for analysis. In addition, the 27 day period of WU-2 HICAT flight operations over southeastern Australia were included in the analysis. The 100 mb level averages close to 53,000 ft.

For purposes of the analysis the Northern Hemisphere data were divided by season defined as winter (Jan-Mar), spring (Apr-Jun), summer (Jul-Sep), and fall (Oct-Dec). The results are presented in terms of the standard deviation of the 24 hour temperature change  $\sigma\Delta_T$  and are shown in Figures 48-51 corresponding

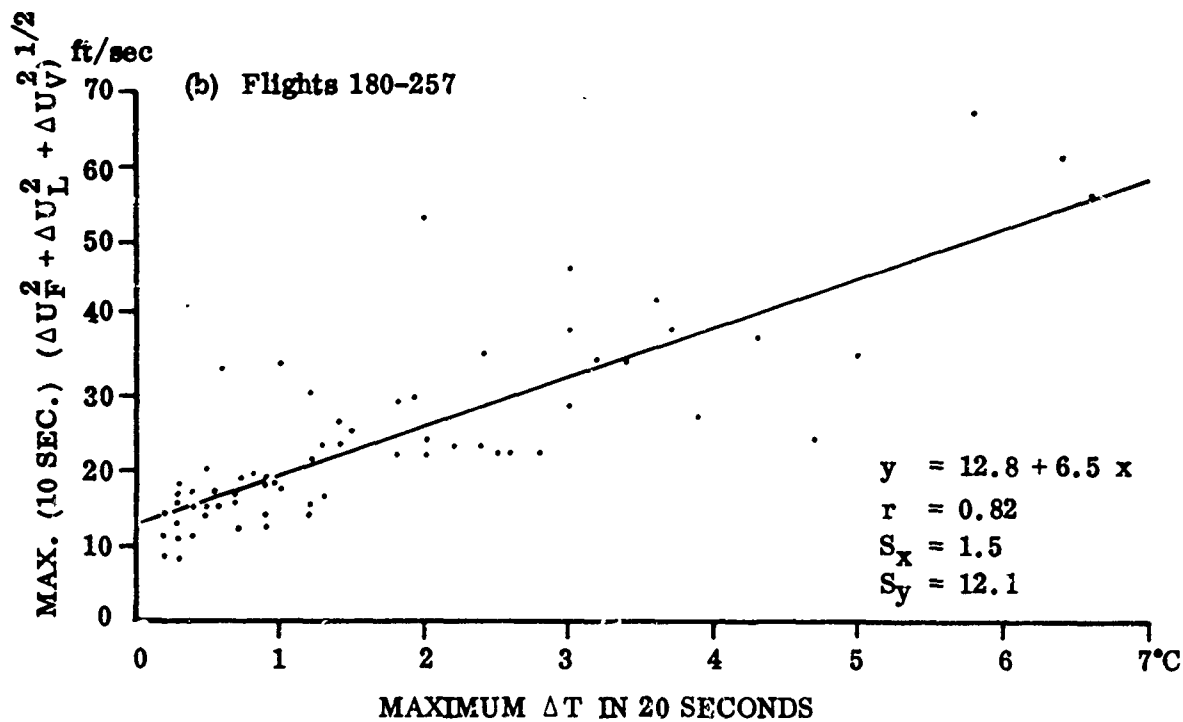
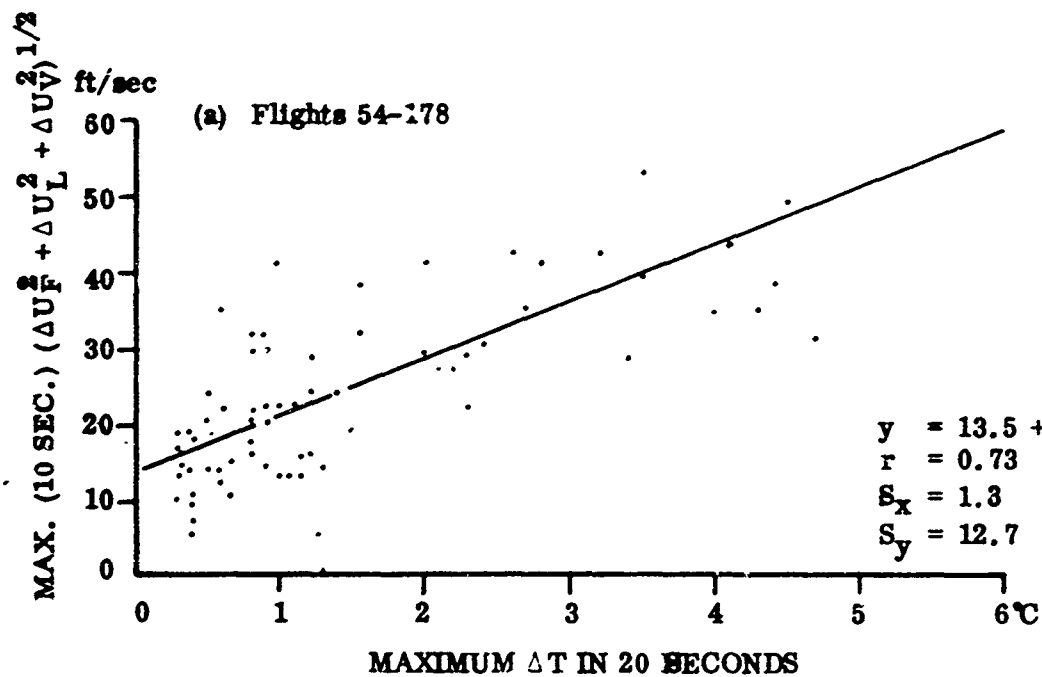


Figure 47. Correlation Between Temperature and Gust Velocity Changes

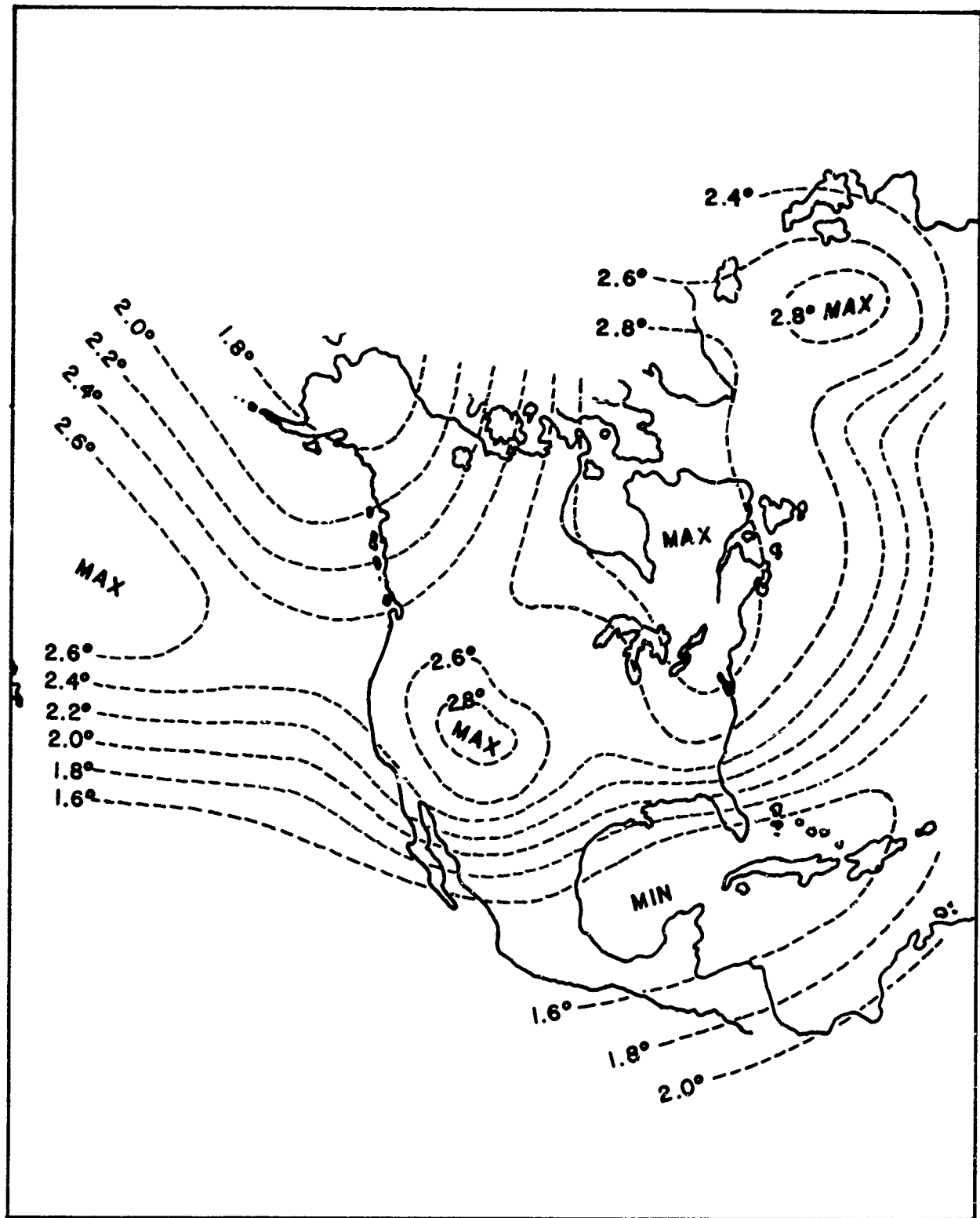


Figure 48. Standard Deviation of 24 Hour Temperature Change at 106 mb.  
(Jan-Mar 1964)

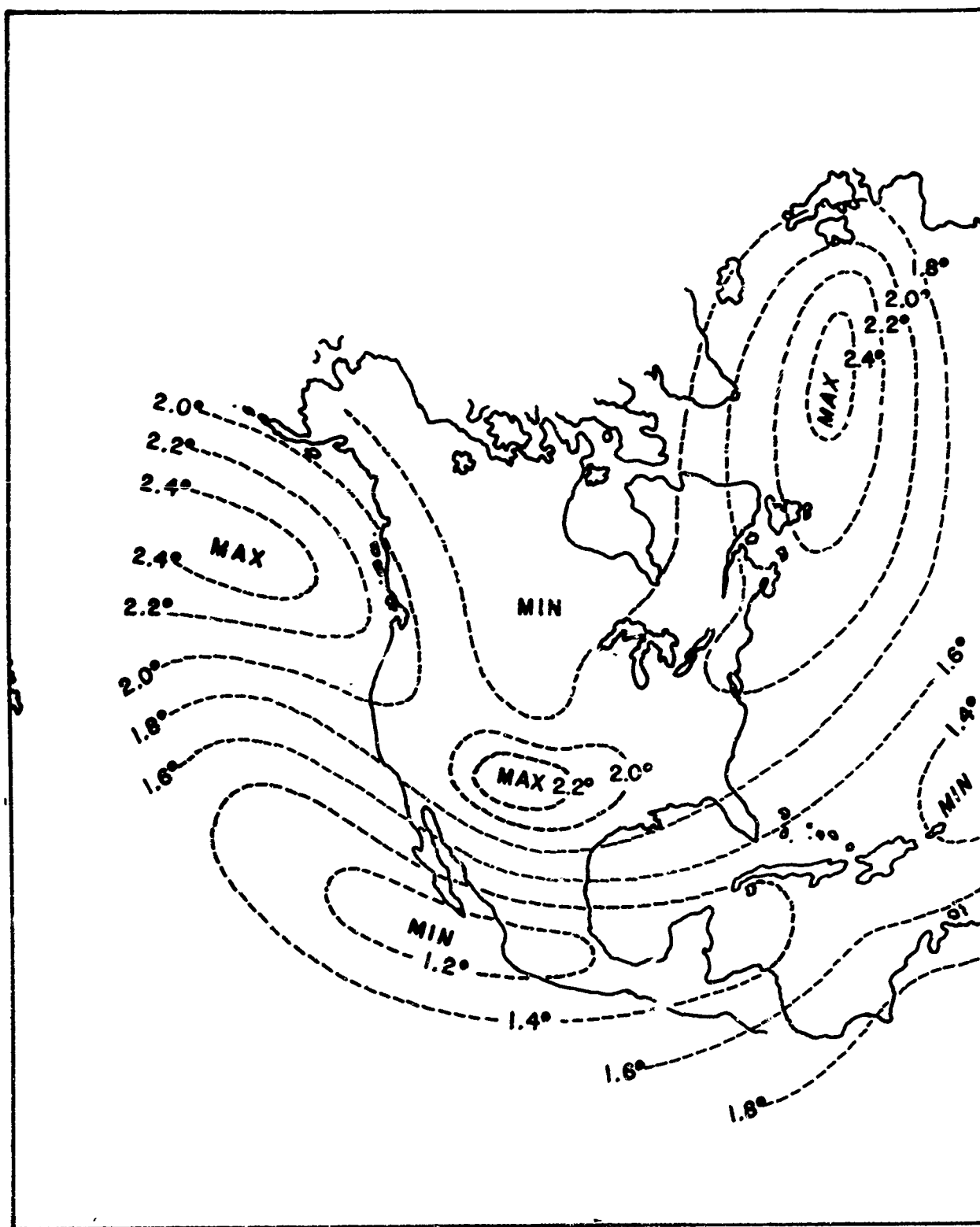


Figure 49. Standard Deviation of the 24 Hour Temperature Change at 100 mb.  
(Apr-Jun 1964-5)

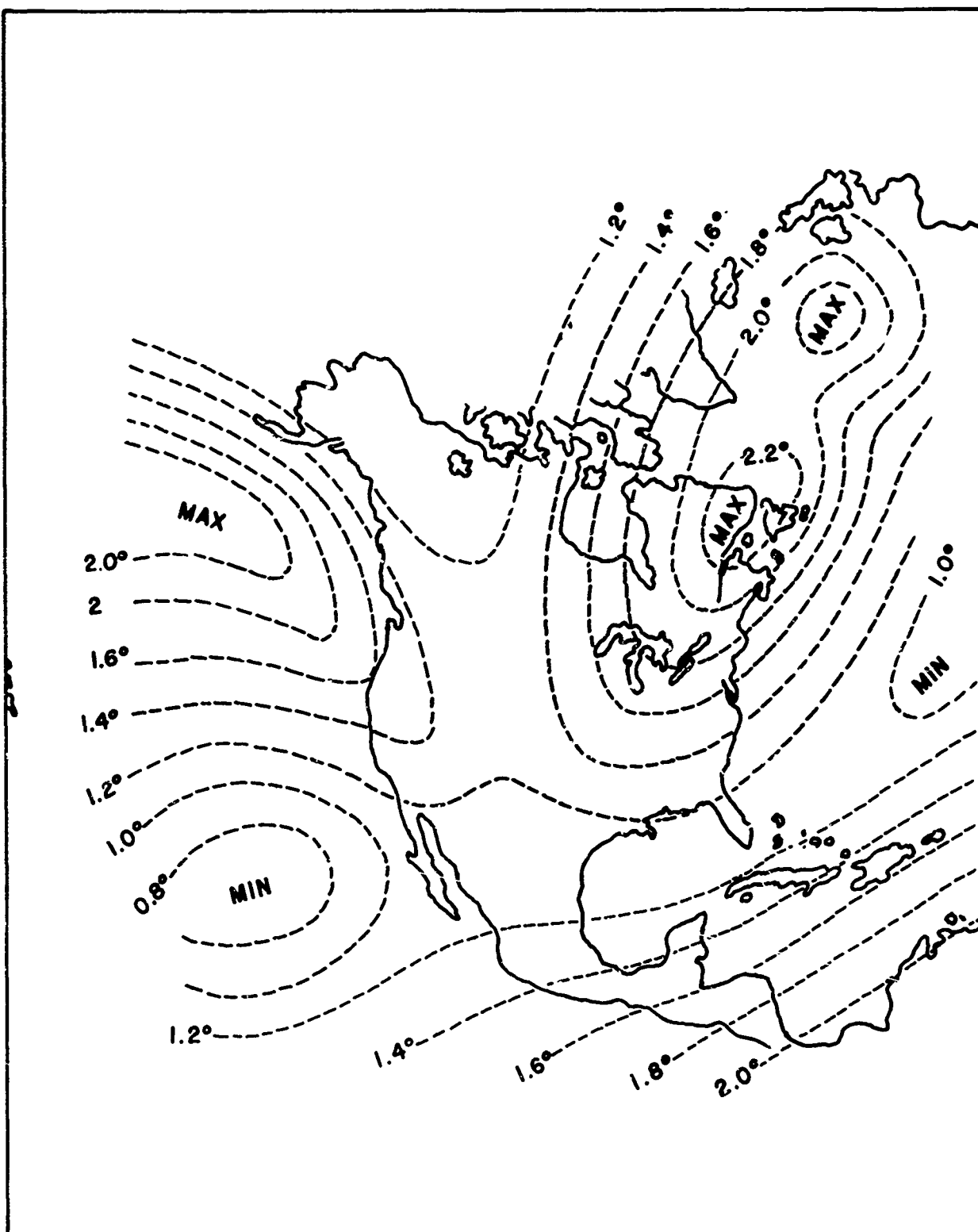


Figure 50. Standard Deviation of 24 Hour Temperature Change at 100 m.  
(Jul-Sep 1964-5)

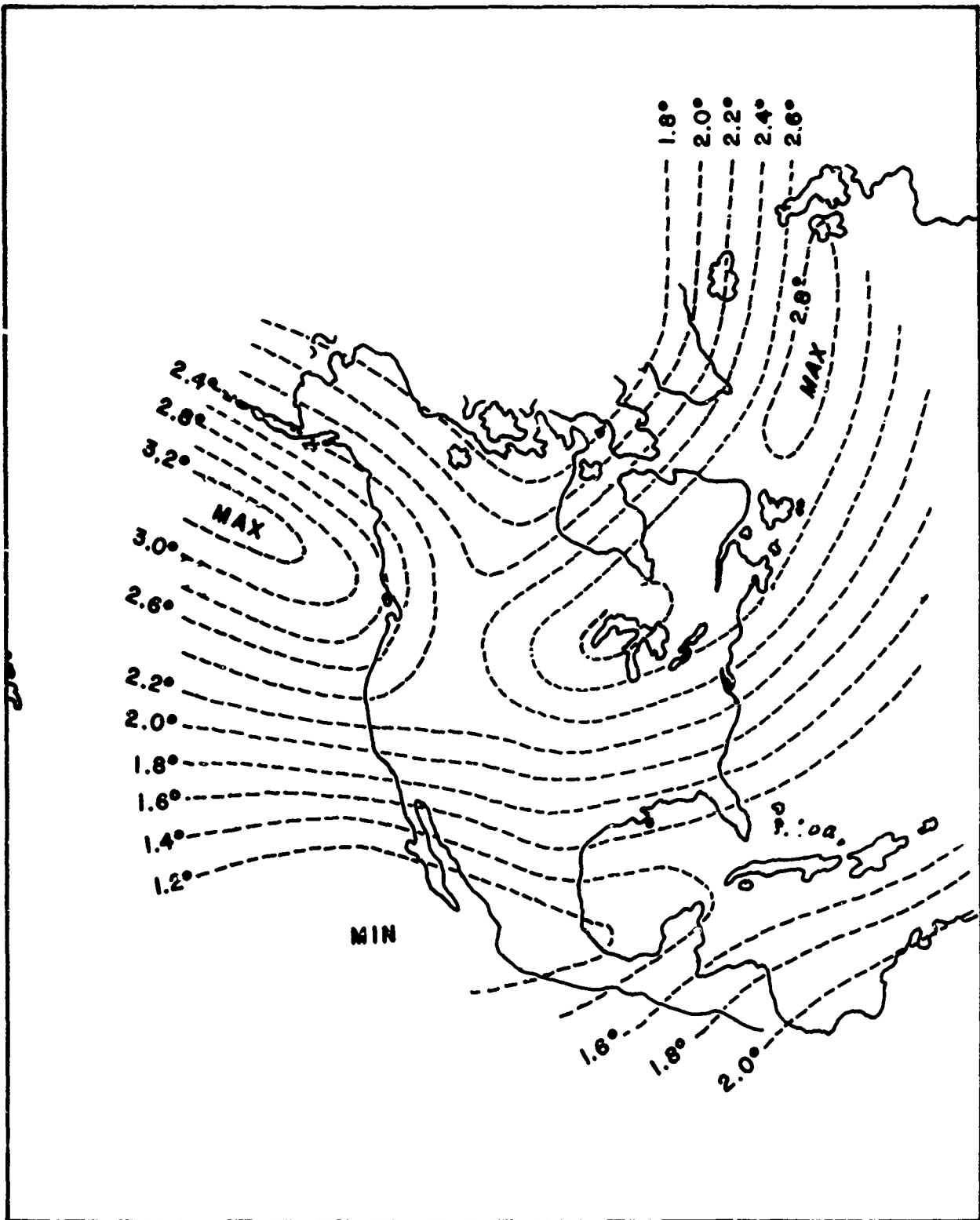


Figure 51. Standard Deviation of 24 Hour Temperature Change at 100 mb.  
(Oct-Dec 1964-5)

to the four seasons. Figure 48 for winter shows maximum  $\sigma\Delta_T$  values near and probably north of Hawaii, over the Rocky Mountains, and from the northeastern U.S. and eastern Canada eastward across southern Greenland and south of Iceland to Great Britain.

In spring (Figure 49) the values decrease nearly everywhere except in the Gulf of Alaska. Maximum values also occur over the southern Rockies and from the northeastern U.S. across the North Atlantic. In summer (Figure 50), maximum values persist in the Gulf of Alaska and from the northern U. S. and eastern Canada eastward across the North Atlantic. In fall (Figure 51), peak values occur in the Gulf of Alaska and from the Great Lakes eastward across the North Atlantic.

A similar analysis for southeastern Australia is shown in Figure 52 for the 27 day period of flight operations only. It is interesting to note that nearly all the turbulence encountered occurred in the areas of maximum  $\sigma\Delta_T$ , primarily from Broken Hill and Cobar southeastward to the coast and northward along the coast through Williamstown.

For most areas, some problems arise in attempting to establish approximate relationships between  $\sigma\Delta_T$  and numerical values for frequency of occurrence of turbulence. In the first place, the aircraft frequently went far from its base of operations so that the average  $\sigma\Delta_T$  over the flight route might vary considerably from the value at the operations base. In addition, flight tracks frequently varied from one day to the next. This required estimating an average value for  $\sigma\Delta_T$  for a relatively large area surrounding most bases.

The Australian data present the best possibilities of establishing an approximate relationship between  $\sigma\Delta_T$  and percentage of time in turbulence. The  $\sigma\Delta_T$  values are fairly uniform over most of the flight routes which correspond closely to the areas of maximum  $\sigma\Delta_T$ . It must be assumed, of course, that the 52 hours of flight on 11 different days are representative of the average conditions prevailing during the 27 day period of meteorological data. In Australia, the observed time in turbulence in the altitude band 50-55,000 ft was 13% of the total flight time in this band, and the average value of  $\sigma\Delta_T$  over the routes where the turbulence occurred is estimated as 3.2°C from Figure 52.

The  $\sigma\Delta_T$  values in the Northern Hemisphere (Figures 48-51) do not correspond to the flight times, but were derived from a longer record so that a more nearly average picture, (but still not a true climatological one) could be presented. When the above relationship between percentage of time in turbulence and  $\sigma\Delta_T$  values based on the Australian data are extrapolated to the Northern Hemisphere, we can compare the observed percentage of time in turbulence at each site with the longer term normal. The results are shown in Table V. The computed values are based on a linear relationship between  $\sigma\Delta_T$  and frequency and using the Australian data as a base, i.e., the computed percentages of time in turbulence are based on the relationship  $\% = 13 (\sigma\Delta_T/3.2)$ . An average value for  $\sigma\Delta_T$  was estimated from Figures 48-51 for each operational base depending upon the season and routes of the actual flights. In some cases, the flights extended for hundreds of miles from the operational base so that  $\sigma\Delta_T$  had to be estimated for a fairly large area.

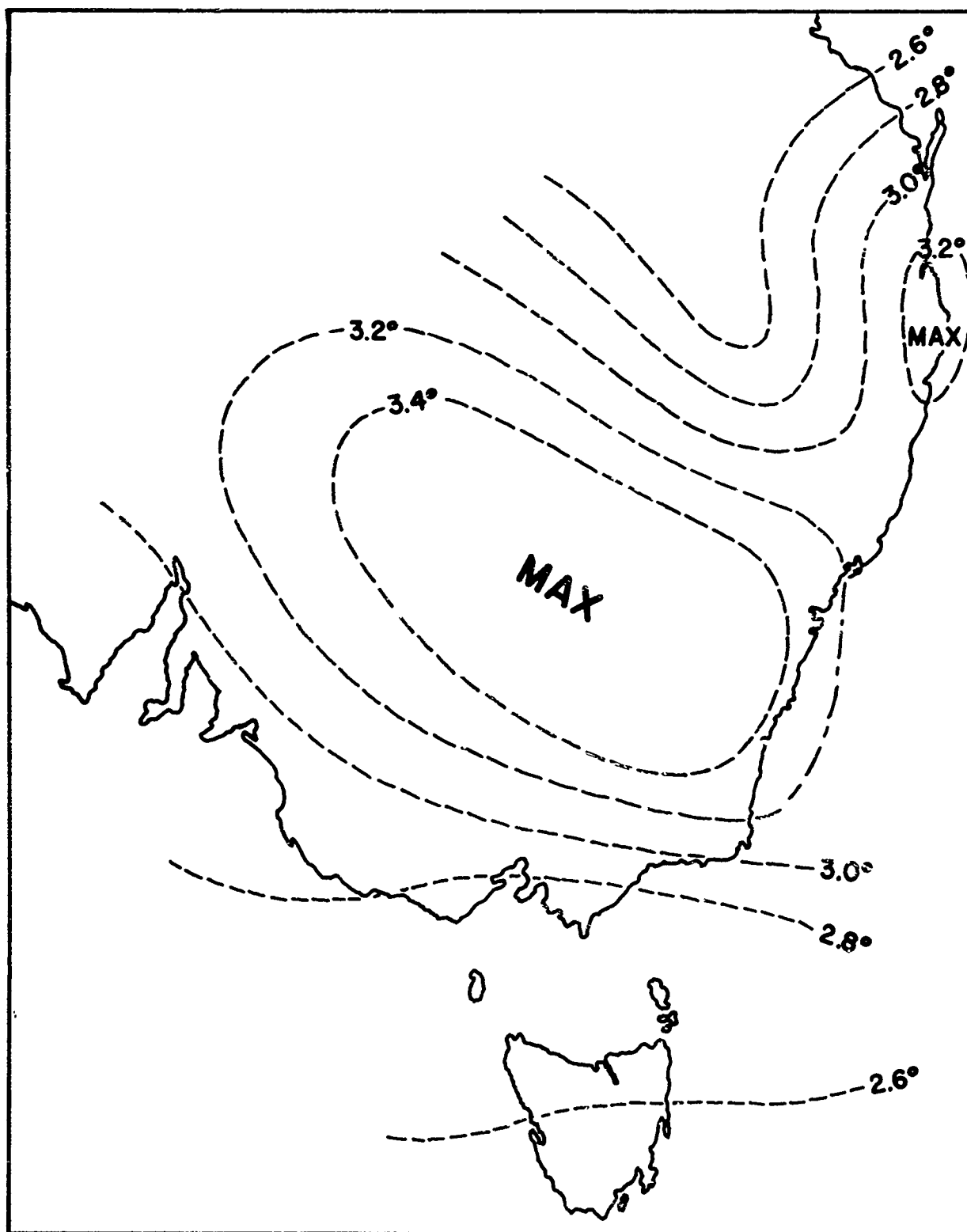


Figure 52. Standard Deviation of 24 Hour Temperature Changes at 100 mb.  
(Southeastern Australia 17 Jul - 12 Aug 1966)

TABLE V

COMPUTED AND OBSERVED PERCENTAGE OF TIME IN TURBULENCE AND  
 $\sigma \Delta_T$  VALUES FOR VARIOUS SEASONS AND AREA

<u>Area</u>	<u>Season</u>	<u>Est. Av. <math>\sigma \Delta_T</math> from Figs. 48-52</u>	<u>% of Time in Turbulence at 50-55,000 ft</u>	
			<u>Computed</u>	<u>Observed</u>
Australia	Winter	3.20		13
Edwards, Calif.	Fall, Winter	2.50	10	12
Hawaii	Spring	2.25	9	7
Hanscom, Mass.	Summer, Fall	2.20	9	9
Elmendorf, Alaska	Winter	1.80	7	7
Ramey, P. R.	Fall	1.50	6	11

A comparison of the computed and observed values for percentage of time in turbulence in Table V shows that they are in good agreement for all areas except Puerto Rico where most of the turbulence was encountered several hundred miles away, mostly to the north or east. It is possible that had more computational points been used in this area in constructing the  $\sigma \Delta_T$  maps, a more representative value could have been obtained. On the other hand, it is also possible that the meteorological conditions which existed during the month of flight operations were not representative of the longer term average.

The results of this analysis illustrated in Figures 48-52 and Table V indicate that the standard deviation of the 24 hour temperature change at HICAT flight levels may be a useful guide for indicating geographical regions of maximum frequency of occurrence of high altitude clear air turbulence. Further study of this method of approach is warranted.

## SECTION VI

### CLASSIFICATION OF HICAT BY CHARACTERISTICS OF THE EARTH'S SURFACE

Monsoon winds, sea breezes, and waves in the atmosphere on the lee side of mountain ridges are examples of the association between macro and mesoscale meteorological conditions and the characteristics of the surface of the earth. In the regions of the atmosphere that are relatively close to the earth's surface the relationship between the occurrence of clear air turbulence and the nature of the underlying surface is relatively well established. Correlations between HICAT and terrain features have also been confirmed and the results are presented below.

The first step taken in the search for significant correlations was to classify the observations of turbulence and non-turbulence according to the characteristics of the surface of the earth in the region over which the WU-2 was flying. Desirable features of such a classification system are:

- a) The system be objective to the maximum practicable extent
- b) The number of categories be small enough to have an adequate number of samples for statistically significant results
- c) The boundaries between the categories be chosen to produce a minimum number of marginal samples.

Crooks, Hoblit, and Prophet (2) classified each turbulence run for WU-2 flights 54 to 175 according to a system which used four terrain categories. The assignment to a specific category was determined by the character of the earth's surface directly below the aircraft. No specific cone of view or area was specified. A detailed study indicated that more significant correlations could be obtained between turbulence and related terrain if the categories were modified and reduced to three. The original and modified classifications are as follows, where  $h$  refers to relief differences:

<u>Crooks, et. al. (2)</u>	<u>Modified System</u>
Water	Water
Flatland ( $h < 500$ ft)	Flatland ( $h < 3000$ ft)
Hills ( $500 < h < 2500$ ft)	--
Mountains ( $h > 2500$ ft)	Mountains ( $h > 3000$ ft)

The field of view in the modified category was designated as 50 miles upwind. If a mountain range was within 50 miles upwind of the NADIR point of the aircraft then the observation was placed within the mountain category. Isolated peaks on plains or islands were classified as flatland or water, respectively. The application of the modified classification to WU-2 flights 54 through 175 gave results that are summarized and compared to those of the initial classification in Table IV.

TABLE VI  
HICAT OBSERVATIONS BY TERRAIN CATEGORY

<u>Terrain Type</u>	<u>Number of Turbulent Runs</u>	
	<u>Crooks, et. al.(2)</u>	<u>Modified System</u>
Water	190	189
Flatland	39	58
Hills	56	--
Mountains	99	147

A comparison has been made between the three categories of terrain and the percent of turbulence miles per flight miles, encountered for WU-2 flights 54 to 175. The geographical distance covered and the distance in turbulence were measured from flight track maps for each terrain type. Search pattern tracks were treated as straight line distances, thereby eliminating some of the bias in data analysis that results from flying several passes through a turbulent region.

The influence of terrain on HICAT is evident (Table VII).

TABLE VII  
TOTAL FLIGHT MILES (IN HUNDREDS OF MILES) FOR EACH TERRAIN TYPE  
AND PERCENT OF FLIGHT MILES IN TURBULENCE, FLIGHTS 54 TO 175

	<u>Water</u>	<u>Flatland</u>	<u>Mountains</u>	<u>Total</u>	<u>≥ Moderate</u>
Edwards	0	5 (0)	98 (7.1)	103 (6.8)	(1.2)
Hickam	206 (5.9)	0	36 (6.5)	242 (6.5)	(0.8)
Christchurch	90 (5.9)	0	73 (13.0)	163 (9.0)	(2.7)
Laverton	1 (0)	94 (8.9)	71 (13.0)	166 (10.6)	(5.4)
Hanscom	2 (45.0)	196 (2.5)	69 (4.6)	177 (3.8)	(0.2)
Ramey	132 (5.0)	0	0	132 (5.0)	(0.8)
Elmendorf	46 (2.8)	0	173 (1.9)	219 (2.1)	(0.6)
All Bases	477 (5.5)	205 (5.4)	520 (6.9)	1202 (6.1)	(.16)
≥ Moderate	(1.0)	(1.8)	(2.1)	(1.6)	

The percent of flight miles in turbulence is 6.9% over mountains and approximately 5.5% over water and flatland. At five bases a higher percent of flight miles were turbulent over mountains than over flatland or water. Flights from Elmendorf,

Alaska, had more turbulence over water than mountains but the total turbulent miles were small (2.1%). On the other hand, flights flown out of Christchurch, New Zealand, and Laverton, Australia, encountered turbulence 13% of the distance over mountains and significantly lesser amounts over other terrain.

The amount of moderate turbulence over mountains for all bases (2.1%) was greater than over flats (1.8%) and water (1.0%). The figure for the mountains is probably lower than that which might be expected for a sample covering all types of terrain for all latitudes. In Alaska, where 33% of the total miles over mountains were flown, only a small amount of turbulence was measured. Had some of these miles been flown over water and flatlands, it is likely that the percent of turbulence would not have been greater.

Table VIII presents an average of the vertical gust velocity root mean square (RMS  $U_V$ ) values for each terrain category. All available RMS values for flights 54 to 281 were used in this comparison.

TABLE VIII

AVERAGE RMS  $U_V$  VALUES FOR EACH TERRAIN TYPE AND PERCENT OF OCCURRENCES EXCEEDING CERTAIN LIMITS, FLIGHTS 54 TO 281

	<u>Water</u>	<u>Flatland</u>	<u>Mountains</u>
No. of Spectra	53	73	107
Avg. RMS $U_V$	0.86	1.02	1.89
RMS $U_V \geq 1.00$ ft/sec	23%	41%	81%
RMS $U_V \geq 2.00$ ft/sec	2%	8%	36%

The effect of mountainous terrain on turbulent conditions in the stratosphere is evident, considering that the data were collected over all four seasons and from several geographical areas.

Terrain features themselves are not the controlling factors in high altitude clear air turbulence. For example, if a water surface were chosen as one category then there would be little variation of clear air turbulence over the earth because most of the earth's surface is ocean. In addition, terrain features such as high mountains may have dissimilar effects upon clear air turbulence under differing meteorological conditions. Strong winds perpendicular to the mountain ridge would probably yield significantly more turbulence than light winds parallel to the ridge. The direction of flight with reference to a mountain ridge may have an important effect.

## SECTION VII

### CONCLUSIONS

An analysis of the data obtained from the HICAT flight program and of the pertinent meteorological data has led to the following conclusions:

1. The power spectra representing the clear air turbulence observed over mountains have slopes and characteristics that are distinctly different from the slopes and characteristics of the spectra obtained from flights over flatlands. The sample obtained from flights over water was too small to justify specific conclusions.
2. No conclusive evidence was found for a significant relationship between category of power spectra and meteorological conditions associated with HICAT.
3. Theoretical analyses indicated definite relationships between large horizontal atmospheric temperature gradients and turbulence and between relatively large changes in vertical temperature gradients and turbulence.
4. The turbulent and non-turbulent cases had distinctly different scalar and vector vertical wind shears of the horizontal winds.
5. Richardson's number for the HICAT levels was significantly higher than that reported in the literature for turbulent situations in the troposphere. However, Richardson's number did serve to distinguish between turbulent and non-turbulent cases to a useful extent.
6. Practical forecasting experience for the HICAT flight program has indicated that strong horizontal temperature gradients and layers with large changes in the vertical temperature gradients are excellent indicators of regions of turbulence. Conversely, small horizontal temperature gradients and layers with uniform vertical temperature gradients indicate regions of smooth flying conditions.
7. Relatively large temperature changes were observed along the flight path when the aircraft was in moderate or severe turbulence. During smooth flight conditions small or no temperature changes were observed.
8. The standard deviation of the 24 hour temperature changes at the 100 mb level for the western part of the northern hemisphere and for southeastern Australia were computed for each of the four seasons. Geographical regions for which the standard deviation was relatively high appear to coincide with regions of relatively high incidence of turbulence. Thus, this technique may be used to determine the world-wide distribution of turbulent and non-turbulent regions.
9. Turbulence was observed during 6.9% of the flight miles over mountains and 5.5% of the flight miles over water. The RMS of the vertical gust velocity during HICAT was 0.86 over water, 1.02 over flatland and 1.89 over mountains.

## SECTION VIII

### REFERENCES

1. Crooks, W. M., "High Altitude Clear Air Turbulence Interim Report," Contract AFFDL-TR-65-112, Lockheed-California Company, Burbank, Calif. (1965), 114 pp.
2. Crooks, W. M., F. M. Hoblit, and D. Prophet, "Project HICAT. An Investigation of High Altitude Clear Air Turbulence," Tech. Report AFFDL-TR-67-123, Lockheed-California Company, Burbank, Calif. (1967), 3 Vol., 1131 pp.
3. Hildreth, W. W., A. Court, T. Ioffer, G. E. Abrahms, E. Ashburn, L. Gates, and J. R. Cook, "High Altitude Clear Air Turbulence," Final Report. Contract AF 33(657)-9364, Lockheed-California Company, Burbank, Calif. (1963), 202 pp.
4. Hildreth, W. W., A. Court, and G. E. Abrahms, "High Altitude Rough Air Model Study," Tech. Report AFFDL-TR-15-112. Lockheed-California Company, Burbank, Calif. (1965), 109 pp.
5. Anonymous, "Critical Atmospheric Turbulence (ALLCAT)," Experimental Mechanics Branch, A.F. Flight Dynamics Lab., Wright-Patterson A.F.B., Ohio (1967) 17 pp.
6. Von Karman, T., "Progress in the Statistical Theory of Turbulence," J. Marine Res. 7, 252-64, (1948).
7. Houbolt, J. C., R. Steiner, and K. G. Pratt, "Dynamic Response of Airplanes to Atmospheric Turbulence Including Flight Data on Input and Response," Tech. Report R-199, National Aeronautics and Space Administration, Washington, D.C., (1964), 116 pp.
8. Rhyne, R. H., and R. Steiner, "Power Spectral Measurement of Atmospheric Turbulence in Severe Storms and Cumulus Clouds," Technical Note TN D-2469, National Aeronautics and Space Administration, Washington, D.C. (1964), 50 pp.
9. Hoblit, F. M., N. Paul, J. D. Shelton, and E. E. Asaford, "Development of a Power-Spectral Gust Design Procedure for Civil Aircraft," Report No. FAA-ADS-53, Contract FA-WA-4768, Federal Aviation Agency, Washington, D.C., (1966), 479 pp.
10. Stauffer, W. A., W. W. Hildreth, and W. M. Crooks, "CAT and the SST," Paper presented at the Institute of Navigation - Society of Automotive Engineers Conference - Clear Air Turbulence, Washington, D.C., (Feb. 1966).
11. Hildreth, W. W., and W. M. Crooks, "Preliminary Results of the HICAT Measurement Program," Paper presented at the Sixth Conference on Applied Meteorology, Los Angeles, California (1966).

12. Reiter, E. R., and A. Burns, "Atmospheric Structure and Clear Air Turbulence," *Atm. Sci. Paper No. 65*, Colorado State Univ., Ft. Collins, Colo. (1965), 18 pp.
13. Eliaseen, A., and E. Palm, "On the Transfer of Energy in Stationary Mountain Waves," *Geophys. Publ.* 22, 1-23 (1961).
14. Townsend, A. A., "Internal Waves Produced by a Convective Layer," *J. Fluid Mech.* 24, 307-20 (1966).
15. Reiter, E. R., and A. Burns, "The Structure of Clear-Air Turbulence Derived from "TOPCAT" Aircraft Measurements," *J. Atm. Sci.* 23, 206-12 (1966).
16. Pinus, N. Z., E. R. Reiter, G. N. Shur, and N. K. Vinnichenko, "Power Spectra of Turbulence in the Free Atmosphere," *Tellus* 19, 206-13 (1967).
17. Kolmogoroff, A. N., "The Local Structure of Turbulence in an Incompressible Viscous Fluid for Very Large Reynolds Number," *Akad. Nauk., SSSR, Dokl.* 30, 301-5 (1941).
18. Scorer, R. S., *Natural Aerodynamics*, (Pergamon, New York, 1958) 312 pp.
19. Haymond, CWO-4 F.B., "The Forecasting of CAT Above the Tropopause," ALLCAT Conference Agenda, Air Weather Service (MAC), Scott A.F.B., Ill. (1967).
20. King, H. W., *Handbook of Hydraulics*, (McGraw-Hill, New York, 1939) 611 pp.
21. Queny, P., G. A. Corby, N. Gerbier, H. Keschmieder, and J. Zierep., "The Air Flow Over Mountains," WMO Technical Note No. 34, World Meteorological Organization, Geneva, Switz. (1960), 132 pp.
22. Holmboe, J., G. E. Forsythe, and W. Gustin, *Dynamic Meteorology*, (Wiley, New York, 1945), 378 pp.
23. Briggs, J., and W. T. Roach, "Aircraft Observations Near Jet Streams," *Quart. J. Roy. Meteorol. Soc.* 89, 225-47 (1963).
24. Endlich, R. M., and R. L. Mancuso, "On the Analysis of Clear Air Turbulence by Use of Rawinsonde Data," *Mon. Wea. Rev.* 93, 47-58 (1965).
25. Reiter, E. R., and P. F. Lester, "The Dependence of Richardson Number on Scale Length," *Atm. Sci. Paper No. 111*, Colorado State Univ., Ft. Collins, Colo. (1967), 39 pp.
26. Serebreny, S. M. and E. J. Wiegman, "Certain Characteristic Features of the Jet Stream and Their Application to Airline Operations," *Meteorological Report*, Pan American World Airways, Inc., Pacific-Alaska Division (1954) 37 pp.

27. Reiter, E. R., and R. W. Hayman, "On the Nature of Clear-Air Turbulence," Contract N 189 (188) 538-28A, Atm. Sci. Paper No. 28 Colorado State Univ., Ft. Collins, Colo. (1962), 42 pp.
28. Kadlec, P.W., "Flight Observations of Atmospheric Turbulence," Final Report, Contract FA66WA-1449, Eastern Airlines, Miami, Fla. (1966), 52 pp.
29. Kadlec, P.W., "Exploration of the Relationship Between Atmospheric Temperature Change and Clear Air Turbulence," Proceedings, National Air Meeting on Clear Air Turbulence, Society of Automotive Engineers, New York, N.Y., 44-50 (Feb. 1966).
30. George, J. J., "Airline Practices in Forecasting Clear Air Turbulence," Proceedings, National Air Meeting on Clear Air Turbulence, Society of Automotive Engineers, New York, N.Y., 172-80 (Feb. 1966).
31. Helvey, R. A., "Observations of Stratospheric Clear Air Turbulence and Mountain Waves over the Sierra Nevada Mountains," Final Report, Contract AF 13(628)-4146, University of California, Los Angeles, Calif. (1967), 60 pp.

SECTION IX  
BIBLIOGRAPHY

- Anonymous, "Airborne Infrared System for Clear Air Turbulence Detection,"  
Pull. 14-601, Barnes Engineering Co., Stamford, Conn. (1968), 7 pp.
- Anonymous, "Atmospheric Turbulence Research, USSR," JPRS 37855, Joint  
Publications Research Service, Washington, D.C. (1966), 56 pp.
- Anonymous, "Critical Atmospheric Turbulence (ALLCAT)," Experimental  
Mechanics Branch, A.F. Flight Dynamics Lab., Wright-Patterson A.F.B.,  
Ohio (1967), 17 pp.
- Anonymous, "Report of the National Committee for Clear Air Turbulence to the  
Federal Coordinator for Meteorological Services and Supporting Research,"  
U.S. Dept. of Commerce, Washington, D.C. (1966), 51 pp.
- Anonymous, Society of Automotive Engineers, "National Air Meeting on Clear  
Air Turbulence," Proceedings, New York, New York (Feb. 1966) 198 pp.
- Anonymous, U.S. Air Force Cambridge Research Labs., "Radar Detection of  
Clear Air Turbulence," Office Aerospace Res., Res. Rev. 5, 15-7 (1966).
- Aanensen, C. J. M., "Turbulence in Clear Air Near a Warm Front Surface,"  
Meteorol. Mag. 77, 209-10 (1948).
- Allan, R. M., "High Altitude Clear Air Turbulence," Technical Note No.  
AERO 2122, Royal Aircraft Establishment, Farnborough, Eng. (1951),  
12 pp.
- Arakawa, H., "Possible Heavy Turbulent Exchange Between the Extratropical  
Tropospheric Air and the Polar Stratospheric Air," Tellus 3, 208-11 (1951).
- Atlas, D., "Optimizing the Radar Detection of Clear Air Turbulence," J. Appl.  
Meteorol. 5, 450-60 (1966).
- Ball, J. T., "A Multiple-Discriminant Analysis of Clear-Air Turbulence,"  
Contract FAA/BRD-363, Tech. Publ. No. 22, The Travelers Research  
Center, Inc., Hartford, Conn. (1962), 25 pp.
- Balzer, M. E., and H. T. Harrison, "The Nature of High Level Clear Air  
Turbulence," Meteorol. Circ. No. 48, United Air Lines, Denver, Colo.  
(1959), 29 pp.

- Bannon, J. K., "Severe Turbulence Encountered by Aircraft Near Jet Streams," Meteorol. Mag. 80, 262-9 (1951).
- Bannon, J. K., "Weather Systems Associated with Some Occasions of Severe Turbulence at High Altitude," Meteorol. Mag. 81, 97-101 (1952).
- Batchelor, G. K., The Theory of Homogeneous Turbulence, (Cambridge Univ. Press, London, 1953) 197 pp.
- Beard, M. G., "Status Report on Latest Development in Clear Air Turbulence," J. Aircraft 3, 443-8 (1966).
- Beliaev, V. P., "Some Results of the Experimental Investigations of the Atmospheric Turbulence Using Radiosondes," Tech. Transl. F-246, National Aeronautics and Space Administration, Washington, D.C. (1965), 66 pp.
- Beliaev, V. P., "Some Results of Comparisons Between Radiosonde and Aircraft Measurements of Turbulence in the Free Atmosphere," Translation -392 (M), Joint Publications Research Service, Washington, D.C. (1967), 5 pp.  
Moscow Tsent. Aerolog. Observ. 63, 109-13 (1965).
- Berggren, R., "The Distribution of Temperature and Wind Connected with Active Tropical Air in the Higher Troposphere and Some Remarks Concerning Clear Air Turbulence at High Altitude," Tellus 4, 43-53 (1952).
- Binding, A.A., "Association of Clear Air Turbulence with 300 mb - Contour Patterns," Meteorol. Mag. 94, 11-9 (1965).
- Boockholdt, J., (Ed), "ALLCAT Conference Agenda," Air Weather Service (MAC), Scott A.F.B., Ill. (1967), 150 pp.
- Boone, J. P., "High Altitude Critical Atmospheric Turbulence Data System," Tech. Report No. AFFDL-TR-67-1, A.F. Flight Dynamics Lab., Wright-Patterson A.F.B., Ohio (1967), 23 pp.
- Briggs, J., "Widespread Severe Clear Air Turbulence, 13 November 1958," Meteorol. Mag. 90, 234-9 (1961).
- Briggs, J., "High-Level Turbulence Over Europe and the Mediterranean," Inst. Navigation J. 16, 220-6 (1967).
- Briggs, J., and W. T. Roach, "Aircraft Observations Near Jet Streams," Quart. J. Roy. Meteorol. Soc. 89, 225-47 (1963).
- Brochet, G., "Contribution to the Statistical Study of Clear Air Turbulence," Meteorol. (France) 81, 3-24 (1966).
- Buckler, S. J., "An Analysis of the Meteorological Conditions During a Case of Severe Turbulence," CIR-4211, TEC-563, Dept. of Transport-Meteorological Branch, Toronto, Canada, (1965), 17 pp.

- Burns, A., T. W. Harrold, J. Burnham, and C. S. Spavins, "Turbulence in Clear Air Near Thunderstorms," Technical Memorandum; ERTM-NSSL-3Q, Environmental Sciences Services Administration, Washington, D.C., (1966), 24 pp.
- Burns, A., and C. K. Rider, "Project TOPCAT: Power Spectral Measurements of Clear Air Turbulence Associated with Jet Streams," Tech. Report No. 65210, Royal Aircraft Establishment, Farnborough, England (1965), 11 pp.
- Clarke, R. H., "Turbulence and a Detailed Structure of a Sub-Tropical Jet Stream." J. Atm. Sci. 23, 516-30 (1966).
- Clem, H., "Clear Air Turbulence Over the U.S.," Aeronaut. Eng. Rev. 16, 63-8 (1957).
- Clodman, J., G. N. Morgan, and J. T. Ball, "High Level Turbulence," Final Report, Contract AF 19(604)-5208, New York Univ., New York, N.Y. (1960) 83 pp.
- Coleman, T. L., and M. T. Meadows, "Airplane Measurements of Atmospheric Turbulence at Altitudes Between 20,000 and 55,000 Feet for Four Geographic Areas," Memo 4-17-59J, National Aeronautics and Space Administration, Washington, D.C. (1959), 21 pp.
- Coleman, T. L., and R. Steiner, "Atmospheric Turbulence Measurements Obtained from Airplane Operations at Altitudes Between 20,000 and 70,000 Feet for Several Areas of the Northern Hemisphere," NASA TN D-548, Langley Aeronautical Lab., Hampton, Va. (1960), 24 pp.
- Colson, D., "Analysis of Clear Air Turbulence Data for March 1962," Mon. Wea. Rev. 91, 73-82 (1963a).
- Colson, D., "Summary of High Level Turbulence Over U.S.," Mon. Wea. Rev. 91, 605-9 (1963b).
- Colson, D., "Analysis of Clear Air Turbulence During Selected 5-Day Data Periods," SRDS Report No. RD-66-79, Final Report, Contract FA66WAI-106, Systems Development Office, Environmental Sciences Services Administration, Washington, D. C., (1966).
- Colson, D., and H. A. Panofsky, "An Index of Clear Air Turbulence," Quart. J. Roy. Meteorol. Soc. 91, 507-13 (1965).
- Cook, J. R., "Technique for Measuring Long Scale Length Atmospheric Perturbations," Report No. LR 16461, Lockheed-California Company, Burbank, Calif. (1962), 37 pp.
- Corwin, H. G., "Operational Use of Richardson Number in the Analysis of Clear-Air Turbulence," Meteorol. Tech. Bull. No. 62-1, Trans. World Airlines, Kansas City, Mo. (1962), 8 pp.

- Court, A., "Undulance and Turbulence," *Quart. J. Roy. Meteorol. Soc.* 91, 234-5 (1965).
- Coy, R. G., "Atmospheric Turbulence Spectra from B-52 Flight Loads Data," Tech. Report AFFDL-TR-67-13, Univ. of Dayton Research Institute, Dayton, Ohio (1967), 50 pp.
- Crooks, W., "High Altitude Clear Air Turbulence Interim Report," Contract AFFDL-TR-65-112, Lockheed-California Company, Burbank, Calif. (1965) 114 pp.
- Crooks, W. M., F. M. Hoblit, and D. Prophet, "Project HICAT. An Investigation of High Altitude Clear Air Turbulence," Tech. Report AFFDL-TR-67-123, Lockheed-California Company, Burbank, Calif. (1967), 3 Vol., 1131 pp.
- Crooks, W. M., W. A. Stauffer, and W. W. Hildreth, "Clear Air Turbulence," *Lockheed Horizons* 5, 2nd Quarter, 78-96 (1966).
- Cummingham, N. W., "A Study of the Duration of Clear-Air Turbulence Near the Jet Stream and its Relation to Horizontal Temperature Gradient," Wind Field Near the Tropopause, Final Report, Contract AF 19(604)-1565, Texas A. & M., College Station, Texas, 75-85 (1958).
- Davidson, B., "Some Turbulence and Wind Variability Observations in the Lee of the Mountain Ridges," *J. Appl. Meteor.* 2, 463-72 (1963).
- Doos, B. R., "A Mountain Wave Theory Including the Effect of the Vertical Variation of Wind and Stability," *Tellus* 13, 305-19 (1961).
- Dutton, J. A., "Belling the Cat in the Sky," *Bull. Am. Meteorol. Soc.* 48, 813-20 (1967).
- Endlich, R. M., "The Mesoscale Structure of Some Regions of Clear-Air Turbulence," *J. Appl. Meteorol.* 3, 261-76 (1964).
- Endlich, R. M., and J. W. Davies, "The Feasibility of Measuring Turbulence in the Free Atmosphere from Rising Balloons Tracked by FPS-16 Radar," *J. Appl. Meteor.* 6, 43-7 (1967).
- Endlich, R. M., and G. S. McLean, "Empirical Relationships Between Gust Intensity in Clear-Air Turbulence and Certain Meteorological Quantities," *J. Appl. Meteorol.* 4, 222-7 (1965).
- Endlich, R. M., and R. L. Mancuso, "Clear-Air Turbulence and its Analysis by Use of Radiosonde Data," Final Report, Contract Cwb-10624, Stanford Research Institute, Menlo Park, Calif. (1964), 55 pp.
- Endlich, R. M., and R. L. Mancuso, "Objective Analysis and Forecasting of Clear-Air Turbulence," Final Report, Contract Cwb-10871, Stanford Research Institute, Menlo Park, Calif. (1965a), 56 pp.

- Endlich, R. M., and R. L. Mancuso, "On the Analysis of Clear-Air Turbulence by Use of Rawinsonde Data," *Mon. Wea. Rev.* 93, 47-58 (1965b).
- Endlich, R. M., and R. L. Mancuso, "Forecasting Clear-Air Turbulence by Computer Techniques," Final Report, Contract FA 66WA-1442, Stanford Research Institute, Menlo Park, Calif. (1967), 86 pp.
- Endlich, R. M., R. L. Mancuso, and J. W. Davies, "Techniques for Determining a World-Wide Climatology of Turbulence Through Use of Meteorological Data," Contract AF 19(628)-5173, Stanford Research Institute, Menlo Park, Calif. (1966), 62 pp.
- Endlich, R. M., and W. Viezee, "Detailed Structure of the Atmosphere in Regions of Clear-Air Turbulence," Final Report, Contract Cwb-10324, Stanford Research Institute, Menlo Park, Calif. (1963), 62 pp.
- Estoque, M. A., "Some Characteristics of Turbulence at High Altitudes," Research Notes No. 4, Geophysical Research Directorate, Cambridge, Mass. (1958), 10 pp.
- Foltz, H. P., "Prediction of Clear Air Turbulence," *Atm. Sci. Paper No. 106*, Colorado State Univ., Ft. Collins, Colo. (1967), 144 pp.
- George, J. J., "Prediction of Clear Air Turbulence," *Shell Aviation News* 273, 1-7 (1961).
- George, J. J., "Airline Practices in Forecasting Clear Air Turbulence," Proceedings, National Air Meeting on Clear Air Turbulence, Society of Automotive Engineers, New York, New York, 172-80 (Feb. 1966).
- Gould, R. C., "The Relation of Upper-Air Turbulence to Tropopause Layers," NAVORD Report 6544, NOTS TP 2242, U.S. Naval Ordnance Test Station, China Lake, Calif. (1959), 27 pp.
- Gruzinova, L. G., and E. I. Sofiev, "Relationship Between the Richardson Number and Atmospheric Turbulence," Contract AF 19(628)-3880, A. F. Cambridge Research Labs., Bedford, Mass. (1966), 9 pp.
- Hanson, D., L. Rothernberg, D. Colson, M. F. Grace, and S. Simplicio, "Procedures for Forecasting Clear Air Turbulence," Tech. Note No. 5, Office of Forecast Development, U.S. Dept. of Commerce, Washington, D.C. (1962), 13 pp.
- Harrison, H. T., "The Use of Horizontal Wind Shear in Forecasting High Level Clear Air Turbulence," *Meteorol. Circ. No. 49*, United Air Lines, Denver, Colo. (1959), 22 pp.
- Harrison, H. T., "Progress in Forecasting High Level Clear Air Turbulence," *Meteorol. Circ. No. 52*, United Air Lines, Denver, Colo. (1961), 30 pp.

- Harrison, H. T., and D. F. Sowa, "Mountain Wave Exposure on Jet Routes of Northwest Airlines and United Airlines," Meteorol. Circ. No. 60, United Airlines, Chicago, Ill., (1966), 68 pp.
- Haymond, CWO-4 F.B., "The Forecasting of CAT Above The Tropopause," ALLCAT Conference Agenda, Air Weather Service (MAC), Scott A.F.B., Ill., (1967).
- Helvey, R. A., "Observations of Stratospheric Clear-Air Turbulence and Mountain Waves Over the Sierra Nevada Mountains," Final Report, Contract AF 19(628)-4146, University of California, Los Angeles, Calif. (1967), 60 pp.
- HICAT Project, Australia, "Preliminary Notes," Bureau of Meteorology, Melbourne, Australia (1966), 3 pp.
- Hildreth, W. W., and G. E. Abrahms, "Program to Develop a World Wide Turbulence Model for Altitudes Between 50,000 and 80,000 Feet," Report No. LR 19092, Lockheed-California Company, Burbank, Calif. (1965), 58 pp.
- Hildreth, W. W., A. Court, and G. Abrahms, "High Altitude Rough Air Model Study," Tech. Report AFFDL-TR-15-112, Lockheed-California Company, Burbank, Calif. (1965), 109 pp.
- Hildreth, W. W., A. Court, T. Hoffer, G. E. Abrahms, E. Ashburn, L. Gates, and J. R. Cook, "High Altitude Clear Air Turbulence," Final Report, Contract AF 33(657)-9364, Lockheed-California Company, Burbank, Calif. (1963), 202 pp.
- Hodge, M. W., and C. Harmantas, "Compatibility of U.S. Radiosondes," Mon. Wea. Rev. 93, 253-6 (1965).
- Hodge, M. W., "Large Irregularities of Rawinsonde Ascensional Rates Within 100 Nautical Miles and 3 Hours of Reported Clear Air Turbulence," Mon. Wea. Rev. 95, 99-106 (1967).
- Hodges, R. R., Jr., "Generation of Turbulence in the Upper Atmosphere by Internal Gravity Waves," J. Geophys. Res. 72, 3455-8 (1967).
- Holmboe, J., G. E. Forsythe, and W. Gustin, Dynamic Meteorology, (Wiley, New York, 1945), 378 pp.
- Houbolt, J. C., "Preliminary Development of Gust Design Procedures Based on Power Spectral Techniques," Tech. Report AFFDL-TR-66-58, A.F. Flight Dynamics Lab., Wright-Patterson A.F.B., Ohio (1966), 2 vol., 65 pp.
- Houbolt, J. C., R. Steiner, and K. G. Pratt, "Dynamic Response of Airplanes to Atmospheric Turbulence Including Flight Data on Input and Response," Tech. Report R-199, National Aeronautics and Space Administration, Washington, D.C. (1964), 116 pp.

- Jefferson, C. J., "An Incident of Severe Low-Level Turbulence," *Meteorol. Mag.* 95, 279-85 (1966).
- Jones, R. F., "Clear Air Turbulence," *Science J.* 3, 34-9 (1967).
- Joseph, P. V., and R. Singh, "Nomograms for Evaluating Richardson Number for Forecasting Clear Air Turbulence," *Indian J. Meteorol. Geophys.* 17, 411-4 (1966).
- Kadlec, P. W., "An In-Flight Study of the Relation Between Jet Streams, Cirrus, and Wind Shear Turbulence," Final Report, Contract Cwb-10356, Eastern Airlines, Miami, Fla. (1963), 48 pp.
- Kadlec, P. W., "A Study of Flight Conditions Associated with Jet Stream Cirrus, Atmospheric Temperature Change, and Wind Shear Turbulence," Final Report, Contract Cwb-10674, Eastern Airlines, Miami, Fla. (1964), 45 pp.
- Kadlec, P. W., "Flight Data Analysis of the Relationship Between Atmospheric Temperature Change and Clear Air Turbulence," Final Report, Contract Cwb-10888, Eastern Airlines, Miami, Fla. (1965), 43 pp.
- Kadlec, P. W., "Flight Observations of Atmospheric Turbulence," Final Report, Contract FA66WA-1449, Eastern Airlines, Miami, Fla. (1966a), 52 pp.
- Kadlec, P. W., "Exploration of the Relationship Between Atmospheric Temperature Change and Clear Air Turbulence," Proceedings, National Air Meeting on Clear Air Turbulence, Society of Automotive Engineers, New York, N. Y., 44-50 (Feb. 1966b).
- Kao, S. K., "Analysis of Clear Air Turbulence Near the Jet Stream," *J. Geophys. Res.* 71, 3799-805 (1966).
- Kao, S. K., and H. D. Woods, "Energy Spectra of Meso-Scale Turbulence Along and Across the Jet Stream," *J. Atm. Sci.* 21, 513-19 (1964).
- Kolmogoroff, A. N., "The Local Structure of Turbulence in an Incompressible Viscous Fluid for Very Large Reynolds Number," *Akad. Nauk, SSSR, Dokl.* 30, 301-5 (1941).
- Kronebach, G. W., "An Automated Procedure for Forecasting Clear-Air Turbulence," *J. Appl. Meteorol.* 3, 119-25 (1964).
- Kuettner, J. I., "On the Possibility of Soaring on Traveling Waves in the Jet Stream," *Aeronaut. Eng. Rev.* 11, 1-7 (1952).
- Lake, H., "A Meteorological Analysis of Clear Air Turbulence," Research Papers No. 47, Geophysical Research Directorate, Cambridge, Mass. (1956), 63 pp.

- Loving, N. V., "High Altitude Clear Air Turbulence (HICAT) - A Menace to the Aerial Highway," AMS/AIAA Paper No. 66-362, American Meteorological Society/American Institute of Aeronautics and Astronautics Conference on Aerospace Meteorology (Mar. 1966), 12 pp.
- Ludlam, F. H., "Characteristics of Billow Clouds and Their Relation to Clear-Air Turbulence," Quart. J. Roy. Meteorol. Soc. 93, 419-35 (1967).
- Lumley, J. L., and H. A. Panofsky, The Structure of Atmospheric Turbulence, (Interscience (Wiley), New York, 1964) 239 pp.
- MacCready, P. B., Jr., "The Inertial Subrange of Atmospheric Turbulence," J. Geophys. Res. 67, 1051-9 (1962).
- McLean, G. S., "An Investigation into the Use of Temperature Gradients as an In-Flight Warning of Impending Clear-Air Turbulence," Environmental Res. Papers No. 85, A.F. Cambridge Research Labs., Bedford, Mass. (1965), 20 pp.
- McLean, J. C., "Synoptic Analysis of Clear Air Turbulence," Proceedings, National Air Meeting on Clear Air Turbulence, Society of Automotive Eng. New York, N. Y., 15-20 (Feb. 1966).
- Mancuso, R. L. and R. M. Endlich, "Clear Air Turbulence Frequency as a Function of Wind Shear and Deformation," Mon. Wea. Rev. 94, 581-5 (1966).
- Mather, G. K., "Some Measurements of Mountain Waves and Mountain Wave Turbulence Made Using the NAE T-33 Turbulence Research Aircraft," Quart. Bull. No. 2, National Research Council, Div. of Mech. Eng. and National Aeronaut. Estab., Ottawa, Can., 1-27 (1967).
- Miller, A. J., "Note on Vertical Motion in the Lower Stratosphere," Beitr. Phys. Atmos. 40, 29-48 (1967).
- Moore, R. L., and T. N. Krishnamurti, "Atmospheric Clear Air Turbulence," Nature 209, 462-64 (1966a).
- Moore, R. L., and T. N. Krishnamurti, "A Theory of Generation of Clear Air Turbulence," Proceedings, National Air Meeting on Clear Air Turbulence, Society of Automotive Engineers, New York, N. Y., 13-20 (Feb. 1966b).
- Nanevich, J. E., E. F. Vance, and S. M. Serebreny, "Correlation Between Clear Air Turbulence and Aircraft Electrical Activity," Proceedings, National Air Meeting on Clear Air Turbulence, Society of Automotive Engineers, New York, N. Y. 77-83 (Feb. 1966).
- Norman, S. M., and N.H. Nacoy, "Inference of Clear Air Turbulence by Means of An Airborne Infrared System," J. Aircraft 3, 289-96 (1966).

- Obukhov, A. M., and A. M. Iaglom, "Progress in Atmospheric Turbulence Investigations," *Atm. Oceanic Phys.* 3, 207-11 (1967).
- Oort, A. H., "Energetics of Mean and Eddy Circulations in the Lower Stratosphere," *Tellus* 16, 309-26 (1964).
- Panofsky, H. A., and R. A. McCormick, "Turbulence Spectra," *Quart. J. Roy. Meteorol. Soc.* 80, 546-64 (1954).
- Panofsky, H. A., and J. C. McLean, "Physical Mechanisms of Clear Air Turbulence," *Meteorology Report*, Penn. State Univ., College Park, Pa. (1964), 20 pp.
- Penn, S., and T. A. Pisinski, "Mesoscale Structure of the Atmosphere in Regions of Clear Air Turbulence, Volume I," *A. F. Surv. Geophys.* 190, Report No. AFCRL-67-0115, A. F. Cambridge Research Labs., Hanscom Field, Mass., (1967), 96 pp.
- Pinus, N. Z., "Atmospheric Turbulence," Tech. Report R, F-246, National Aeronautics and Space Administration, Washington, D. C. (1965), 129 pp.
- Pinus, N. Z., E. R. Reiter, G. N. Shur, and N. K. Vinnichenko, "Power Spectra of Turbulence in the Free Atmosphere," *Tellus* 19, 206-13 (1967).
- Pinus, N. Z., and S. M. Shmeter, Atmospheric Turbulence Affecting Aircraft Bumping, (Hydrometeorol., Moscow, 1962) 167 pp.
- Port, W. G. A., "High Altitude Gust Investigation," Report No. AERO 2341, Royal Aircraft Establishment, Farnborough, Eng. (1949), 24 pp.
- Prophet, D. T., "A Mechanism for Clear Air Turbulence Development," Contract AF 33(657)-11143, Lockheed-California Company, Burbank, Calif. (1967) 19 pp.
- Queney, P., G. A. Corby, N. Gerbier, H. Koschmieder, and J. Zierep, "The Air Flow Over Mountains," WMO Technical Note No. 34, World Meteorological Organization, Geneva, Switz. (1960), 132 pp.
- Rai Sircar, N. C., and K. P. Varghese, "Study of High Level Clear Air Turbulence Reports Received from Aircraft," *Indian J. Meteorol. Geophys.* 14, 433-40 (1963).
- Reiter, E. R., "A Case Study of Severe Clear Air Turbulence," Contract No. N 189 (188) 55120A, *Atm. Sci. Paper No. 30*, Colorado State Univ., Ft. Collins, Colo. (1962b), 15 pp. *Arch. Meteorol., Geophys. Bioklimatol., Ser. A.*, 13, 379-89 (1963).
- Reiter, E. R., "Nature and Observation of High Level Turbulence Especially in Clear Air," *J. Aircraft* 1, 94-6 (1964a).

- Reiter, E. R., "CAT and SCAT," *Astronaut. Aeronaut.* 2, 60-5 (1964b).
- Reiter, E. R., "Problem of Clear-Air Turbulence (CAT): Possible Future Developments," *Astronaut. Aeronaut.* 5, 56-8 (1967).
- Reiter, E. R., D. W. Beran, J. D. Mahlman, and G. Wooldridge, "Effect of Large Mountain Ranges on Atmospheric Flow Patterns as Seen from TIROS Satellites," *Atm. Sci. Paper No. 69*, Colorado State Univ., Ft. Collins, Colo. (1965).
- Reiter, E. R., and A. Burns, "Atmospheric Structure and Clear Air Turbulence," *Atm. Sci. Paper No. 65*, Colorado State Univ., Ft. Collins, Colo. (1965), 18 pp.
- Reiter, E. R., and A. Burns, "The Structure of Clear-Air Turbulence Derived from 'TOPCAT' Aircraft Measurements," *J. Atm. Sci.* 23, 206-12 (1966).
- Reiter, E. R., and H. P. Foltz, "The Prediction of Clear Air Turbulence Over Mountainous Terrain," *J. Appl. Meteorol.* 6, 549-56 (1967).
- Reiter, E. R., and R. W. Hayman, "On the Nature of Clear-Air Turbulence," Contract N 189 (188) 538-28A, *Atm. Sci. Paper No. 28*, Colorado State Univ., Ft. Collins, Colo. (1962), 42 pp.
- Reiter, E. R., and P. F. Lester, "The Dependence of the Richardson Number on Scale Length," *Atm. Sci. Paper No. 111*, Colorado State Univ., Ft. Collins, Colo. (1967), 39 pp.
- Reiter, E. R., and A. Nania, "Jet-Stream Structure and Clear-Air Turbulence (CAT)," *J. Appl. Meteorol.* 3, 247-60 (1964).
- Richardson, N. N., "Clear Air Turbulence," Scientific Services Tech. Note 6, Offutt A. F. B., Nebraska (1963), 29 pp.
- Rustenbeck, J. D., "Association of Richardson's Criterion with High Level Turbulence," *Mon. Wea. Rev.* 91, 193-8 (1963).
- Sasaki, J., "A Theory and Analysis of Clear Air Turbulence," Contract AF 19(604)-1565, Texas A. & M., College Station, Tex. (1958).
- Sastry, P. S. N., "A Note on Evaluation of the Richardson Number in Relation to Forecasting Clear Air Turbulence," *Indian J. Meteorol. Geophys.* 17, 415-8 (1966).
- Saxton, D. W., "Nature and Causes of Clear-Air Turbulence," *J. Aircraft* 4, 356-9 (1967).

- Scherhag, R., G. Warnecke, and W. Wehry, "Meteorological Parameters Affecting Supersonic Transport Operations," *Inst. Navigation J.* 20, 53-63 (1967).
- Scorer, R. S., "Theory of Waves in the Lee of Mountains," *Quart. J. Roy. Meteorol. Soc.* 75, 41-56 (1949).
- Scorer, R. S., "Clear Air Turbulence in the Jet Stream," *Weather* 12, 275-82 (1957).
- Scorer, R. S., *Natural Aerodynamics*, (Pergamon, New York, 1958) 312 pp.
- Scrase, F. J., "Turbulence in the Upper Air As Shown by Radar Wind and Radiosonde Measurements," *Quart. J. Roy. Meteorol. Soc.* 80, 369-76 (1954).
- Shur, G. N., "The Spectral Structure of Turbulence in a Free Atmosphere based on Data Obtained by Aircraft," *RSIC-543*, U. S. Redstone Scientific Information Center, Redstone Arsenal, Ala. (1966), 15 pp.
- Smigielski, F. J., "A Note on Clear Air Turbulence During April and May, 1960," *Mon. Wea. Rev.* 88, 91-3 (1960).
- Sorenson, J. E., "Synoptic Patterns for Clear Air Turbulence," *Meteorol. Circ.* 56, United Airlines, Chicago, Ill. (1964), 64 pp.
- Spillane, K. T., "Atmospheric Structures Associated with Turbulence in the Free Atmosphere," *Australian Meteorol. Mag.* 50, 44-5 (1965).
- Spillane, K. T., "Clear Air Turbulence and Supersonic Transport," *Nature* 214, 237-9 (1967).
- Steiner, R., "A Review of NASA High Altitude Clear Air Turbulence Sampling Programs," *J. Aircraft* 3, 48-52 (1966).
- Stephens, J. J., and E. R. Reiter, "Estimating Refractive Index Spectra in Regions of Clear Air Turbulence," *J. Appl. Meteorol.* 6, 911-3 (1967).
- Tillotson, K. C., and D. Colson, "Wave-Cloud Formation at Denver," *Weatherwise* 7, 34-5 (1954).
- Vasil'ev, A. A., "Use of Scorer's Parameter for Forecasting Turbulence on the Leeward Side of Mountains," *NLL-M 7028*, Joint Publications Research Service, Washington, D.C. (1967), 9 pp. *Trudy, Tsentr. Inst. Prognozov* 158, 90-8 (1966).
- Venkiteshwaran, S. P., and B. B. Huddar, "A Method of Estimating the Vertical Component of Gusts in Turbulence in the Upper Air," *Indian J. Meteorol. Geophys.* 17, 563-6 (1966).

- Vinnichenko, N. K., "Clear Air Turbulence at Heights of 6-12 KM," *Atm. Oceanic Phys.* 2, 701-4 (1966).
- Vinnichenko, N. K., N. Z. Pinus, and G. N. Shur, "Some Data on Turbulence in the Upper Troposphere and Stratosphere Causing Airplane Buffeting," *Meteorol. Hydrol.* 11, 35-47 (1967).
- Von Karmen, T., "Progress in the Statistical Theory of Turbulence," *J. Marine Res.* 7, 252-64 (1948).
- Wells, E. W., "Project TOPCAT: Summary of Meteorological Observations and Aircraft Measurements During Routine Flights in the Australian Jet Stream," Tech. Report 66122, Royal Aircraft Establishment, Farnborough, Eng. (1966), 44 pp.
- Wiegman, E. J., "Distribution of Clear Air Turbulence Reports and Cloud Patterns as Seen in Satellite Photographs," Final Report, Contract Cwb-10791, Stanford Research Institute, Menlo Park, Calif. (1965), 101 pp.
- Zirkle, R. E., Jr., "Study of Techniques for Detection and Measurement of Clear Air Turbulence," Final Report, Contract AF 19(628)-2376, Honeywell, Inc., Roseville, Minn. (1966) 125 pp.

Unclassified

Security Classification

DOCUMENT CONTROL DATA - R&D		
(Security classification of title, body of abstract and indexing annotation must be entered when the overall report is classified)		
1. ORIGINATING ACTIVITY (Corporate author) Lockheed-California Company P. O. Box 551 Burbank, California		2a. REPORT SECURITY CLASSIFICATION Unclassified
		2b. GROUP
3. REPORT TITLE HIGH ALTITUDE CLEAR AIR TURBULENCE MODELS FOR AIRCRAFT DESIGN AND OPERATION		
4. DESCRIPTIVE NOTES (Type of report and inclusive dates) Final Report 1 March 1966 - 30 June 1968		
5. AUTHOR(S) (Last name, first name, initial) Ashburn, Edward V.; Prophet, David T.; and Waco, David E.		
6. REPORT DATE July 1968	7a. TOTAL NO. OF PAGES 131	7b. NO. OF REFS 31
8a. CONTRACT OR GRANT NO. AF 33(615)-3639	9a. ORIGINATOR'S REPORT NUMBER(S) LR 21501	
b. PROJECT NO. 1367		
c. Task No. 136702	9b. OTHER REPORT NO(S) (Any other numbers that may be assigned this report)	
10. AVAILABILITY/LIMITATION NOTICES This document is subject to special export controls and each transmittal to foreign governments or foreign nationals may be made only with prior approval of the Air Force Flight Dynamics Laboratory (FDTR), Wright-Patterson AFB, Ohio 45433		
11. SUPPLEMENTARY NOTES	12. SPONSORING MILITARY ACTIVITY Flight Dynamics Laboratory Air Force Systems Command Wright-Patterson Air Force Base, Ohio	
13. ABSTRACT <p>This report presents the results of an analysis of the turbulence data derived from the high altitude clear air turbulence (HICAT) flight investigation and from the pertinent meteorological and geophysical data. The curves representing the power spectra have various slopes and shape. These curves are grouped into categories. One group of categories are predominantly cases of flights over mountains. A second group of categories are mostly from flights over flatland. Theoretical, statistical, and practical forecasting analyses in addition to flight records all indicate that large horizontal temperature gradients and large changes in vertical temperature gradient are closely associated with HICAT and conversely small horizontal temperature gradients and nearly constant vertical temperature gradients are closely associated with smooth air.</p> <p>Evidence is presented that the relative frequency of occurrence of high altitude clear air turbulence by geographic area may be deduced from an analysis of the standard deviation of the 24 hour temperature changes at the HICAT flight altitude.</p> <p>Turbulence was observed during 6.9% of the flight miles over mountains and 5.5% of the flight miles over water. The RMS of the vertical gust velocity during HICAT was 0.86 over water, 1.02 over flatland and 1.89 over mountains.</p> <p>This document is subject to special export controls and each transmittal to foreign governments or foreign nationals may be made only with prior approval of the Air Force Flight Dynamics Laboratory (FDTR), Wright-Patterson AFB, Ohio 45433.</p>		

DD FORM 1 JAN 64 1473 0101-807-6800

Unclassified

Security Classification

Unclassified

Security Classification

14 KEY WORDS	LINK A		LINK B		LINK C	
	ROLE	WT	ROLE	WT	ROLE	WT
High Altitude Clear Air Turbulence Models of Clear Air Turbulence Meteorological Conditions Associated with Clear Air Turbulence						

**INSTRUCTIONS**

1. **ORIGINATING ACTIVITY:** Enter the name and address of the contractor, subcontractor, grantee, Department of Defense activity or other organization (*corporate author*) issuing the report.

2a. **REPORT SECURITY CLASSIFICATION:** Enter the overall security classification of the report. Indicate whether "Restricted Data" is included. Marking is to be in accordance with appropriate security regulations.

2b. **GROUP:** Automatic downgrading is specified in DoD Directive 5700.10 and Armed Forces Industrial Manual. Enter the group number. Also, when applicable, show that optional markings have been used for Group 3 and Group 4 as authorized.

3. **REPORT TITLE:** Enter the complete report title in all capital letters. Titles in all cases should be unclassified. If a meaningful title cannot be selected without classification, show title classification in all capitals in parenthesis immediately following the title.

4. **DESCRIPTIVE NOTES:** If appropriate, enter the type of report, e.g., interim, progress, summary, annual, or final. Give the inclusive dates when a specific reporting period is covered.

5. **AUTHOR(S):** Enter the name(s) of author(s) as shown on or in the report. Enter last name, first name, middle initial. If military, show rank and branch of service. The name of the principal author is an absolute minimum requirement.

6. **REPORT DATE:** Enter the date of the report as day, month, year; or month, year. If more than one date appears on the report, use date of publication.

7a. **TOTAL NUMBER OF PAGES:** The total page count should follow normal pagination procedures, i.e., enter the number of pages containing information.

7b. **NUMBER OF REFERENCES:** Enter the total number of references cited in the report.

8a. **CONTRACT OR GRANT NUMBER:** If appropriate, enter the applicable number of the contract or grant under which the report was written.

8b, 8c, & 8d. **PROJECT NUMBER:** Enter the appropriate military department identification, such as project number, subproject number, system numbers, task number, etc.

9a. **ORIGINATOR'S REPORT NUMBER(S):** Enter the official report number by which the document will be identified and controlled by the originating activity. This number must be unique to this report.

9b. **OTHER REPORT NUMBER(S):** If the report has been assigned any other report numbers (*either by the originator or by the sponsor*), also enter this number(s).

10. **AVAILABILITY/LIMITATION NOTICES:** Enter any limitations on further dissemination of the report, other than those imposed by security classification, using standard statements such as:

- (1) "Qualified requesters may obtain copies of this report from DDC."
- (2) "Foreign announcement and dissemination of this report by DDC is not authorized."
- (3) "U. S. Government agencies may obtain copies of this report directly from DDC. Other qualified DDC users shall request through \_\_\_\_\_."
- (4) "U. S. military agencies may obtain copies of this report directly from DDC. Other qualified users shall request through \_\_\_\_\_."
- (5) "All distribution of this report is controlled. Qualified DDC users shall request through \_\_\_\_\_."

If the report has been furnished to the Office of Technical Services, Department of Commerce, for sale to the public, indicate this fact and enter the price, if known.

11. **SUPPLEMENTARY NOTES:** Use for additional explanatory notes.

12. **SPONSORING MILITARY ACTIVITY:** Enter the name of the departmental project office or laboratory sponsoring (*paying for*) the research and development. Include address.

13. **ABSTRACT:** Enter an abstract giving a brief and factual summary of the report, even though it may also appear elsewhere in the body of the technical report. If additional space is required, a continuation sheet shall be attached.

It is highly desirable that the abstract of classified reports be unclassified. Each paragraph of the abstract shall end with an indication of the military security classification of the information in the paragraph, represented as (TS), (S), (C), or (U).

There is no limitation on the length of the abstract. However, the suggested length is from 150 to 225 words.

14. **KEY WORDS:** Key words are technically meaningful terms or short phrases that characterize a report and may be used as index entries for cataloging the report. Key words must be selected so that no security classification is required. Identifiers, such as equipment model designation, trade name, military project code name, geographic location, may be used as key words but will be followed by an indication of technical context. The assignment of links, roles, and weights is optional.

Unclassified

Security Classification